Role of Bmi-1 in Epigenetic Regulation During Early Neural Crest Development

Thesis by

Jane I. Khudyakov

In Partial Fulfillment of the Requirements

for the Degree of

Doctor of Philosophy

California Institute of Technology

Pasadena, California

2009

(Defended April 30, 2009)

©2009

Jane I. Khudyakov

All Rights Reserved

ACKNOWLEDGEMENTS

First and foremost, I would like to express gratitude to my thesis advisor, Marianne Bronner-Fraser, without whose constant support, motivation, encouragement, and unfailing optimism it would have been impossible to navigate through a complex and challenging project. I am also grateful to my co-advisor, Tatjana Sauka-Spengler, for giving me the opportunity to study an exciting developmental question, providing me with a good balance of independence and support, facilitating my development as a mature scientist, and constantly encouraging me to believe in my own abilities. I would also like to thank members of my thesis committee: Scott Fraser, Angela Stathopoulos, Paul Sternberg, and Kai Zinn, for their critical advice and guidance through my graduate project.

I am grateful to my family, especially my father, Igor Khudyakov, for support during my time at Caltech and for the helpful advice and input that they have provided as fellow scientists. I would also like to thank my fiancé, Joseph Schramm, without whose persistent encouragement, support, kindness, and infinite patience I would never have been able to reach this point. I would like to thank the current and former members of the Bronner-Fraser group that have enriched my years in the lab with interesting discussions, helpful suggestions, motivation, friendship, and constant entertainment. In particular, I am exceedingly grateful to the support and friendship of Meghan Adams, Sonja McKeown, Sujata Bhattacharyya, Lisa Taneyhill, Saku Jayasena, Marcos Simoes-Costa, Ed Coles, and Natalya Nikitina. I am also especially grateful for the invaluable assistance of Mary Flowers and Matt Jones during my time in the Bronner-Fraser lab.

I would also like to thank my undergraduate advisor, Larysa Pevny, for inspiring me to pursue a graduate degree at Caltech, as well as Beverly Koller, in whose lab at UNC-Chapel Hill I first acquired an interest in scientific research. Last but not least, I would like to thank Cortney Tribu, Michael Brown, Jennifer Klamo and the wonderful Schramm family for their encouragement, friendship, cheerleading, and support.

ABSTRACT

The neural crest is a transient, multipotent cell population in the developing vertebrate embryo that migrates extensively and contributes to a staggering diversity of cell lineages. Neural crest progenitors are specified at the neural plate border during gastrulation; however, commitment to the neural crest lineage does not occur for some time. I find that the chick neural plate border is characterized by co-expression of several neural crest specifier genes, previously considered "late" signals, which often overlap with "early" neural plate border genes. This suggests that continuously expressed members of the neural crest gene regulatory network may be modulated or repressed for proper maintenance of the multipotent state. Consistent with this possibility, several members of the Polycomb Group of epigenetic repressors are expressed at these early stages. For example, the stem cell factor Bmi-1 is expressed in the neural plate border, dorsal neural folds, and migrating neural crest, but is extinguished in differentiated derivatives. Morpholino-mediated knock-down of Bmi-1 causes early upregulation of *Msx1*, *FoxD3*, and *Sox9* in the chick neurula without affecting cell proliferation. Conversely, Bmi-1 over-expression causes a downregulation of *Msx1*, suggesting that it negatively regulates neural crest network genes. I find that several alternatively spliced variants of Bmi-1 are expressed in the developing chick and that a truncated N-terminal variant, V4, acts as a dominant-negative regulator of the full-length protein by up-regulating *Msx1* expression. Taken together, these results suggest that neural crest progenitors are exposed to numerous signals during gastrulation, some of which are regulated by Polycomb Group factors such as Bmi-1. The activity of Bmi-1, in turn, is modulated by alternatively spliced variants, demonstrating an additional level of regulatory complexity acting during early neural crest development.

TABLE OF CONTENTS

Chapter 4:

Chapter 5:

LIST OF FIGURES

Chapter 1

Chapter 2

Chapter 3

Chapter 4

Chapter 5

Chapter 1: Introduction

Molecular and Epigenetic Regulation of Development

Neural crest as a stem cell model

A fundamental question in developmental biology is how a pluripotent precursor can generate an amazing diversity of specialized cell types. This involves the process by which stem cells become restricted in their fate potential over time, undergo lineage commitment, and finally differentiate into specific cell types and tissues. Restriction of stem cell potential occurs gradually over time. This necessitates maintenance of a degree of multipotency and plasticity throughout development and even into adulthood, since some tissues contain progenitors with the capacity to de- or trans-differentiate during tissue repair or oncogenesis (Pietersen and van Lohuizen, 2008). In an attempt to understand these important events, much research has been directed at identifying mechanisms that regulate multipotency and understanding the signals that orchestrate lineage-specific differentiation.

The neural crest has been a useful model system to study these processes *in vivo* because of its capability to differentiate into a large number of diverse cell types, its capacity to proliferate, and the persistence of multipotent progenitors within differentiated tissues. In addition, slowly developing model systems like the chicken embryo are amenable to embryological perturbation because of their accessibility and ease of manipulation, thus proving very useful for understanding neural crest development (Le Douarin, 2004). Neural crest precursors are specified during early gastrulation at the border of the presumptive neural plate, and come to reside within the dorsal neural folds by morphological rearrangements during neurulation. Upon neural tube closure, neural crest cells emigrate from its dorsal aspect and undergo one of the most extensive migrations in the vertebrate body, coming to populate almost every

developing tissue. They differentiate into cell types as diverse as cranial bone and cartilage, sensory, parasympathetic, and enteric ganglia, pigment cells, and secretory endocrine cells, among many others (Le Douarin and Kalcheim, 1999). It has been suggested that this highly specialized cell type, which was a major driving force during evolution of the vertebrate predator, should be considered a fourth germ layer (Gans and Northcutt, 1983; Hall, 2000).

Lineage-tracing experiments using the chick embryo have been instrumental in identifying neural crest precursors. These studies have demonstrated that neural crest progenitors are indistinguishable from the rest of the neuroepithelium prior to their emigration from the dorsal neural tube, and that progeny of single-labeled dorsal neuroepithelial cells can contribute to both neural crest or dorsal neural tube derivatives such as roof plate and commissural neurons (Bronner-Fraser and Fraser, 1988, 1989; Selleck and Bronner-Fraser, 1996). Intriguingly, even dorsal neural tube cells expressing canonical "pre-migratory neural crest" markers can contribute to either of these lineages, suggesting that the neural crest is not committed prior to emigration, despite exposure to a number of specification signals (LaBonne and Bronner-Fraser, 1999). Furthermore, clonogenic analyses of migrating neural crest cells have demonstrated that they remain largely multipotent throughout their journey and that fate restriction occurs gradually, at least in a portion of the progenitors. However, a pool of multipotent, if not pluripotent, neural crest stem cells persists even after differentiation in tissues such as the sensory, sympathetic, and enteric ganglia and peripheral nerves, which are able to self-renew in culture. This population is heterogeneous and contains both multipotent neural crest progenitors as well as cells that differentiate into only one or two cell types

(Crane and Trainor, 2006). Nevertheless, even the apparently lineage-restricted progenitors demonstrate a high degree of plasticity and can de-differentiate upon back-transplantation into younger embryo hosts, and trans-differentiate appropriately into alternative lineages in response to novel signals (Le Douarin, 2004). It is likely that this ability may contribute to the oncogenic potential of neural crest cells in neurocristopathies such as neuroblastoma and Schwannoma. However, the highly plastic and multipotent nature of the neural crest also makes it a promising candidate for stem cell therapy, such as for use in peripheral nerve repair (Crane and Trainor, 2006). Not surprisingly, a large amount of research has been dedicated to understanding the timing and mechanisms regulating emergence of this fascinating cell type during early embryogenesis.

Establishment of the neural plate border

It is now widely accepted that neural crest cells are first specified during gastrulation and preceding the emergence of a definitive neural plate, in all vertebrates examined including the chicken embryo. Explants of early chick gastrula-stage medial epiblast generate migratory neural crest cells in culture in the absence of inducing factors, and are able to autonomously differentiate into bona fide crest derivatives such as melanocytes and neurons (Basch et al., 2006). The precise region of the epiblast from which neural crest progenitors arise has been examined by fate mapping and found to coincide with the junction between future neural plate and non-neural ectoderm. This “neural plate border” region is fairly wide and also contains progenitors of neural plate, epidermis, and placodes that are highly intermixed and indistinguishable from each other either

morphologically or molecularly (Garcia-Martinez et al., 1993; Fernandez-Garre et al., 2002; Ezin et al., 2009). In order to understand how progenitors within the neural plate border acquire their distinct cell fates, one must first consider the signaling events that segregate neural tissue from non-neural ectoderm, therefore generating this specialized "in-between" region.

For some time, the process of neural plate induction and specification of the neural lineage was thought to be a relatively simple and "default" process occurring during gastrulation, involving inhibition of bone morphogenetic proteins (BMP) by diffusible factors emerging from a specialized mesodermal signaling center, the "organizer." Accordingly to this scenario, the ectodermal germ layer had an inherent predisposition to a neural fate in the absence of epidermal-derived BMP signals (Hemmati-Brivanlou and Melton, 1997). Moreover, diffusion of BMP inhibitors from the organizer was found to generate a concentration gradient which specified positional information such that epidermal cells were specified at high BMP levels, the neural plate formed where they were absent or low, and intermediate BMP concentrations at the neural plate border specified neural crest fate (LaBonne and Bronner-Fraser, 1999). While experimental support for this "default model" of neural induction came from studies using the *Xenopus* model system and primarily involved data from *in vitro* experiments, investigation of this process in amniotes, as well as more careful reexamination of inductive events in the frog have generated a more complicated picture involving integration of several distinct molecular pathways.

Current data suggest that pre-patterning of the ectoderm and specification of the neural fate occurs prior to gastrulation and that mesoderm induction and

the organizer are dispensable for neural induction in both anamniotes and amniotes (Pera et al., 1999; Kuroda et al., 2004). In chick and mouse, BMP inhibition by organizer-derived inhibitors is neither necessary nor sufficient for neural induction. Rather, FGF signaling appears to play a major role both independently and together with BMP repression (Wilson et al., 2000). Consequently, the only area of the chick epiblast which is affected by direct perturbation of BMP signaling is the border of the prospective neural plate, suggesting that the role of these factors in neural induction may be to maintain the boundary of neural plate formation (Streit and Stern, 1999). Following these reports in the chick, additional studies in *Xenopus* also found a requirement for the FGF pathway in neural induction, as well as for formation of the neural plate border, and consequently, the neural crest (Launay et al., 1996; LaBonne and Bronner-Fraser, 1998). In addition, the canonical Wnt signaling pathway has been implicated in neural induction in chick and *Xenopus*. Two members of the Wnt family are expressed at high levels in lateral epiblast of the chick blastula and have been shown to inhibit neural induction by blocking the ability of FGF to negatively regulate BMP (Wilson et al., 2001). In contrast, Wnt signaling in the *Xenopus* blastula is necessary for BMP inhibition in dorsal ectoderm, prior to diffusion of neuralizing factors from the organizer (Baker et al., 1999). Although the mechanism by which Wnt functions in neural induction varies between *Xenopus* and chick, this pathway is necessary in both organisms for induction of the third ectodermal derivative, the neural crest (LaBonne and Bronner-Fraser, 1998; Garcia-Castro et al., 2002). In summary, specification of the neural plate and neural plate border occurs very early in development in both amniotes and anamniotes, by processes that are generally conserved in other vertebrate model

systems, such as zebrafish and mouse. The neural plate is distinguished from non-neural ectoderm by the integration of signals from three separate pathways: BMP, FGF, and Wnt. In *Xenopus*, neural induction occurs primarily through BMP inhibition in dorsal ectoderm by early Wnt and FGF signals and later signals from the organizer. Cell fates at the neural plate border are specified by cooperative activity of intermediate ectodermal BMP levels and mesodermally derived FGF and Wnt signals. In chick, FGF plays a main role in neural induction by independently promoting neural fate as well as inhibiting BMP in medial epiblast, while high concentrations of ectodermal Wnt in lateral epiblast regulate the lateral extent of the neural plate. Neural plate border fates are specified at the edge of the presumptive neural plate by high levels of BMP and lateral diffusion of ectodermal Wnt, and later maintained by FGF signals emanating from paraxial mesoderm (LaBonne and Bronner-Fraser, 1999; Wilson and Edlund, 2001; Knecht and Bronner-Fraser, 2002). Therefore, by late gastrulation, diffusible growth factor signals have regionalized the ectoderm and the presumptive neural plate border has been established. However, specification of distinct neural plate border fates, including that of the neural crest, requires precise transcriptional readout of these early inductive signals.

Gene regulatory interactions driving early neural crest development

Understanding of transcriptional regulation of neural crest development is largely derived from functional studies in which putative neural crest specifier genes were perturbed by over-expression, dominant-negative inhibition, or antisense oligonucleotide knock-down. Unfortunately, the classical vertebrate model systems used to study neural crest development are not easily amenable

to the kind of genomic *cis*-regulatory analysis that has enabled formulation of detailed gene regulatory circuits for tissue-specific development in other organisms (Davidson et al., 2002). However, a putative gene regulatory network for neural crest development (NC-GRN) has been proposed based on the large collection of data from neural crest perturbation studies and examinations of epistatic relationships between vertebrate neural crest genes (Fig. 1.1, Meulemans and Bronner-Fraser, 2004). The NC-GRN proposes that the inductive events responsible for ectodermal patterning (BMP, FGF, Wnt) activate of group of transcription factors (Msx1, Dlx3/5, Pax3/7, Zic1) at the junction between neural and non-neural ectoderm, specifying this area as the neural plate border. Subsequently, highly coordinated activity of the "neural plate border specifiers" leads to the activation of "neural crest specifier" genes (Snail1/2, FoxD3, SoxE group, Myc, AP-2, Id) specifically in neural crest progenitors residing within the neural plate border (neighboring placode progenitors are specified by an alternative combination of signals). Expression of neural crest specifier genes confers competency to form bona fide neural crest by inducing effector genes which are necessary for delamination from the neural tube, migration along appropriate pathways, and cell type-specific differentiation (Sauka-Spengler and Bronner-Fraser, 2008).

The molecular events leading to specification of the neural plate border are reiterative and highly complex. For example, BMP signals at the edges of the neural plate in combination with Wnt signals from ectoderm induce *Msx1* and *Pax7* in the prospective neural plate border (Tribulo et al., 2003; Monsoro-Burq et al., 2005; Basch et al., 2006). The combination of high concentrations of FGF and low BMP activates the neural specifier *Zic1*, which also functions as a neural

plate border specifier by collaborating with *Msx* and *Pax* to induce downstream neural crest genes (Merzdorf, 2007). In contrast, high levels of ectodermal BMP and Wnt induce the ectoderm specifiers *Dlx5* and *Dlx3*, which function indirectly to position the neural plate border by repressing neuronal fate (Bang et al., 1997; Suzuki et al., 1997; Pera et al., 1999; Streit and Stern, 1999; Luo et al., 2001a; Tribulo et al., 2003; Monsoro-Burq et al., 2005). The fact that many of the neural plate border specifiers do not function uniquely in this region (e.g., Msx1 and Dlx3/5 genes are also ectodermal specifiers, while Zic1 is a neural gene) makes it incredibly difficult to precisely map the neural plate border using gene expression analysis. While we are currently unable to obtain cellular resolution of this process, we do know that the neural plate border region is established by cooperative activity and cross-regulatory interactions between neural plate border specifiers (Meulemans and Bronner-Fraser, 2004).

Some of the regulatory relationships between neural plate border and neural crest specifiers have been described, and attempts at dissection of *cis*-regulatory interactions are currently underway in a number of organisms. For example, one of the earliest neural crest-specific genes activated by Pax3 and Zic1 in *Xenopu*s is *FoxD3*, which promotes neural crest fate by inducing and maintaining expression of other neural crest specifiers such as the *SoxE* genes, and by segregating the neural crest lineage from other cell fates in the dorsal neural tube (Dottori et al., 2001; Kos et al., 2001; Montero-Balaguer et al., 2006; Stewart et al., 2006). Pax3/7 and Zic1 also cooperate with Msx1 to induce the neural crest specifier *Snail2*, which is essential for neural crest migration and also functions as an anti-apoptotic factor and regulator of *SoxE* expression (Nieto et al., 1994; Mayor et al., 1995; LaBonne and Bronner-Fraser, 2000; del Barrio and

Nieto, 2002; Monsoro-Burq et al., 2005; Sato et al., 2005; Taneyhill LA, 2007). Interactions between neural crest specifiers are highly complex, involving extensive auto- and cross-regulation, so that perturbation of one member of this group usually affects expression of all others (Meulemans and Bronner-Fraser, 2004). Interestingly, some neural crest specifiers perform several temporally distinct functions during development. For example, *AP2α* is activated during early development by high levels of BMP in non-neural ectoderm and specifies ectodermal fate by maintaining *Msx1* and *Dlx5* expression (Luo et al., 2002). However, during late neurulation, *AP2α* becomes recruited to the dorsal neural tube and functions in a feedback loop with Slug and Sox9 to maintain neural crest identity (Luo et al., 2003). Other transcription factors that are considered neural crest specifiers, such as c-myc, N-myc, and Id, function mainly as proliferation and survival factors and inhibitors of differentiation (Bellmeyer et al., 2003; Light et al., 2005). The regulatory targets of neural crest specifiers and their function in later stages of neural crest development are reviewed elsewhere (Meulemans and Bronner-Fraser, 2004; Sauka-Spengler and Bronner-Fraser, 2008).

In summary, specification of the neural crest lineage occurs via step-wise and highly coordinated activation of discrete groups of genes during early development. Although a simplistic view of the NC-GRN would suppose that transcriptional events during neural crest development proceed in a hierarchical fashion, we know that interactions between induction factors, neural plate border specifiers, and neural crest specifiers are characterized by a large degree of cross- and auto-regulation and are therefore highly complex. Precise timing of

induction of NC-GRN factors is still largely unknown, and studies in *Xenopus* and lamprey suggest that some neural crest specifiers are expressed as early as gastrulation concomitant with the neural plate border genes (Huang and Saint-Jeannet, 2004; Sauka-Spengler et al., 2007). In addition, expression of inducers such as *BMP* and neural plate border specifiers such as *Msx1* and *Pax7* persists throughout early neural crest development, suggesting the possibility of late roles in maintenance of the neural crest fate and continued regulation of neural crest specifiers. The complexity of the NC-GRN interactions, together with the fact that neural crest progenitors remain multipotent despite continuous exposure to a plethora of specifying signals, suggests the existence of modulatory factors that regulate early neural crest progenitor development.

Epigenetic regulation of embryonic development

The advent of whole-genome analysis by technologies such as ChIP-on-Chip and ChIP-Seq has enabled researchers to obtain a large-scale view of molecular events operating during stem cell development, lineage commitment, and differentiation (Mendenhall and Bernstein, 2008). Data from such studies have demonstrated that a ubiquitous and important mechanism for regulating gene expression during development involves epigenetic modification of chromatin structure. Chromatin state maps have illustrated that the majority of transcription factor families involved in cell type-specific determination are transcriptionally inactive in pluripotent stem cells and are correlated with high levels of trimethylation of histone H3 on lysine 27 ($H3K27me^3$), a mark of compacted heterochromatin. In contrast, in response to differentiation signals, developmental regulator genes become associated with activated polymerase II

and a methylation mark of active transcription, H3K4me^3 (histone H3 trimethylated on lysine 4), resulting in high expression. Concurrently, genes that are involved in maintenance of pluripotency (Oct4, Sox2, Nanog) or in specification of alternative cell lineages become repressed and labeled by H3K27me^3 during differentiation (Mikkelsen et al., 2007).

A recent pivotal study that examined methylation patterns in mouse embryonic stem cells (ESC) demonstrated that surprisingly, a large number of promoters of transcriptionally inactive developmental regulator genes are marked by both repressive and active chromatin marks (H3K27me^3 and H3K4me^3), which have been termed "bivalent" regions. Upon differentiation, genes that were characterized by bivalent domains in stem cells resolve to either one or the other methylation mark, and become preferentially activated or repressed (Bernstein et al., 2006). Based on these findings, it has been suggested that the bivalent domain may function to keep key developmental regulators "poised" to undergo a rapid change in transcriptional activity upon receiving differentiation signals. Therefore, epigenetic chromatin modifications play a vital role during development by regulating transcriptional events, preventing premature activation of lineage specification factors, and modulating inputs of developmental signals by enabling rapid and flexible changes in transcription of target genes (Pietersen and van Lohuizen, 2008). Not surprisingly, dysregulation of epigenetic mechanisms is regularly observed in a large number of human diseases and cancers (Delcuve et al., 2009).

The Polycomb Group of epigenetic repressors

The enzymatic complexes responsible for H3K27 and H3K4 trimethylation, the Polycomb Group (PcG) and Trithorax Group (TxG), have been extensively studied in a number of organisms and developmental processes and are highly conserved throughout evolution in both plants and animals (Schuettengruber et al., 2007; Whitcomb et al., 2007). PcG genes were first identified in *Drosophila* by E. B. Lewis as repressors of the Hox complex, as reflected in their names which describe the homeotic transformations that characterized the mutants (Lewis, 1978). Identification of vertebrate Polycomb orthologs has demonstrated that their role in axial patterning is conserved (Alkema et al., 1995; van der Lugt et al., 1996). Interestingly, PcG proteins play a critical role in maintenance and self-renewal of stem cells by repression of transcriptional regulators (Fig. 1.2A).

Isolation of PcG proteins and their characterization by biochemical assays has demonstrated that this group functions as two separate and sequentially acting complexes: Polycomb Repressive Complex 2 (PRC2) and Polycomb Repressive Complex 1 (PRC1), each of which consists of a set of core components in *Drosophila* and a large number of paralogs in vertebrates (Fig. 1.2B). The PRC2 subunit Enhancer of Zeste (E(z), or vertebrate Ezh1/2) is the key enzymatic partner responsible for trimethylation of histone H3 lysine 27. Three other core components of PRC2, which stimulate its methyltransferase activity, include Extra sex combs (Esc, or vertebrate Eed), Suppressor of Zeste (Su(z)12, or vertebrate Suz12), and Nurf55 (Sparmann and van Lohuizen, 2006; Schuettengruber et al., 2007). The downstream PRC1 complex is thought to recognize the PRC2-catalyzed methylation mark via a chromodomain of the

Polycomb protein (Pc, or vertebrate Cbx2/4/6/7/8). Core PRC1 components also include Polyhomeotic (Ph, or vertebrate Mph1/2 and Phc3), Posterior sex combs (Psc, or vertebrate Bmi-1 and Mel-18), and dRing (vertebrate Ring1B and Ring1A). The Ring1B protein possesses catalytic activity which is used to monoubiquitylate lysine 119 of histone H2A (Schuettengruber et al., 2007; Schwartz and Pirrotta, 2007). This mark is necessary for maintenance of PcG repressive activity, which is lost in Ring1B mutants despite persistence of H3K27me^3 (Wang et al., 2004). Furthermore, presence of all PRC1 and PRC2 core components is necessary for their expression and repressive activity, suggesting extensive auto-regulation as a means of maintaining complex integrity (Boyer et al., 2006; Lee et al., 2006; van der Stoop et al., 2008).

The importance of PcG-mediated gene repression during development has been demonstrated by PcG transgenic mouse models, which exhibit an inability to maintain the embryonic stem cell state, drastic loss of stem cell populations, and embryonic lethality. Analogously, many human cancers are characterized by increased expression of Polycomb genes (Sparmann and van Lohuizen, 2006). In ChIP-on-Chip studies, binding of both PRC2 and PRC1 proteins in mouse and human embryonic stem cells was enriched at the silent promoters of a large number of genes involved in vertebrate development. The PcG target genes included members of such highly conserved transcription factor families as *Hox*, *Dlx*, *Irx*, *Lhx*, *Pou*, *Pax*, *Six*, *Sox*, and *Tbx*, among many others. Upon stimulation with differentiation factors, the Polycomb complexes were removed from chromatin, causing de-repression of target genes and subsequent differentiation. Interestingly, it was the PcG target genes that were preferentially activated upon stem cell differentiation. Similar de-repression of transcription

factor targets was observed in stem cells carrying mutations for one or more PRC members, causing inappropriate differentiation in culture (Boyer et al., 2006; Bracken et al., 2006; Lee et al., 2006).

Furthermore, promoter regions of PcG-target genes are primarily characterized by bivalent domains and often exhibit co-occupancy by PRC1 and PRC2 members, Trithorax group proteins, and RNA polymerase II that is in a "paused" biochemical conformation (Stock et al., 2007; Ku et al., 2008). Therefore, the Polycomb proteins function as critical regulators of development by repressing differentiation-promoting transcription factors in stem cells while maintaining them in a poised state, enabling rapid and highly coordinated activation upon reception of inductive signals. In addition, lineage-appropriate specification requires activation of cell type-specific genetic programs coincident with suppression of signals mediating alternative fates, states which can still be reversed prior to lineage commitment and therefore involve a large degree of plasticity. Finally, terminal differentiation necessitates maintained activation of specialized cell type markers and stable repression of multipotency factors and genes involved in other tissue functions. ChIP-on-Chip analysis of Polycomb binding and histone methylation in a variety of lineage precursors and differentiated cell types have demonstrated that the PcG participates in regulation of all of these processes and aspects of development (Bracken et al., 2006; Pasini et al., 2007; Mohn et al., 2008).

Structure and function of Bmi-1 in stem cell development

The vertebrate PRC1 ortholog of *Drosophila posterior sex combs*, Bmi-1, was one of the first Polycomb genes to be studied as a stem cell and oncogenic factor.

Bmi-1 was first identified in the mouse as a retrovirus-induced cooperator in lymphomagenesis with c-myc, and subsequently named "**B**-cell type specific **M**oloney murine lymphoma retrovirus **i**nsertion site **1** (Haupt et al., 1991). In these transgenic mice, over-expression of Bmi-1 induced lymphomas by inhibiting c-myc-mediated apoptosis in hematopoietic stem cells (Jacobs et al., 1999b). Conversely, Bmi-1 knockout mice exhibited gross defects in the hematopoetic system due to failure of hematopoietic stem cells to proliferate and self-renew (Lessard and Sauvageau, 2003; Park et al., 2003). Mice deficient in Bmi-1 also exhibit defects in self-renewal of other stem cell types, such as CNS (subventricular zone) and PNS (enteric neural crest) progenitors (Molofsky et al., 2003). The targets through which Bmi-1 functions to positively regulate the cell cycle in mouse were identified by double knockout experiments, and involve the $p16^{Ink4a}/p19^{Arf}$ locus of cell cycle repressors (Jacobs et al., 1999a; Molofsky et al., 2005). Subsequent ChIP experiments have demonstrated that Bmi-1 negatively regulates this locus by direct association, and this interaction has been extensively studied due to its role in cell senescence during aging (Bracken et al., 2007). In addition, Bmi-1 functions in stem cell development by regulating a number of differentiation-specific transcription factors in cooperation with other Polycomb members (Bracken et al., 2006). During later development, Bmi-1 is necessary for maintenance of postnatal stem cell populations and regulation of axial patterning by direct repression of homeotic genes (van der Lugt et al., 1994; Molofsky et al., 2003; Cao et al., 2005).

Bmi-1 is a ~40 kDa protein which is characterized by three distinct functional domains (Fig. 1.3A). A highly conserved cysteine-rich RING finger domain located near the N-terminus mediates protein-protein interactions with

the other RING- containing PRC1 members Ring1A and Ring1B (Hemenway et al., 1998; Satijn and Otte, 1999). Since the presence of Bmi-1 in the PRC1 complex has been shown to stimulate ubiquitination activity of Ring1B, it is not surprising that this key interaction domain is also necessary for the oncogenic potential and repressive activity of Bmi-1 (Alkema et al., 1997b; Itahana et al., 2003; Wang et al., 2004). The Bmi-1 protein also contains a conserved helix-turn-helix-turn-helix-turn (HTHTHT) domain which is necessary for interaction with Mph proteins, the mammalian orthologs of *Drosophila polyhomeotic*, and for the ability to repress transcription of Hox genes and other targets (Cohen et al., 1996; Alkema et al., 1997a). A proline, glutamine, serine, threonine-rich, or PEST, domain is localized in the C-terminus of Bmi-1, which may function to target the protein for rapid degradation, although this has not been definitively demonstrated *in vitro* (Alkema et al., 1997b). A putative MAPK-pathway phosphorylation site within this domain may be involved in subcellular translocation of Bmi-1 in response to external signals (Voncken et al., 2005). Based on biochemical protein interaction assays, it has been suggested that Bmi-1 may function as a tethering protein that maintains structural integrity of PRC1 (Fig. 1.3B, Cao et al., 2005).

In addition, the biochemical deletion studies that identified Bmi-1 functional domains also demonstrated that truncated portions of the protein could dimerize with full-length Bmi-1 and other PRC1 proteins, and exhibit dominant-negative effects (Hemenway et al., 1998; Satijn and Otte, 1999; Itahana et al., 2003). Based on these data, an intriguing possibility is that the function of Bmi-1 may be mediated by naturally occurring alternatively spliced isoforms which contain differential combinations of functional domains, therefore modulating the activity of Bmi-1 and the complex. Indeed, there is mounting

evidence that a number of Polycomb proteins and other critical developmental specifiers are regulated by alternative splicing (Alkema et al., 1997a; Yamaki et al., 2002; Tajul-Arifin et al., 2003; Li et al., 2005). Therefore, cell lineage diversification and differentiation during development likely involves several complex layers of regulation: transcriptional specification signals, their modification by epigenetic repressor complexes, and in turn, the modulation of those complexes by alternatively spliced isoforms.

Figure 1.1: Gene regulatory network for neural crest development

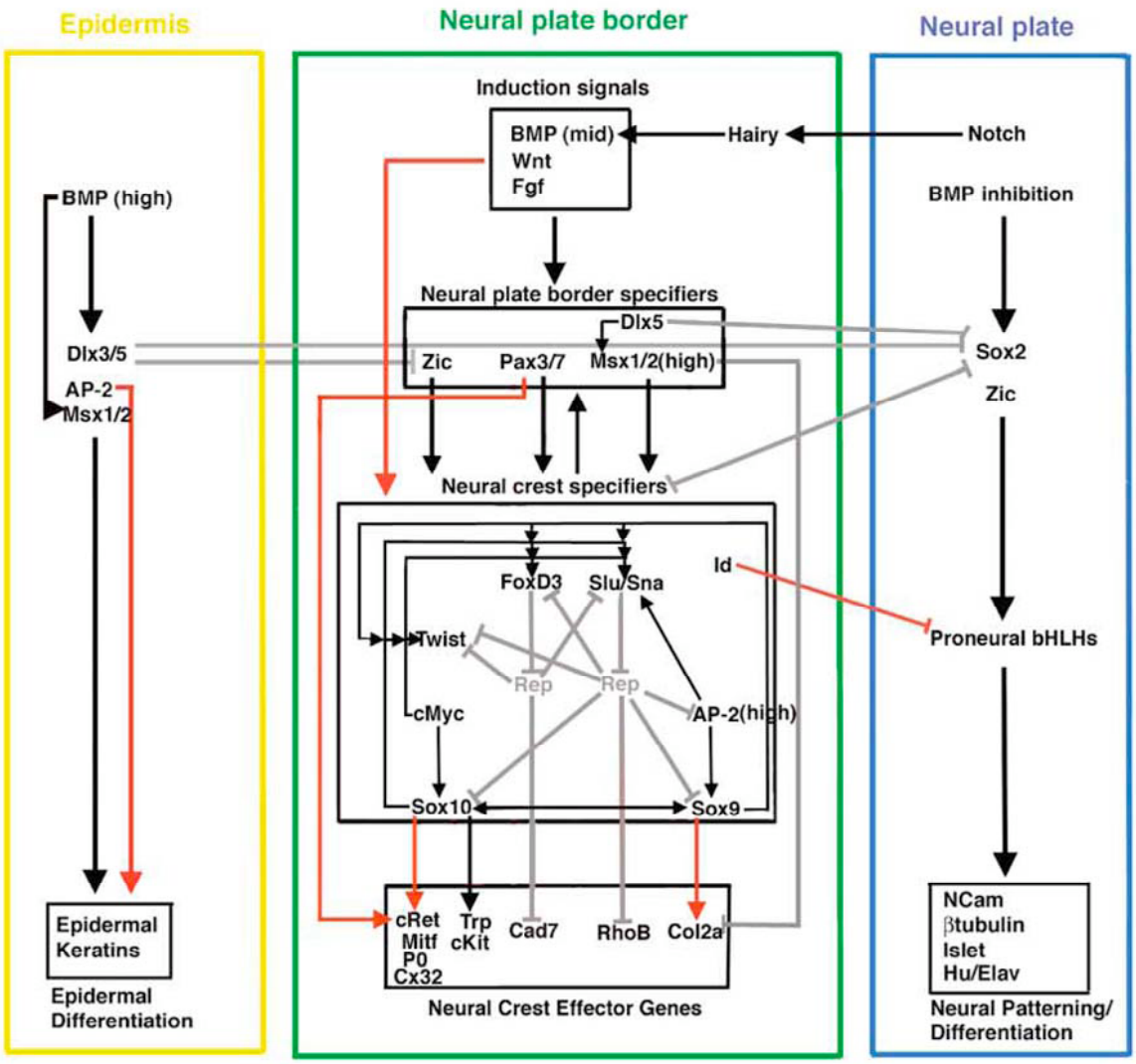

Figure 1.1. Putative gene regulatory network proposed by Meulemans and Bronner-Fraser to describe signaling and transcriptional events at the neural plate border during vertebrate neural crest development (Meulemans and Bronner-Fraser,2004).

Figure 1.2: Biochemical composition of Polycomb Repressive Complexes

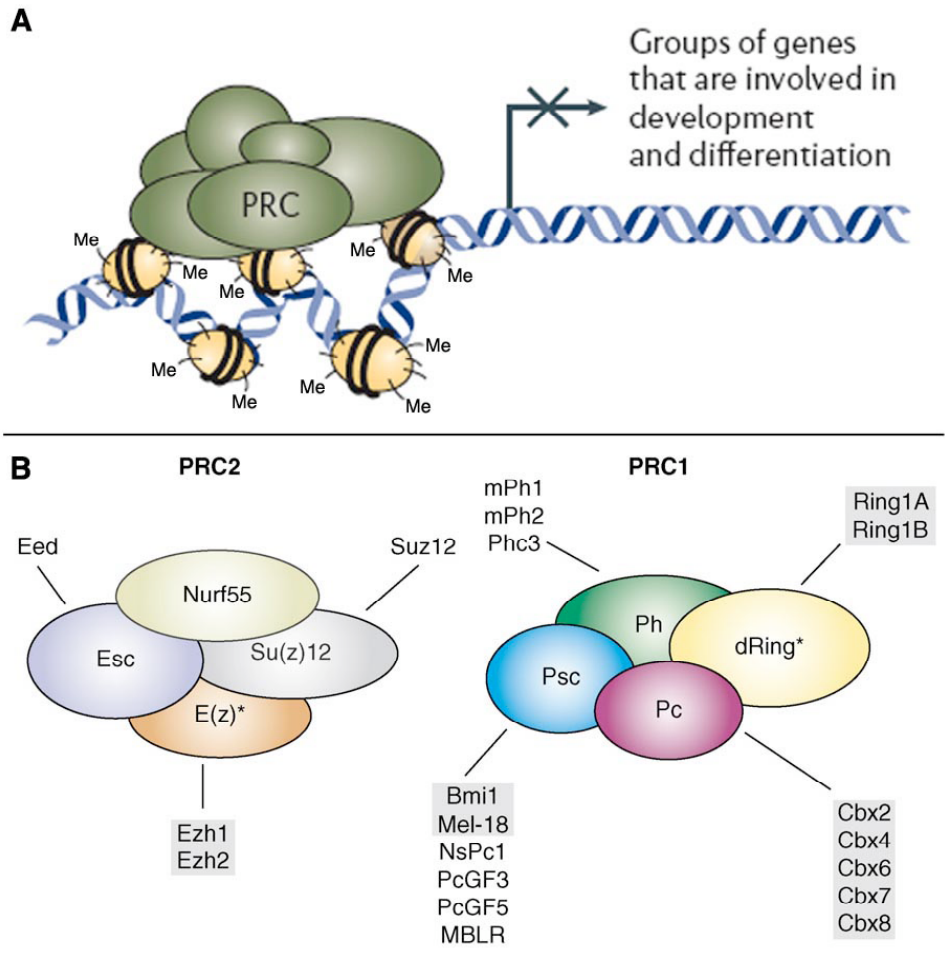

Figure 1.2. The Polycomb Group consists of two discrete complexes with a large number of highly conserved protein partners. **A.** In a simplistic schematic, the Polycomb complex is shown to associate with regulatory regions of genes involved in development and differentiation, causing histone methylation, compaction of heterochromatin, and transcriptional repression. Adapted from Baylin and Ohm, 2006. **B.** Diagram illustrating the core components of *Drosophila* Polycomb Repressive Complex 2 (PRC2) and Polycomb Repressive Complex 1 (PRC1), and their mammalian paralogs. From Whitcomb et al., 2007.

Figure 1.3: Biochemical structure of Bmi-1 protein

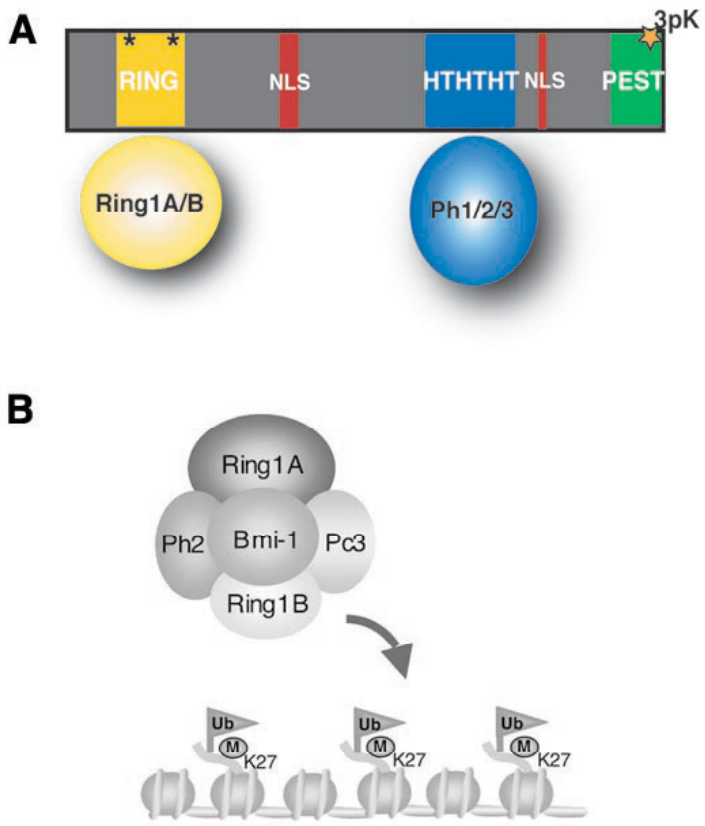

Figure 1.3. A. The PRC1 member Bmi-1 is characterized by several conserved motifs necessary for interaction with other complex members. The RING finger domain (yellow) mediates interaction with RING-containing proteins Ring1A and Ring1B, for which the presence of two conserved cysteine residues (asterisks) is required. The helix-turn-helix-turn-helix-turn (HTHTHT, blue) domain mediates interactions with polyhomeotic proteins Ph1, Ph2, and Phc3. A proline-glutamine-serine-threonine-rich (PEST, green) domain may be involved in protein degradation. A putative downstream MAPK pathway phosphorylation site (orange star) lies within this domain. **B.** Bmi-1 has been biochemically purified as a tethering protein in a complex containing Ring1A,

Ring1B, Ph2, and Pc3 (Cbx8). PRC1 (via Ring1B) ubiquitinates histone H2A on lysine 119 within genomic regions targeted by PRC2. From Cao et al., 2005.

Chapter 2:

Comprehensive Spatiotemporal Analysis of Early Chick Neural Crest Network Genes

The majority of this chapter has been published as:

Khudyakov J and Bronner-Fraser M. (2009) Comprehensive spatiotemporal analysis of early chick neural crest network genes. Dev Dyn 238:716-723. © Wiley-Liss, Inc.

Reprinted with permission of Wiley-Liss, Inc. a subsidiary of John Wiley & Sons, Inc.

ABSTRACT

Specification of neural crest progenitors begins during gastrulation at the neural plate border, long before migration or differentiation. Neural crest cell fate is acquired by progressive activation of discrete groups of transcription factors that appear to be highly conserved in vertebrates; however, comprehensive analysis of their expression has been lacking in chick, an important model system for neural crest development. To address this, we analyzed expression of ten transcription factors that are known specifiers of neural plate border and neural crest fate and compared them across developmental stages from gastrulation to neural crest migration. Surprisingly, we find that most neural crest specifiers are expressed during gastrulation, concomitant with and in similar domains as neural plate border specifiers. This suggests that interactions between these molecules may occur much earlier than previously thought in the chick, an important consideration for interpretation of functional studies.

INTRODUCTION

Neural crest cells are a transient, multipotent population of migratory cells that arise during development in dorsal neural tissue. After emigrating from the neural tube, they travel extensively throughout the body to form diverse derivatives in the periphery (Sauka-Spengler and Bronner-Fraser, 2008). Many of the processes and molecules that govern neural crest induction, commitment, migration, and differentiation have been uncovered over the past several decades through experimentation on a number of vertebrate models. In particular, the *Xenopus* embryo has been invaluable to our understanding of neural crest induction and underlying gene cascades. In addition, genetic studies using mouse and zebrafish have resolved many of the molecular interactions operating during neural crest development. Due to its easy accessibility to manipulation as well as optical clarity, the chick embryo has added much to our knowledge of neural crest formation and migration. In addition, its relatively slow development compared to other vertebrates and recently available genome have been advantageous for resolving early genetic events in neural crest development (Le Douarin and Kalcheim, 1999; Le Douarin, 2004).

Neural crest cells acquire their identity early in development, at gastrula stages, and often retain stem cell-like properties during migration (Le Douarin, 2004; Basch et al., 2006; Crane and Trainor, 2006). Fate map studies in the chick show that cells originating from the junction of neural and non-neural ectoderm, known as the presumptive "neural plate border" region, are progenitors of dorsal neural folds, dorsal neural tube, and migrating neural crest cells (Ezin et al., 2009). Furthermore, when explanted from the embryo, tissue from this region

executes a neural crest cell program in the absence of exogenous factors (Basch et al., 2006). Therefore, progenitor cells in the prospective neural plate border have already received instructive signals that specify them as neural crest in the gastrula. However, the nature of these early signals remains largely unknown.

Comparison of molecular data from several model organisms has led to the formulation of a putative neural crest gene regulatory network (NC-GRN) to help explain the signaling and transcriptional events underlying neural crest development (Meulemans and Bronner-Fraser, 2004; Sauka-Spengler and Bronner-Fraser, 2008). The NC-GRN suggests that hierarchical relationships between distinct groups of genes contribute to progressive acquisition of neural crest cell fate. As such, the first signals are received during gastrulation, when diffusible "induction factors" (BMP, FGF, Wnt) subdivide the ectoderm into neural plate and non-neural ectoderm. A specific, finely tuned combination of such signals at the junction between neural and non-neural tissues induces a cadre of transcription factors that specify this region as the neural plate border (Bang et al., 1997; Suzuki et al., 1997; Pera et al., 1999; Streit and Stern, 1999; Luo et al., 2001a; Tribulo et al., 2003; Monsoro-Burq et al., 2005). These "neural plate border specifiers" (Msx1, Zic1, Pax7, Dlx5, Dlx3) cooperate to delineate the neural plate border, which contains a heterogeneous population of progenitor cells including those fated to become neural crest, placodes, and dorsal neural tube (McLarren et al., 2003; Tribulo et al., 2003; Woda et al., 2003; Sato et al., 2005; Hong and Saint-Jeannet, 2007; Merzdorf, 2007). Acquisition of these distinct cells fates depends on particular combinations of downstream molecules. Specifically in neural crest progenitors, the aforementioned "neural plate border specifiers" induce a group of "neural crest specifiers" (FoxD3, Snail2, c-myc, N-myc, AP-2α,

Sox9, Sox10, among others) that function to impart bona fide neural crest characteristics, such as migratory ability on these progenitors. In addition, these genes play a crucial role in cell survival and differentiation, and their expression in pre-migratory and migrating neural crest is maintained by extensive cross- and auto-regulation (Wakamatsu et al., 1997; LaBonne and Bronner-Fraser, 2000; Dottori et al., 2001; Kos et al., 2001; Sasai et al., 2001; Bellmeyer et al., 2003; Cheung and Briscoe, 2003; Luo et al., 2003; McKeown et al., 2005; Sakai et al., 2006; Stewart et al., 2006; Taneyhill et al., 2007; Teng et al., 2008). Finally, the neural crest specifiers activate effector genes that regulate differentiation of distinct neural crest derivative lineages. These include Col2a (chondrocyte), Trp (melanocyte), c-Ret (enteric neuron), and many others (Sauka-Spengler and Bronner-Fraser, 2008).

Comparative studies of NC-GRN in modern vertebrates (zebrafish, frog, chick and mouse), basal vertebrate (lamprey), and non-vertebrate chordates (amphioxus and ascidian) suggest that neural plate border genes are remarkably conserved throughout chordate evolution but that expression of neural crest specifier genes at the neural plate border is unique to vertebrates (Meulemans and Bronner-Fraser, 2004; Sauka-Spengler et al., 2007; Yu et al., 2008). Recent studies in the lamprey suggest that some neural crest specifier genes, such as *AP-2* and *c-myc*, may be activated much earlier than previously thought, concomitant with neural plate border specifiers during gastrulation (Sauka-Spengler et al., 2007). Likewise in *Xenopus*, neural crest specifiers *Snail2* and *FoxD3* are co-expressed in the neural plate border with *Msx1* and *Pax3* during gastrulation (Huang and Saint-Jeannet, 2004). Orthologs of these genes have been identified and studied individually, but there is little information regarding their onset,

duration, or overlap of expression in the chick. Although expression patterns of chick NC-GRN members have been examined in detail at neurula stages, much less is known about their early deployment. Such information represents a critical backdrop for interpretation of functional perturbation studies.

Here, we characterize and carefully compare the expression patterns of transcription factors of the neural plate border and neural crest specifier category in chick embryos from stages of gastrulation to neural crest migration. Surprisingly, we find that a number of neural crest specifier genes are co-expressed with neural plate border specifiers during gastrulation in remarkably similar expression domains, implying possible early regulatory relationships. This suggests that interactions between chick specifier genes in the NC-GRN may be more complex and occur earlier than previously thought.

MATERIALS AND METHODS

Chick embryo incubation

Fertilized chicken eggs were obtained from AA Enterprises (Ramona, CA) and incubated at 38°C in a humidified incubator (Lyon Electric, Chula Vista, CA). Embryos were staged according to the Hamburger and Hamilton chick staging system (Hamburger and Hamilton, 1992).

Whole-mount *in situ* hybridization

Chick embryos were dissected in Ringer's solution and fixed in 4% paraformaldehyde at 4°C overnight. Whole-mount *in situ* hybridization was performed as described previously (Nieto et al., 1996; Xu and Wilkinson, 1998), with some modifications involving more extensive washing adapted from a lamprey *in situ* protocol (Sauka-Spengler et al., 2007). Stained embryos were photographed in 50% glycerol on a Zeiss Stemi SV11 microscope using AxioVision software (Release 4.6) and processed using Photoshop 7.0 (Adobe Systems).

Cryosectioning

To obtain transverse sections for histological analysis, embryos were equilibrated in 15% sucrose (in phosphate-buffered saline (PBS)) for 2 hours at room temperature, then transferred to 30% sucrose and incubated overnight at 4°C. Embryos were embedded in O.C.T. Compound (Tissue-Tek, catalog #4583) and frozen at -80°C. Sections 20 or 25 μm thick were obtained by cryosectioning at a

temperature of -23°C on a Microm HM550 cryostat. For imaging, slides were washed twice for 10 minutes in PBS with 0.1% Tween, rinsed in double-distilled water, and mounted with PermaFluor Mountant Medium (Thermo Electron Corporation, catalog #434990). Sections were imaged on a Zeiss Axioskop 2 Plus and processed as described for whole-mount images.

In situ mRNA probes

Many of the templates for mRNA probe synthesis were obtained from the BBSRC ChickEST Database (http://www.chick.umist.ac.uk). The following clones were used: Msx1 (ChEST900p21), Zic1 (ChEST459n6), c-myc (ChEST191o11), N-myc (ChEST895e1), AP-2α (ChEST765g1), and Irx1 (ChEST523e4). The other template plasmids used were: Pax7 (Basch et al., 2006), Dlx5 (Bhattacharyya et al., 2004), Dlx3 (Brown et al., 2005), Snail2 (Nieto et al., 1994), and FoxD3 (Kos et al., 2001). Linearized DNA was used to synthesize digoxigenin- and fluorescein-labeled antisense probes with Promega buffers and RNA polymerases (Promega Corp). RNA probes were purified with illustra ProbeQuant™ G-50 Micro Columns (GE Healthcare, product code 28-9034-08).

RESULTS

Here, we present a detailed analysis of the expression of ten transcription factors that are part of the putative neural crest gene regulatory network in chick embryos using whole-mount mRNA *in situ* hybridization. We compare their expression patterns across each stage of development from gastrulation (Hamburger and Hamilton (HH) stage 4) to cranial neural crest migration (HH stage 10; Hamburger and Hamilton, 1992).

HH4

The expression patterns of known neural plate border specifiers were compared with early expression domains of neural crest specifiers during chick gastrulation. Surprisingly, the results show that many neural crest specifiers are already present in the gastrula that and their distribution patterns are strikingly similar to those of canonical neural plate border specifiers. When compared at stage 4, these markers loosely group into three expression categories: 1, neural plate border and posterior epiblast; 2, neural plate, neural plate border, and anterior epiblast; and 3, non-neural ectoderm adjacent to and including part of the neural plate border.

Msx1 and *c-myc* fall into the first category. Similar to observations in *Xenopus* and zebrafish and previous work in the chick, we find that *Msx1* is expressed in posterior epiblast (ventrolateral ectoderm and mesodermal progenitors) and in the posterior and lateral edges of the neural plate (Fig. 2.1B,B'; Streit and Stern, 1999; Tribulo et al., 2003; Phillips et al., 2006). *c-myc* is also expressed at high levels in prospective mesoderm progenitors in the

posterior epiblast. Its anterior boundary of expression encompasses the neural plate border, similar to *Msx1* (Fig. 2.1C,C').

Zic1, *FoxD3*, *N-myc*, and *Dlx3* fall in the second category. *Zic1* is a known neural specifier that is also expressed in the neural plate border and in the anterior epiblast region which contains placodal progenitors (Fig. 2.1D,D'; Merzdorf, 2007). Interestingly, neural crest specifiers *FoxD3* and *N-myc* are also expressed during gastrulation in a domain remarkably similar to that of *Zic1*. Namely, *FoxD3* transcripts are present in anterior neural plate, where their rostral-most boundary of expression is adjacent to and slightly overlapping with that of *Dlx5*, the neural plate border and placodal specifier (Fig. 2.1F,F'; Fig. 2.3B). However, *FoxD3* does not overlap with *Msx1* in the posterior neural plate border (Fig. 2.3A). Some of the *FoxD3*-positive cells anterior to the node are likely notochord progenitors, since *FoxD3* functions in development of this structure at later stages (Odenthal and Nusslein-Volhard, 1998). However, *FoxD3* appears to be mainly restricted to the neural plate, as it does not overlap with ectodermal specifier *AP-2α* (data not shown). The oncogene *N-myc* is expressed at very high levels in the neural plate border, and to a lesser extent, in anterior epiblast surrounding the presumptive neural plate (Fig. 2.1E,E'). It overlaps in the neural plate border with *Msx1* (Fig. 2.3C). *Dlx3* is a known specifier of ectoderm and placode fates and also functions indirectly to position the neural plate border by repressing adjacent neural fates (Woda et al., 2003). Therefore, we were surprised to find low levels of chick *Dlx3* transcripts in a large swath of epiblast tissue encompassing the presumptive neural plate border and lateral portions of the prospective neural plate, suggesting an additional novel role for *Dlx3* in the chick. *Dlx3* transcripts are concentrated at higher levels in the anterior epiblast,

which contains the pre-placodal region (Fig. 2.1G,G'). In contrast, *Dlx3* in the frog is never expressed in the neural plate border (Luo et al., 2001b).

The third category of neural crest gene expression at stage 4 includes *Dlx5* and *AP-2α* (henceforth referred to as *AP-2*). We find that *Dlx5* is expressed during gastrulation in anterior epiblast adjacent to the neural plate border that contains the pre-placodal region, consistent with previously published frog and chick studies (Fig. 2.1H,H'; Yang et al., 1998; Luo et al., 2001b; McLarren et al., 2003; Woda et al., 2003; Bhattacharyya et al., 2004). Chick *AP-2* is expressed broadly throughout non-neural ectoderm at all axial levels (Fig. 2.1I,I'). It is co-expressed anteriorly with *Dlx5* in the pre-placodal region that is defined by *Irx1* expression (Fig. 2.3E,F). Surprisingly, *AP-2* transcripts also overlap in the posterior neural plate border with *Msx1* (Fig. 2.3D).

HH5

At stage 5, when the primitive streak begins to regress and leave notochord tissue in its wake, network genes become more clearly resolved at the neural plate border. *Msx1* is maintained in posterior epiblast but its expression at the neural plate border becomes more refined, and also begins to extend anteriorly (Fig. 2.1K). In the lateral and posterior portions of the neural plate border, *Msx1* expression domain is identical to that of the border specifier *Pax7*, which becomes upregulated at this stage (Fig. 2.1J,J'). *c-myc* is maintained in posterior epiblast and posterior neural plate border, but unlike *Msx1*, does not extend anteriorly (Fig. 2.1L). *Zic1* persists in anterior neural tissue and begins to accumulate more strongly at the edges of the neural plate (Fig. 2.1M). Likewise, *N-myc* expression is maintained in the neural plate and its border, where it

extends posteriorly as the embryo elongates (Fig. 2.1N). The expression domain of *Dlx3* is almost identical to that of *N-myc* (Fig. 2.1P). Conversely, *FoxD3* is no longer expressed in the neural plate or its border and is almost exclusively localized to the notochord (Fig. 2.1O). *Dlx5* and *AP-2* remain in the non-neural ectoderm, with *AP-2* marking ectoderm at all axial levels and *Dlx5* being concentrated anteriorly (Fig. 2.1Q,R).

HH6 and HH7

At stages 6 and 7, neural folds begin to thicken and elevate, allowing for better resolution of gene expression at their edges. During this time, *Pax7* is expressed exclusively in cells at the neural plate border caudal to the anterior prominence of the neural folds (Fig. 2.1S,S',BB). Likewise, *Msx1* becomes refined in the neural plate border both anteriorly (similarly to the *Dlx* genes) and posteriorly, and it is also maintained in open neural plate in the tail (Fig. 2.1T,T',CC). With progressive development, the neural plate closes anteriorly, while staying open at the caudal end of the embryo where the streak has not yet fully regressed. Gene expression at the open neural plate level recapitulates events that occur earlier at rostral levels. Expression of *c-myc* in the caudal open neural plate is markedly similar to *Pax7* and *Msx1*, but it is not expressed more anteriorly prior to the definitive appearance of the neural folds (Fig. 2.1U,U'). However at stage 7, very low levels of *c-myc* transcripts begin to accumulate in the anterior-most neural folds, becoming more distinct at later stages (Fig. 2.1DD). *Zic1* and *N-myc* are both maintained in the neural plate and upregulated at its edges, although *Zic1* becomes primarily restricted to the anterior neural folds (Fig. 2.1V,V',W,W',EE,FF). A stripe of enhanced *N-myc* expression is visible

in the region of the first forming somite at stage 7 (Fig. 2.1FF). *FoxD3* transcripts continue to mark the notochord, but also begin to accumulate at low levels in the anterior neural folds beginning at stage 6 (Fig. 2.1X,X',GG). *Dlx3* is expressed most prominently in the anterior neural ridge and placode region where it shares its domain with *Dlx5* (Fig. 2.1Y,Y',HH). Low levels of *Dlx3* remain in neural tissue at all axial levels. *Dlx5* and *AP-2* are expressed in ectoderm directly adjacent to the neural folds (Fig. 2.1Z,Z',AA,AA',II, JJ).

HH8

At the 3 to 6 somite stage (HH stage 8), neural folds are markedly elevated and begin to fuse anteriorly. At this time, most of the genes examined are co-expressed in the dorsal neural folds. *Msx1* and *Pax7* show almost identical expression in dorsal neural folds and border of the open neural plate (Fig. 2.2A,A',B,B'). Strong *Snail2* expression is present in the dorsal neural folds at the mid- and hindbrain level (Fig. 2.2C,C'). Likewise, *FoxD3* is recruited to the dorsal neural folds, where it is co-expressed in the mid- and hindbrain with *Snail2* and in the forebrain with *Zic1*, *N-myc*, and *c-myc* (Fig. 2.2D,D'). *Zic1* and *N-myc* have almost identical expression patterns in the anterior neural folds, though *N-myc* is also found in heart mesoderm and in posterior lateral plate mesoderm (Fig. 2.2E,E',F,F'). At this stage, we first see clear expression of *c-myc* in the anterior-most neural folds (Fig. 2.2G,G'). Intriguingly, its expression seems to be divided into two completely separate domains: anterior neural folds and posterior lateral plate mesoderm. The expression domain of *Dlx3* also resolves cleanly at this stage. It has disappeared from the neural folds and is expressed exclusively in the anterior neural ridge and surrounding ectoderm, where it is co-expressed

with *Dlx5* (Fig. 2.2H,H'). However, the *Dlx5* expression domain extends more caudally to the level of the hindbrain and medially into the lateral-most edge of the dorsal neural folds (Fig. 2.2I,I'). At this stage, *AP-2* transcripts are also recruited to the lateral edge of the neural folds (Fig. 2.2J,J').

HH9

At the 7 to 9 somite stage (HH stage 9) the neural folds have completely fused in the head, and neural crest precursors that arose from the neural plate border come to lie in the dorsal neural tube and begin to emigrate. Many of the neural plate border and neural crest specifiers now mark pre-migratory neural crest in the dorsal neural tube and emigrating cranial neural crest cells. The expression domains of *Msx1* and *Pax7* are identical (Fig. 2.2K,L), marking neural crest progenitors in the head, trunk and tail. *Snail2* and *FoxD3* also exhibit similar expression patterns in emigrating cranial neural crest and trunk dorsal neural tube (Fig. 2.2M,N). However, they are not expressed in the open neural plate like *Msx1* and *Pax7*. At this time, *Zic1*, *Dlx3*, and *Dlx5* expression patterns are similar; their transcripts are almost exclusively restricted to olfactory progenitors in the anterior forebrain (Fig. 2.2O,R,S). However, *Zic1* is additionally expressed in a specific stripe in the hindbrain, and *Dlx3* is present in cranial placogenic ectoderm and prospective otic placode. *N-myc* is maintained in anterior neural tissue at high levels, and is also expressed in lateral plate mesoderm at the level of the heart and in the tail (Fig. 2.2P). *c-myc* is expressed in the forebrain and in emigrating neural crest cells at the level of the midbrain, where its expression is highly similar to that of *Snail2* and *FoxD3*. It is additionally expressed in the blood islands (Fig. 2.2Q). Finally, at this stage *AP-2* is recruited to the dorsal

neural tube at the cranial and vagal trunk levels. Its transcripts also persist in non-neural ectoderm adjacent to the open neural plate (Fig. 2.2T).

HH10

At the 9 to 11 somite stage (HH stage 10), migrating neural crest cells can be identified by their characteristic "cobra hood" pattern in the head. Many neural crest specifiers are expressed in these cells, including *Snail2*, *FoxD3*, *c-myc*, and *AP-2* (Fig. 2.2W,W',X,X',AA,AA',DD,DD'). They are also maintained in pre-migratory trunk neural crest. Likewise, the neural plate border specifiers *Pax7* and *Msx1* persist in migrating cranial and pre-migratory trunk neural crest cells, suggesting a role in maintenance of neural crest traits (Fig. 2.2U,U',V,V'). However, the other specifier genes are excluded from neural crest at this stage and are instead expressed in other cell types such as placodes (*Zic1*, *Dlx3*, *Dlx5* (Fig. 2.2Y,BB,BB',CC,CC')) and neural tissue and somites (*Zic1* (Fig. 2.2Y,Y')). *N-myc* is also not expressed by migrating neural crest cells despite transcripts being concentrated in the dorsal neural tube (Fig. 2.2Z,Z'). It has been shown that *N-myc* plays a role in neural crest migration at much later stages (Wakamatsu et al., 1997).

DISCUSSION

Expression patterns of ten transcription factors that are members of the chick NC-GRN were compared between HH stages 4 to 10. We show that transcripts of most neural crest specifiers are already expressed in or around the presumptive neural plate border at gastrulation stages. Thus, this work challenges our current formulation of gene interactions within the chick NC-GRN. The remarkable similarities in expression patterns of neural plate border and neural crest specifiers at gastrulation suggests that regulatory events are occurring much earlier than previously thought. For instance, the shared expression domain of *Zic1* and *FoxD3* hints at a direct interaction between these two molecules at HH4. In addition, the overall similarity in expression of most specifiers at the neural plate border and in the dorsal neural tube support data from ongoing studies that demonstrate extensive cross- and auto-regulation between these genes. Importantly, comparison of NC-GRN specifier expression patterns as they are resolved throughout development lays crucial groundwork for functional studies aimed at understanding the interactions between these transcription factors. Namely, such comprehensive and comparative expression data provide key information on when and where genes should be inactivated or activated during functional studies. Finally, resolving the overlap between all of these molecules brings us closer to defining the "neural plate border" and the location of neural crest progenitors within it, which is summarized in Fig. 2.5A. Interestingly, there is strong conservation of early expression patterns of neural crest network genes between chick and *Xenopus* (Fig. 2.5B), suggesting that early

specification of neural crest progenitors is likely to be conserved across vertebrates.

While comparing the expression patterns of neural plate border and neural crest specifiers at each stage of early neural crest development, we found some interesting trends in terms of which genes are maintained and which are differentially expressed from stage to stage. For instance, the canonical neural plate border specifiers *Msx1* and *Pax7* are continuously expressed in neural crest progenitors from gastrulation to migration, suggesting a role in both induction and maintenance of other neural crest genes. In contrast, *Zic1*, *Dlx5*, and *Dlx3* are expressed in or near the neural plate border region at early stages but are later recruited to other regions of the embryo, such as neural tissue, placodes, and somites. This suggests that they play several spatiotemporally separable roles during development, only one of which is specific to neural crest.

Changes in expression patterns of neural crest specifiers are even more interesting. *N-myc* is maintained in neural crest progenitors throughout development like *Msx1* and *Pax7*, but it is also expressed in other areas of the embryo, such as neural, ectodermal, and mesodermal tissues. Being a proto-oncogene, *N-myc* is likely playing a role in proliferation and maintenance of all of these progenitor cell types throughout development. It is surprising, however, that *N-myc* is not expressed in migrating neural crest cells at HH10 since those cells proliferate extensively. In contrast, although *AP-2* is continuously expressed in the gastrula and neurula, it does not definitively appear in neural crest progenitors until HH9, when it is recruited to the dorsal neural tube. Its early role as an ectodermal specifier is highly conserved among chordates, but its recruitment to the dorsal neural tube is a vertebrate-specific event. It is likely that

this event in vertebrates has occurred as a result of the evolution of a novel crest-specific *AP-2* regulatory element that is distinct from the element(s) driving its expression in the ectoderm. We hypothesize that it may also have an earlier function in neural crest development by maintaining ectodermal fate and repressing neuronal markers, therefore contributing to the placement of the prospective neural plate border. It has been shown that the *Dlx3/5* genes function to position the neural plate border in this manner (McLarren et al., 2003; Woda et al., 2003). In addition, we have also found that *AP-2* transcripts overlap in a small portion of the posterior neural plate border, suggesting a more direct role in the formation of this region. Likewise, *Snail2* is not expressed in the neural plate border at HH4 but instead plays a role in epithelial-to-mesenchymal transition of ingressing mesoderm cells during gastrulation (Fig. 2.4A; Nieto et al., 1994). *Snail2* transcripts begin to accumulate in dorsal neural folds only around early HH8 (Fig. 2.4E,E'). Intriguingly, we find two very specific stripes of *Snail2*-positive mesodermal cells directly under the forming neural plate border at HH stages 5-8 (Fig. 2.4B,B',C,C',D, E, E''). We conjecture that that *Snail2* may also play an early role in neural crest specification by participating in a feedback loop to maintain neural plate border specifier expression via signals from underlying mesoderm. The expression pattern of *c-myc* is intriguing in that it is present in the neural plate border and mesoderm progenitors at gastrulation, but is then exclusively expressed in mesoderm until HH8, when it strikingly appears in the anterior neural folds. Likewise, *FoxD3* is expressed in the neural plate at HH4, after which it becomes restricted to the notochord and does not definitively re-appear in neural crest progenitors until HH8. This suggests that *c-myc* and *FoxD3* may play temporally distinct roles in specification and maintenance of cell fates.

These data are highly suggestive of the presence of distinct enhancer elements that drive expression of neural plate border and neural crest specifiers in temporally and spatially separable domains. Identification of such elements is key to elucidating the regulatory interactions between these genes as well as to providing insights into regulatory events that have facilitated neural crest evolution. In conclusion, these results represent an important first step in examining regulatory interactions between transcription factors in the NC-GRN and for comparative analysis with other species.

ACKNOWLEDGEMENTS

We thank Tatjana Sauka-Spengler, Sujata Bhattacharyya, Meyer Barembaum, and Jack Sechrist for their technical advice. This work was supported by NIH Grant number NS36585 to M.B.F.

Figure 2.1: Early expression of neural plate border and neural crest specifiers

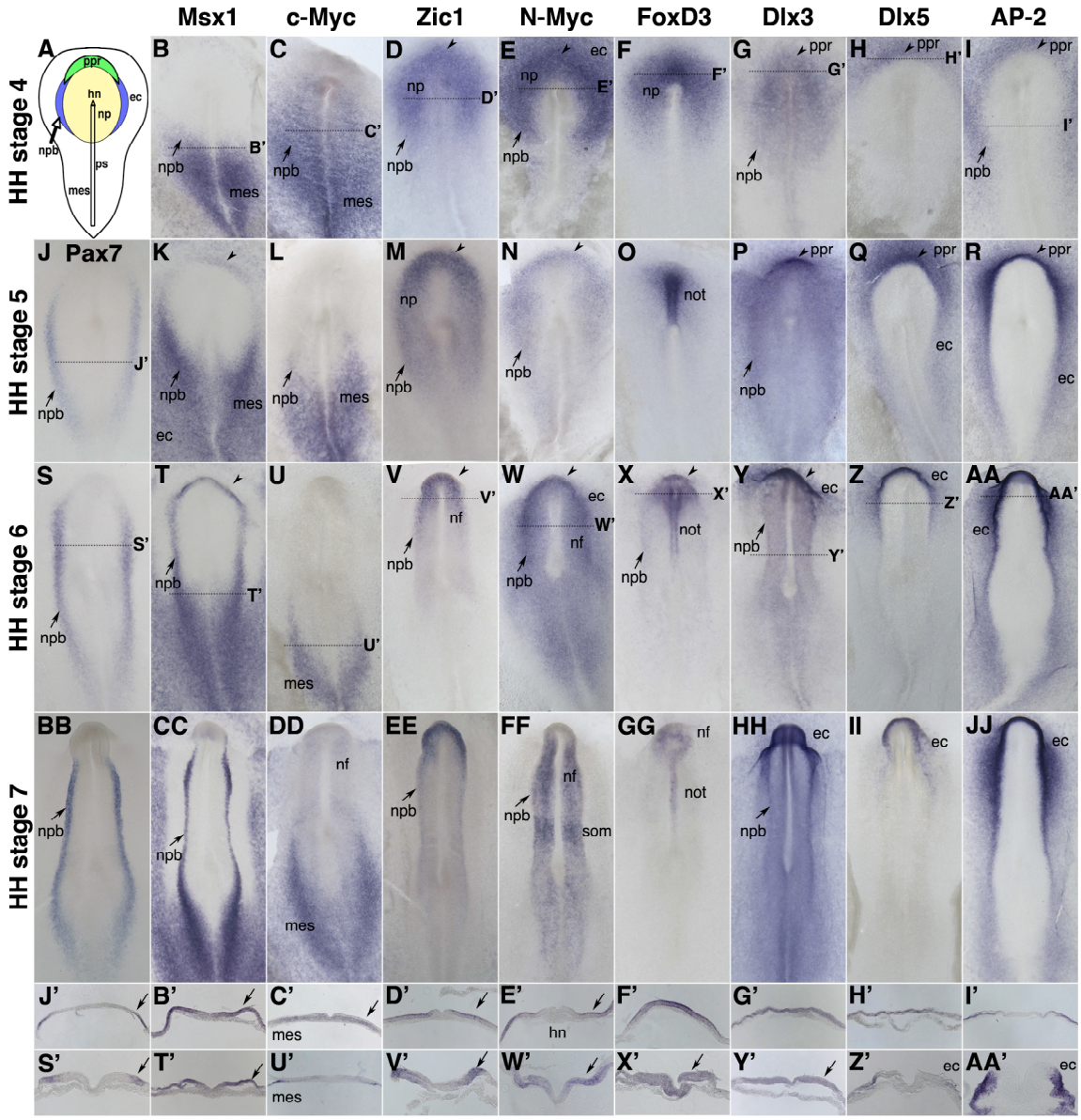

Figure 2.1. A-JJ: Neural plate border and neural crest specifier gene expression during early development. Hamburger and Hamilton (HH) stage 4 (**B-I**), HH5 (**J-R**), HH6 (**S-AA**) and HH7 (**BB-JJ**) embryos were analyzed by whole-mount *in situ* hybridization using digoxigenin (DIG)-labeled RNA probes for chick *Pax7* (**J, S, BB**), *Msx1* (**B, K, T, CC**), *c-myc* (**C, L, U, DD**), *Zic1* (**D, M, V, EE**), *N-myc* (**E, N,**

W, FF), *FoxD3* (**F, O, X, GG**), *Dlx3* (**G, P, Y, HH**), *Dlx5* (**H, Q, Z, II**), and *AP-2α* (**I, R, AA, JJ**). Transverse sections were performed on HH4 (**B'-I'**) and HH6 (**S'-AA'**) embryos as indicated. A rough schematic of a HH4 embryo showing the respective positions of the primitive streak, Hensen's node, neural plate, neural plate border, pre-placodal region, non-neural ectoderm, and mesodermal progenitors is shown in **A**. Gene expression at the neural plate border and pre-placodal region is indicated by arrows and arrowheads, respectively. Ec, non-neural ectoderm; hn, Hensen's node; mes, mesoderm; nf, neural fold; not, notochord; np, neural plate; npb, neural plate border; ppr, pre-placodal region; ps, primitive streak; som, somite.

Figure 2.2: Neural crest network gene expression during late neurulation

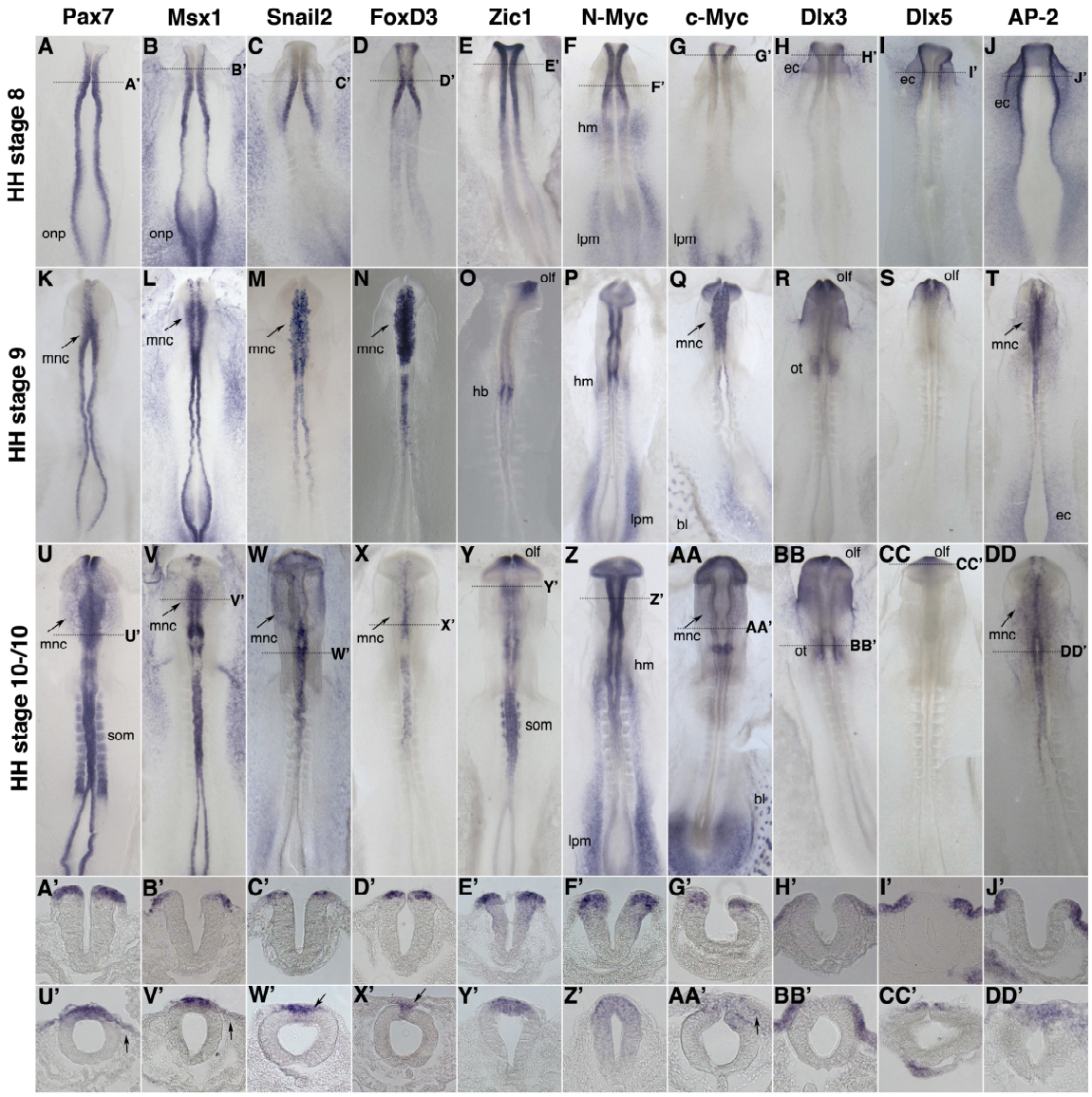

Figure 2.2. Neural plate border and neural crest specifier gene expression during neurulation and neural crest migration. HH8 (**A-J**), HH9 (**K-T**) and HH10-/10 (**U-DD**) embryos were analyzed by whole-mount *in situ* hybridization using digoxigenin (DIG)-labeled RNA probes for chick *Pax7* (**A**, **K**, **U**), *Msx1*, (**B**, **L**, **V**), *Snail2* (**C**, **M**, **W**), *FoxD3* (**D**, **N**, **X**), *Zic1* (**E**, **O**, **Y**), *N-myc* (**F**, **P**, **Z**), *c-myc* (**G**, **Q**,

AA), *Dlx3* (**H**, **R**, **BB**), *Dlx5* (**I**, **S**, **CC**), and *AP-2a* (**J**, **T**, **DD**). Transverse sections were performed on HH stage 8 (**A'-J'**) and HH stage 10 (**U'-DD'**) embryos as indicated. Gene expression in migrating neural crest cells is indicated by arrows. Bl, blood islands; ec, non-neural ectoderm; hb, hindbrain; hm, heart mesoderm; lpm, lateral plate mesoderm; mnc, migrating neural crest; olf, olfactory placode/pit; onp, open neural plate; ot, otic placode; som, somites.

Figure 2.3: Overlap of gene expression at the neural plate border

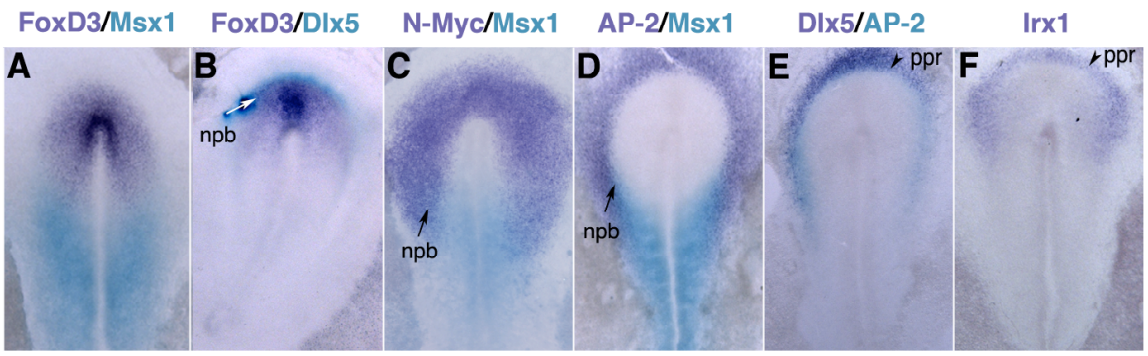

Figure 2.3. Co-expression of neural crest network genes in the chick gastrula. Stage HH4 or HH4+ embryos were analyzed by whole-mount double *in situ* hybridization using digoxigenin (DIG)- and fluorescein (FITC)-labeled RNA probes for chick *Msx1*, *AP-2α*, *FoxD3*, *N-myc*, *Dlx5*, and *Irx1*. **A.** Expression of *FoxD3* and *Msx1* is complementary. *FoxD3* (purple) is expressed in anterior neural plate while *Msx1* (blue) is expressed in posterior epiblast and neural plate border. **B.** *FoxD3* expression domain (purple) in the anterior neural plate border (arrow) lies adjacent to and slightly overlaps with pre-placodal marker *Dlx5* (blue). **C.** *N-myc* (purple) is co-expressed in the posterior neural plate border (arrow) with *Msx1* (blue). **D.** *AP-2* (purple) is co-expressed in posterior neural plate border (arrow) with *Msx1* (blue). **E.** *Dlx5* (purple) and *AP-2* (blue) are co-expressed in the pre-placodal region (arrowhead). **F.** Expression of the placodal marker *Irx1* at stage 4+ is shown for comparison with E. Npb, neural plate border; ppr, pre-placodal region.

Figure 2.4: *Snail2* expression during early development

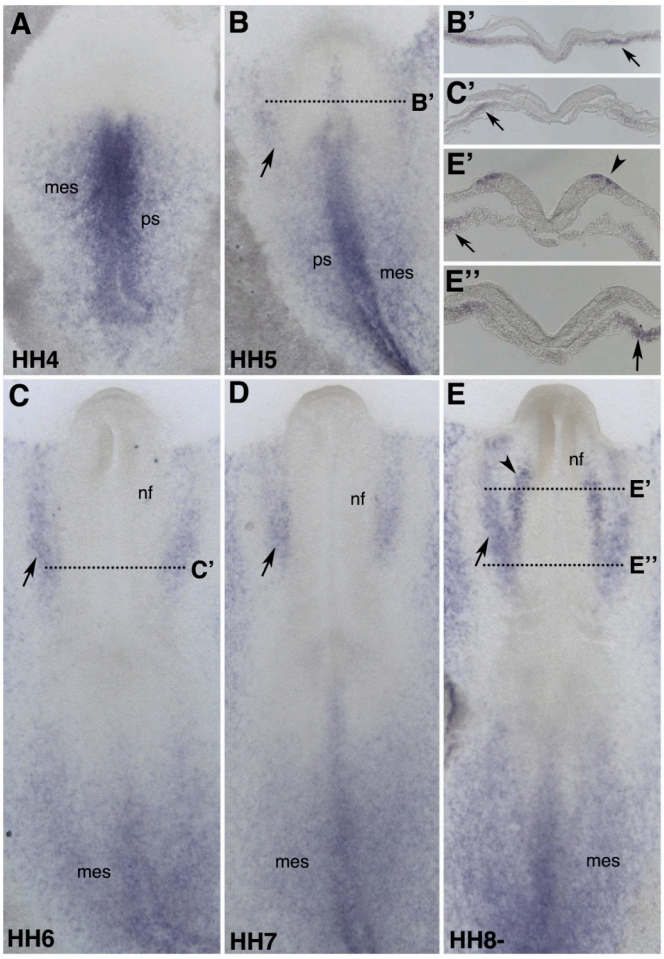

Figure 2.4. *Snail2* expression was examined in HH4-8- chick embryos by whole-mount *in situ* hybridization. **A.** At HH4 *Snail2* is expressed by mesodermal progenitors ingressing through the primitive streak. **B.** By HH5, two *Snail2*-positive stripes are observed in mesoderm beneath the neural plate border (**B′**). **C** and **D.** During HH6 and HH7, *Snail2* expression in mesoderm underlying the neural plate border becomes more obvious (**C′**). **E.** By early HH8, *Snail2* is upregulated strongly in dorsal midbrain neural folds (**E′**) and persists in the mesoderm (**E′′**).

Figure 2.5: Conservation of early neural crest gene expression in vertebrates

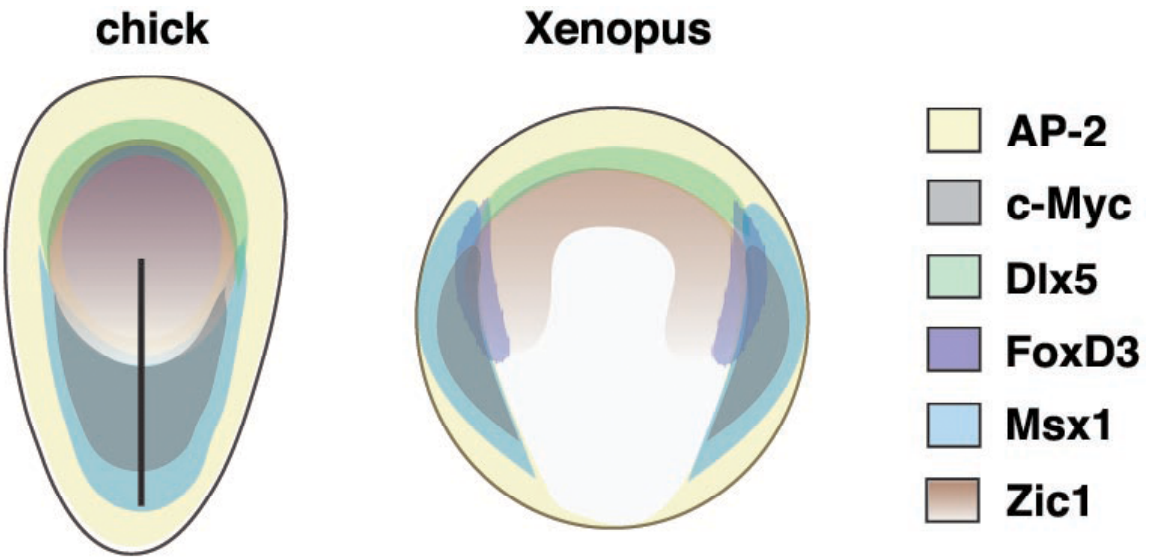

Figure 2.5. Schematic comparison of overlap in neural plate border and neural crest specifier expression domains during mid-gastrulation in chick and *Xenopus*. Expression of *AP-2* (yellow), *c-myc* (gray), *Dlx5* (green), *FoxD3* (purple), *Msx1* (blue) and *Zic1* (brown) are illustrated. During neurulation, expression of these genes overlaps in the neural plate border and dorsal neural tube in both organisms.

Chapter 3:

Regulation of Neural Crest Network Genes by Stem Cell Factor Bmi-1 During Early Chick Development

Jane Khudyakov, Tatjana Sauka-Spengler, and Marianne Bronner-Fraser

INTRODUCTION

The neural crest is a developmentally transient multipotent cell population that emigrates from the dorsal neural tube during neurula stages, migrates extensively throughout the body, and generates a diverse array of differentiated cell derivatives in a variety of target destinations (Le Douarin and Kalcheim, 1999). Neural crest cells are initially specified during gastrulation at the junction of the forming neural plate and non-neural ectoderm, as evidenced by the ability of gastrula-stage explants from this region to generate migratory neural crest cells autonomously in culture (Basch et al., 2006). However, neural crest cells do not differentiate *in vivo* until several days later, suggesting that multipotency is maintained for a significant period of their early development. In fact, back-transplantations and clonogenic assays have demonstrated that some multipotent neural crest cells continue to persist in targets such as the peripheral nerve, dorsal root ganglia, gut, and hair follicle, well into stages when neural crest-derived tissues were thought to be fully and irreversibly differentiated (Morrison et al., 1999; Crane and Trainor, 2006; Sieber-Blum and Hu, 2008). In addition, neuroblastoma tumors in pediatric patients are often neural crest-derived, suggesting that this cell type has the capacity to proliferate expansively and maintain a multipotent state that contributes to oncogenesis (Hemmati et al., 2003; Ross and Spengler, 2007). In light of these studies, the neural crest has been considered a type of stem cell, although some disagreement still exists as to whether it is strictly "stem" or "progenitor," since isolated neural crest populations often contain a combination of both multipotent and lineage-restricted cells (Crane and Trainor, 2006).

Characterizing molecular mechanisms and cues that specify neural crest cells, contribute to maintenance of their plasticity and proliferation, and instruct their lineage-specific fate restriction and differentiation have been subjects of much interest. A putative neural crest gene regulatory network has been proposed which suggests that distinct groups of signals regulate successive steps in neural crest formation (Meulemans and Bronner-Fraser, 2004). For instance, inductive signals are received during gastrulation in the form of diffusible growth factors that subdivide the ectoderm into neural plate and non-neural ectoderm, inducing a group of transcription factors at their junction that specify this region as the neural plate border. These neural plate border specifiers then induce a group of neural crest specifier genes in the dorsal neural folds during neurulation, which label these cells as pre-migratory neural crest (Aybar and Mayor, 2002; Gammill and Bronner-Fraser, 2003). In turn, the neural crest specifiers induce a group of effector genes that enable migratory behavior and differentiation into particular neural crest derivatives (Sauka-Spengler and Bronner-Fraser, 2008). However, we now know that these relationships are not linearly hierarchical. For instance, many neural crest specifiers are co-expressed with neural plate border specifier genes in the chick gastrula in similar spatiotemporal patterns (Khudyakov and Bronner-Fraser, 2009). Therefore, at a time when neural crest cells are thought to be receiving their first specification signals, they already express a combination of induction factors and specifiers of both neural plate border and neural crest fate. This observation suggests that instructive molecular cues are present very early in neural crest development and function in a manner that involves extensive regulatory interactions.

Despite the presence of multiple components of the NC-GRN in the neural plate border during early development, this region contains a heterogeneous and intermixed population of neural crest, placode, and dorsal neural tube precursors which are indistinguishable (Fernandez-Garre et al., 2002; Hong and Saint-Jeannet, 2007; Ezin et al., 2009). Even after neural tube closure, progenitors in the dorsal neural tube can contribute to both neural crest and neural tube derivatives, and it is not until the former undergo an epithelial-to-mesenchymal transition that they become bona fide neural crest cells (Bronner-Fraser and Fraser, 1988; Bronner-Fraser, 1998, 2002). Therefore, although a number of specification factors are expressed continuously throughout neural crest development, the progenitors receiving these signals remain uncommitted and multipotent for quite some time. We hypothesize that maintenance of the multipotent neural plate border progenitor and undifferentiated neural crest cell may require regulation of neural crest network genes by yet unknown repressive mechanism(s).

Global regulation of developmental genes mediated by the Polycomb Group (PcG) of epigenetic repressors has been proposed as one of the main mechanisms involved in maintenance of a stable stem cell state in mouse and human embryonic stem cells (ESC) (Boyer et al., 2006; Bracken et al., 2006; Lee et al., 2006). The Polycomb proteins were first identified in Drosophila over 30 years ago as repressors of homeotic genes, and have subsequently been shown to function in axial patterning in vertebrates in a similar manner (Lewis, 1978; van der Lugt et al., 1996). PcG first began to attract the attention of the stem cell community when several protein partners were found to repress negative regulators of the cell cycle, therefore promoting self-renewal and preventing

premature senescence of hematopoietic and neural stem cells (Jacobs et al., 1999a; Molofsky et al., 2003; Park et al., 2003). More recent studies have demonstrated that PcG proteins serve to maintain ESC in a pluripotent, undifferentiated state by repressing a vast number of transcription factors and signaling molecules involved in development and differentiation (Pietersen and van Lohuizen, 2008; Schwartz and Pirrotta, 2008).

The Polycomb Group consists of two large, separate, and sequentially acting protein complexes, each of which contains a set of core components necessary for repression, as well as a number of other interchangeable protein partners (see Fig. 1.2B, Chapter 1). The core components of Polycomb Repressive Complex 2 (PRC) include the methyltransferase Ezh, which catalyzes addition of three methyl groups to lysine 27 of histone H3 ($H3K27me^3$), a canonical mark of epigenetic repression. Chromodomain-containing protein partners of Polycomb Repressive Complex 1 (PRC1) subsequently recognize this methylation mark and the complex is recruited to the PRC2-associated target chromatin region (Schwartz and Pirrotta, 2007). The catalytically active PRC1 subunit Ring1B ubiquitinates histone H2A at lysine 119, which is thought to aid in stabilizing and maintaining PRC2-mediated repression (Wang et al., 2004; Cao et al., 2005).

While PcG binding sites or "Polycomb Repressive Elements" have been well characterized in *Drosophila*, analogous regions within vertebrate genomes have proven difficult to identify, although some correlations between CpG island distribution patterns and PcG binding have been made (Schwartz and Pirrotta, 2007; Ku et al., 2008). Recent whole-genome profiling studies of Polycomb binding by ChIP-on-Chip have demonstrated that core members of both complexes are associated with an impressive number of transcription factor

groups in stem cells and are often spread over chromatin regions several kilobases in size surrounding the coding regions of these genes (Bracken et al., 2006). As a general rule, PcG target genes, the majority of which represent key developmental regulators, remain transcriptionally silent until ESC are induced to differentiate, at which point the PcG is removed from chromatin and the genes are activated. Not surprisingly, ESC isolated from knockout mice lacking core PRC components differentiate prematurely in culture by inappropriately upregulating Polycomb target genes (Boyer et al., 2006; Lee et al., 2006).

Interestingly, PcG-associated chromatin regions are often marked not only by the repressive methylation mark H3K27me^3 but also by trimethylated lysine 4 (H3K4me^3), a mark of active transcription. These regions have been termed "bivalent" and are associated with genes that are "poised" to undergo a change in transcriptional activity upon differentiation (Bernstein et al., 2006; Ku et al., 2008). It therefore appears that the role of PcG in stem cell development is highly complex and involves maintenance of key developmental regulator genes in a transcriptionally plastic state that can be changed quickly upon reception of instructive signals. Moreover, Polycomb proteins are also necessary for proper cell differentiation because they repress "pluripotency" genes and regulators of alternative cell type pathways during lineage restriction (Pasini et al., 2007; Mohn et al., 2008). Therefore, the PcG proteins are critical regulators of embryonic development that fulfill a number of diverse functions, including (but probably not limited to) cell proliferation, maintenance of pluripotency, cell lineage restriction and differentiation, and axial patterning. Not surprisingly therefore, the Polycomb genes have been highly conserved throughout metazoan evolution (Whitcomb et al., 2007).

Due to the many similarities between ESC and neural crest progenitors, we hypothesized that Polycomb proteins may function analogously during neural crest development by repressing members of the NC-GRN. We chose to focus on PRC1 member Bmi-1 which has a well-studied role in proliferation and self-renewal of neural and hematopoietic stem cells (Park et al., 2004). Although it does not possess any enzymatic activity on its own, Bmi-1 has been shown to stimulate the ubiquitination activity of Ring1B and to maintain integrity of the PRC1 complex, possibly by acting as a tethering protein (Wang et al., 2004; Cao et al., 2005). In addition, ChIP studies have demonstrated that Bmi-1 associates with developmental regulator genes in embryonic stem cells, similarly to other PcG components (Bracken et al., 2006; Dietrich et al., 2007).

Chick *Bmi-1* was previously identified in a macroarray library screen and shown to be present throughout early chick development in a number of tissues, including the neural crest (Fraser and Sauka-Spengler, 2004). In this work, we demonstrate that *Bmi-1*, along with six other PcG genes, is expressed by neural crest progenitors from gastrulation until migration stages. Bmi-1 knock-down by *in vivo* antisense morpholino oligonucleotide electroporation results in an early upregulation of several neural crest network genes of the neural plate border and neural crest specifier categories in the absence of significant changes in cell proliferation within the dorsal neural fold. In contrast, combined over-expression of Bmi-1 and Ring1B in the early embryo results in a downregulation of the neural plate border specifier *Msx1*. Our results suggest that Bmi-1, as part of the PRC1 complex, negatively regulates expression of neural crest network genes during early chick development, possibly as a means of preventing premature

differentiation or modulating appropriate lineage restriction and cell fate decisions.

MATERIALS AND METHODS

Chick embryo incubation

Fertilized chicken eggs were obtained from AA Enterprises (Ramona, CA) and incubated at 38°C in a humidified incubator (Lyon Electric, Chula Vista, CA). Embryos were staged according to the Hamburger and Hamilton chick staging system (Hamburger and Hamilton, 1992).

In situ hybridization

Chick embryos were dissected in Ringer's solution and fixed in 4% paraformaldehyde at 4°C overnight. Whole-mount *in situ* hybridization was performed as described previously (Nieto et al., 1996; Xu and Wilkinson, 1998), with some modifications involving more extensive washing adapted from a lamprey *in situ* protocol (Sauka-Spengler et al., 2007). Stained embryos were photographed in 50% glycerol on a Zeiss Stemi SV11 microscope using AxioVision software (Release 4.6) and processed using Photoshop 7.0 (Adobe Systems).

In situ mRNA probes

The following DNA templates were used for antisense mRNA probe synthesis: cBmi-1 (Fraser and Sauka-Spengler, 2004), Pax7 (Basch et al., 2006), FoxD3 (Kos et al., 2001), Snail2 (Nieto et al., 1994), and Sox10 (McKeown et al., 2005). EST clones obtained from the BBSRC ChickEST Database (http://www.chick.umist.ac.uk) for use as *in situ* probe templates were the following: c-myc (ChEST191o11), Zic1 (ChEST459n6), AP-2α (ChEST765g1), Irx1

(ChEST523e4), Msx1 (ChEST900p21), Ring1B (ChEST852k8), Phc1 (ChEST49d22, ChEST764m2), Cbx2 (ChEST992K16), Cbx8 (ChEST636k11), Eed (ChEST78C3), and Suz12 (ChEST848N23). The HoxA2 clone was obtained from Peter Lwigale. Linearized DNA was used to synthesize digoxigenin- and fluorescein-labeled antisense probes with Promega buffers and RNA polymerases (Promega Corporation). RNA probes were purified with illustra ProbeQuant™ G-50 Micro Columns (GE Healthcare, Cat# 28-9034-08).

Cryosectioning

To obtain transverse sections for histological analysis, embryos were equilibrated in 15% sucrose (in phosphate-buffered saline (PBS)) for 2 hours at room temperature, then transferred to 30% sucrose and incubated overnight at 4°C. Embryos were embedded in O.C.T. Compound (Tissue-Tek, catalog #4583) and frozen at -80°C. Sections 14 to 20 μm thick were obtained by cryosectioning at a temperature of -23°C on a Microm HM550 cryostat. For imaging without subsequent immunostaining, slides were washed twice for 10 minutes in PBS with 0.1% Tween, rinsed in double-distilled water, and mounted with PermaFluor Mountant Medium (Thermo Electron Corporation, Cat# 434990). Sections were imaged on a Zeiss Axioskop 2 Plus microscope and processed as described for whole-mount images.

Antibodies and immunohistochemistry

The distribution of Bmi-1 and Ring1B proteins was examined using the following antibodies: Anti-Bmi-1, clone F6 mouse monoclonal IgG1 (1:200, Upstate, Cat#

05-637), Rabbit polyclonal to Bmi-1 (1:500, Abcam, ab38432), and mouse monoclonal Ring1B (1:2000, Atsuta et al., 2001). Whole chick embryos were fixed in 4% pa\raformaldehyde at 4°C overnight, washed in PBS containing 0.1% Tween-20 (PBTw), and incubated in blocking solution (5% goat serum in PBTw) for 2 hours at room temperature. Primary antibody was added in blocking solution and incubated at 4°C overnight, then washed with PBTw, and replaced with Alexa-Fluor 488 or 568 secondary antibody (1:500 in PBTw, Molecular Probes) and incubated overnight at 4°C. Embryos were then washed, mounted, and imaged on a Zeiss Axioskop 2 Plus microscope and processed using Photoshop 7.0 (Adobe Systems). Alternatively, after the primary antibody step embryos were washed in 0.5% hydrogen peroxide in PBTw for 45 minutes, rinsed with PBTw, and incubated with biotin-labeled secondary antibody (1:750 in PBTw, Jackson Labs, Cat# 715-065-150, 711-065-152) overnight at 4°C. Following PBTw washes, embryos were incubated with 1:750 ABC reagent overnight at 4°C (Vectastain ABC kit, Vector Laboratories, Cat# PK-4000). After several PBTw washes, immunostaining was developed using 0.1 mg/mL DAB reagent in PBTw with 0.01% hydrogen peroxide and 0.001% NiCo (Sigma Fast 3.3 Diaminobenzidine Tablet Sets, Sigma, Cat# D-4293). Embryos were then washed with PBS containing 0.2% sodium azide, rinsed in PBTw, mounted, and imaged as described above. Fluorescent immunostaining on sections was performed using a similar protocol as described for whole-mount and the following primary antibodies: rabbit anti-phospho-histone H3 (1:2000, Upstate, Cat# 06-570), anti-HNK-1 (1:50, American Type Culture Collection Hybridoma), anti-GFP rabbit IgG fraction (1:500, Molecular Probes, Cat#A11122), anti-

HuC/HuD neuronal protein (human), mouse IgG_{2b} (1:500, Invitrogen, Cat#A-21271). Sections were incubated with 0.001% DAPI in PBTw for 5 minutes, rinsed with PBTw, and mounted with PermaFluor Mountant Medium (Thermo Electron Corporation, Cat# 434990). Sections were imaged on a Zeiss Axioskop 2 Plus microscope and processed as described for whole-mount images.

Morpholino design and specificity assay

3′-lissamine-labeled antisense cBmi-1 morpholino oligonucleotides were designed according to manufacturer's criteria (Gene Tools, LLC) as follows: Bmi-1 MO1: 5′-TTTTGATCCTGGTCGTCCGGTGCAT-3′, Bmi-1 MO2: 5′-GTCGTCCGGTGCATTTTGGCGCGGG-3′. The following 3′-lissamine-labeled 5 base pair mismatch cBmi-1 morpholinos were designed as negative controls: Control MO1: TTTTcATCgTGGTgGTCCcGTcCAT-3′, Control MO2: 5′GTCcTCCGcTGgATTTTGGaGCcGG-3′ (mutated bases shown in lower case). A 3′ lissamine-labeled standard control MO (5'-CCTCTTACCTCAGTTACAATTTATA-3') provided by Gene Tools was also used in control experiments. Morpholinos were dissolved in sterile water to a working concentration of 1 mM for chick embryo injection. A *Xenopus laevis* oocyte *in vitro* translation system was used to evaluate MO specificity. Fertilized *Xenopus laevis* embryos at the 1- to 2-cell stage were co-injected with 100 pg of *cBmi-1* mRNA containing a C-terminal myc tag and 10 ng of either Bmi-1, mismatch, or standard control MO. Prior to injection, morpholinos and RNA were combined and incubated at 37°C for 30 minutes to confirm that RNA does not degrade in these conditions. Injected *Xenopus* embryos were collected at gastrula stage and lysed in protein extraction buffer (50mM Tris, 100mM NaCl, 5mM EDTA and 1%

NP-40). Yolk was cleared from protein samples by extraction with an equal volume of Freon (1,1,2-Trichloro 1,2,2 trifluoroethane, Spectrum Laboratories Inc.) and resolved on a 12% SDS-PAGE gel. Anti-myc antibody was used for immunoblotting at 1:2000 concentration (9E10, Santa Cruz Biotechnology, Inc).

Electroporation

HH stage 3-5 chick embryos were explanted on Whatman filter paper rings and placed ventral-side up in Ringer's solution in an electroporation dish containing a platinum plate electrode on the bottom of a shallow well. Bmi-1 or control morpholinos at 1mM concentration were unilaterally injected into the lumen between the epiblast and vitelline membrane targeting the prospective neural plate border. The embryo was covered with a flattened-tip platinum electrode and five 7-volt, 50-millisecond pulses with 100 millisecond pauses in between were applied using a square-pulse electroporator. Embryos were cultured in thin albumin in a humidified 37°C incubator. After 6-24 hours, embryos were fixed in 4% paraformaldehyde for analysis by *in situ* hybridization and subsequently dehydrated to 100% methanol, or dissected and lysed in 100 µL of RNAqueous®-Micro Lysis Buffer (Ambion, Cat# AM1931) for RT-QPCR assay.

Over-expression constructs

Using a high fidelity enzyme (Expand High FidelityPLUS PCR System, Roche, Cat# 03300242001), the open reading frame including endogenous Kozak sequence was amplified using the full-length Bmi-1 clone obtained previously from a chick cDNA library screen as a template (Fraser and Sauka-Spengler,

2004). The resulting fragment was cloned into several expression vectors: pCIG-IRES-GRP (pCIG-Bmi-1-GFP), pCIG-H2B-GFP (pCIG-Bmi-1-H2B-GFP), and pCIG-H2B-RFP (pCIG-Bmi-1-H2B-RFP). Full-length Ring1B was obtained by screening a chick cDNA library using a Ring1B EST clone (ChEST852k8, BBSRC ChickEST Database http://www.chick.umist.ac.uk) (Gammill and Bronner-Fraser, 2002). Similarly, the Ring1B ORF with Kozak sequence was cloned into several expression vectors: pCIG-IRES-GRP (pCIG-Ring1B-GFP), pCIG-H2B-RFP (pCIG-Ring1B-H2B-RFP), and pCIG-mem-RFP (pCIG-Ring1B-memRFP (RFP with a membrane linker)). Maxi preps were prepared using the Qiagen EndoFree Plasmid Maxi Kit (Qiagen, Cat# 12362) and DNA was re-suspended in Buffer EB (Qiagen, Cat# 19086). Plasmids were further diluted to a concentration of 2 to 5 μg/μL with Buffer EB and 0.01% Blue Vegetable Dye (FD&C Blue 1, Spectra Colors Corp, Cat# 3844-45-9) for injection into chick embryos as described for morpholinos. Empty vectors were used as electroporation controls.

RNA and cDNA preparation

Total RNA from electroporated embryos was isolated using the RNAqueous®-Micro Lysis Kit (Ambion, Cat# AM1931). Genomic DNA was digested using TURBO DNA-*free*™ (Ambion, Cat# AM1907) according to manufacturer's protocol with the exception of extended digestion time and increased quantity of enzyme. Clean total RNA was precipitated and concentrated and cDNA was synthesized using random hexamers and SuperScript® II Reverse Transcriptase (Invitrogen, Cat# 18064-022) according to the manufacturer's instructions.

QPCR

QPCR was performed using the 96-well plate ABI 7000 QPCR machine (Applied Biosciences) with SYBRGreen iTaq Supermix with ROX (Bio-Rad, Cat# 172-5101). Primers were used at 450 nM concentration in a 25 μL reaction. Gene-specific primers were designed using the Primer 3 program (http://frodo.wi.mit.edu) and synthesized by IDT. The sequences of primers used are as follows: Msx1 F 5′- GGAACTGTGGCAGAGAAAGG-3′, Msx1 R 5′-ATGGCCACAGGTTAACAGC-3′, Pax7 F 5′-ACTGCGACAAGAAGGAGGAA-3′, Pax7 R 5′-CTCTTCAAAGGCAGGTCTGG-3′, FoxD3 F 5′-TCTGCGAGTTCATCAGCAAC-3′, FoxD3 R 5′-TTCACGAAGCAGTCGTTGAG-3′, Sox9 F 5′-CTCAAGGGCTACGACTGGAC-3′, Sox9 R 5′-CTTCACGTGGGGTTTGTTCT-3′, Gapdh F 5′-GGACACTTCAAGGGCACTGT-3′, Gapdh R 5′-TCTCCATGGTGGTGAAGACA-3′. Each sample was run in three replicates to reduce errors created by pipetting. The baseline and threshold levels were set according to the Applied Biosystem software, and gene expression was calculated by the standard curve assay method as described in the Applied Biosystems protocols. In detail, the results for different samples were interpolated from a line created by running four point standard curves for each primer set and then normalized against results for the *Gapdh* housekeeping gene. The standard cDNA was prepared from chick embryos collected during stages when all the target genes are known to be expressed in measurable quantities. Each plate also held two minus RT controls for each set of primers, which showed no amplification. Fold amplification was calculated as the ratio of

normalized expression levels between the electroporated and control sides of the same embryo.

RESULTS

Bmi-1 is expressed in neural crest progenitors during gastrulation

The expression pattern of chick *Bmi-1* during early development was characterized in detail by whole-mount *in situ* hybridization using a full-length antisense RNA probe (Fraser and Sauka-Spengler, 2004). During early gastrulation (Hamburger and Hamilton (HH) stage 3c, Hamburger and Hamilton, 1992), *Bmi-1* is expressed ubiquitously and at low levels throughout the epiblast (Fig. 3.1A). As gastrulation proceeds, *Bmi-1* transcripts begin to accumulate at the presumptive neural plate border, both posteriorly and anteriorly, and are also maintained at lower levels in the prospective neural plate (Fig. 3.1B and C). *Bmi-1* is restricted to the ectodermal cell layer at HH4 (Fig. 3.1C,C'). *Bmi-1* expression during gastrulation was compared to early expression domains of several neural plate border and neural crest specifier genes. *Bmi-1* is expressed in the neural plate border in a domain similar to that of *Pax7* at HH4+ (Fig. 3.1D). However, *Pax7* is specific to cells in the presumptive neural plate border whereas the expression domain of *Bmi-1* is wider, more closely resembling that of *N-myc* (Fig. 3.1E). *Bmi-1* expression is restricted to the neural plate and its border, similarly to *Zic1*, and does not extend into non-neural ectoderm (Fig. 3.1F).

Bmi-1 expression in the neural plate border at HH4 was further characterized by double *in situ* hybridization. We find that it is co-expressed in the posterior neural plate border with *Msx1* (Fig. 3.1G). Anteriorly, *Bmi-1* is co-expressed with the placodal marker *Irx1* (Fig. 3.1H). It is excluded from non-neural ectoderm marked by *Dlx5* and *Msx1* (Fig. 3.1G and I). Therefore, we find

that chick *Bmi-1* is expressed by progenitors of neural, neural plate border, and placode fates during gastrulation.

***Bmi-1* is maintained in undifferentiated neural crest progenitors**

Bmi-1 transcripts persist in neural crest and neural tube progenitors during neurulation and neural crest migration. *Bmi-1* is expressed in and around the neural plate border at HH5 (Fig. 3.2A). During HH6, when neural folds begin to thicken, *Bmi-1* is expressed throughout the neuroepithelium and is obvious at the neural plate border (Fig. 3.2B,B'). Expression is highest during HH7 and HH8 in the anterior-most neural folds marked by *Zic1*, *c-myc*, and *N-myc* that do not generate neural crest cells (Fig. 3.2C,D; also see Fig. 2.2, Chapter 2). *Bmi-1* transcripts accumulate in the dorsal portion of the neural folds at HH8 (Fig. 3.2D'). After neural tube closure, *Bmi-1* marks pre-migratory neural crest cells in its dorsal aspect, as well as migrating neural crest cells (Fig. 3.2E,F,F',F'').

Bmi-1 protein can be detected as early as HH3 and is localized in essentially the same domain as mRNA at these stages, suggesting that Bmi-1 is actively translated in neural crest progenitors during early development (Fig. 3.3A-F). *Bmi-1* transcript expression is maintained in migrating neural crest cells until they reach their target tissues and begin to express markers of differentiation. For instance, HuC/D-positive neural crest-derived neurons in cranial ganglia do not express *Bmi-1* (Fig. 3.2G,G',G'',H,I). However, *Bmi-1* persists in other regions of the embryo that are not populated by neural crest, such as brain neuroectoderm and dermamyotome, suggesting additional functions in development of other cell types (Fig 3.2G). In conclusion, transcript and protein expression data demonstrate that undifferentiated neural crest

progenitors are marked by Bmi-1 until they populate their target tissues and commence a terminal differentiation programme.

Multiple members of PRC1 and PRC2 are expressed in neural crest progenitors in overlapping domains

Bmi-1 functions as part of a large two-part protein complex, in which the presence of a set of "core" PRC2 and PRC1 partners is necessary for functional repression of target genes (Schwartz and Pirrotta, 2007). Therefore, we hypothesized that a number of other PcG genes may be co-expressed with *Bmi-1* in neural crest progenitors. Indeed, we find that transcripts of four PRC1 genes (*Ring1B*, *Phc1*, *Cbx2*, *Cbx8*) and two PRC2 genes (*Eed*, *Suz12*) are expressed in overlapping, but not identical domains during early neural crest development. During gastrulation (HH4/4+), *Cbx2* and *Eed* are expressed ubiquitously throughout the epiblast (Fig. 3.4C,E). In contrast, *Ring1B*, *Cbx8*, and *Suz12* are localized more specifically in the anterior epiblast corresponding to the prospective neural plate (Fig. 3.4A,D,F). *Phc1* exhibits the most specific expression pattern in the neural plate border, which is strikingly similar to that of *N-myc* (Fig. 3.4B) (Khudyakov and Bronner-Fraser, 2009). During neurulation (HH6-7) all six genes examined are expressed in the neural folds. *Ring1B*, *Cbx2*, *Eed*, and *Suz12* are expressed in neural tissue at all axial levels (Fig. 3.4G,I,K,L), whereas *Phc1* and *Cbx8* are mainly restricted to the anterior neural folds (Fig. 3.4H,J). In addition, *Ring1B*, *Cbx2*, *Eed*, and *Suz12* are expressed in anterior non-neural and non-placogenic ectoderm, and *Phc1* is distributed widely throughout ectoderm and area opaca at all axial levels. Strikingly, at HH8, all six genes are strongly expressed similarly to *Bmi-1* in the anterior-most neural folds, which fail

to generate neural crest (Fig. 3.4M-R). Transcripts also overlap in the open neural plate and lateral plate mesoderm. *Phc1* is the sole member maintained in the area opaca (Fig. 3.4N). During HH10, we find that all of the PcG genes examined are expressed in migrating cranial neural crest cells, trunk neural tube, and open neural plate, as well as in mesodermal and ectodermal tissues (Fig. 3.4S-X). In summary, we find that a number of PRC1 and PRC2 genes are expressed by neural crest progenitors during early development. Although their expression domains are broad, we were surprised to find that they are not ubiquitous, as might be assumed for catalytically active PcG genes that are critical for embryonic development (such as *Ring1B*), and for members of the upstream PRC2 complex (Voncken et al., 2003; Pasini et al., 2004). Although *Phc1* is the only gene with unique and specific expression in the neural plate border, all of the PRC expression domains examined encompass this territory, and all are also co-expressed in migrating cranial neural crest cells around HH10.

Bmi-1 knock-down results in early upregulation of the neural crest network genes

Msx1 is specifically upregulated as a result of Bmi-1 MO electroporation

To examine the role of Bmi-1 in early development of neural crest, we used a morpholino oligonucleotide-based loss-of-function approach. We designed two morpholinos (MOs) targeting the ATG context of chick *Bmi-1* and find that, when co-injected with myc-tagged *Bmi-1* mRNA into *Xenopus* embryos, they inhibit Bmi-1 protein translation (Fig. 3.5I). We used these two MOs interchangeably in our experiments. MO electroporation was performed at HH stage 4 to target the prospective neural plate border region in one half of the

chick gastrula. Electroporated embryos were cultured in albumin until HH6-8 and analyzed by *in situ* hybridization. We find that Bmi-1 knock-down results in a consistent increase of *Msx1* transcripts in dorsal neural tube progenitors, visualized as an increase in staining intensity within its endogenous expression domain on the electroporated side (Fig. 3.5A,A',B,B',C,D,G, n=12/18 embryos, $p<0.01$), which is not seen with control MO (Fig. 3.5E,E',F,F',G, n=2/13 embryos). Phenotypes range in severity and include a slight enhancement of staining along the AP axis of the embryo (Fig. 3.5D, n=5/18), or a strong increase in staining intensity within the neural fold edge and/or at the open neural plate (Fig. 3.5B, n=7/18). The effect is more discernable when electroporated embryos are analyzed at younger stages, and is often strongest within the open neural plate, suggesting that Bmi-1 may have an early role in regulating *Msx1*, and/or that the neural crest population is able to compensate for the MO effect as development proceeds. Interestingly, although the MO was often distributed throughout the whole proximo-distal aspect of the neural fold and the laterally adjacent ectoderm, ectopic expression of *Msx1* was never observed outside of the neural plate border, suggesting that Bmi-1 may act on *Msx1* specifically within this cell population.

We analyzed the effect of Bmi-1 MO on expression of several other neural plate border and neural crest specifier genes. We were unable to detect a statistically significant change in expression of the neural plate border specifier *Pax7* (n=3/13 weak upregulation). Likewise, preliminary *in situ* hybridization analysis did not suggest an effect of Bmi-1 MO on *Zic1*, *c-myc*, or *AP-2* expression. It is likely that while we do not observe a visible change in expression of these genes on the electroporated side of the embryo due to their

wide expression domains (as compared with *Msx1*), the transcript levels may be quantitatively altered. Alternatively, Bmi-1 may be regulating some neural crest network genes selectively.

The effects of Bmi-1 MO on neural crest specifiers are non-specific during late neurulation

In contrast to the effect on *Msx-1*, results of Bmi-1 knockdown on neural crest specifier genes during late neurulation stages were inconsistent. For *Snail2* and *FoxD3* expression, some Bmi-1 MO-electroporated embryos showed either a distinct anterior expansion or an anterior loss or general decrease on the electroporated side when analyzed at HH stage 8+/9, but which was not statistically significant (*Snail2*: n=6/17 upregulation, n=5/17 downregulation; *FoxD3*: n=4/11 downregulation, data not shown). A small number of control MO-electroporated embryos also exhibited non-specific effects when assayed for *FoxD3* (n=2/9) and *Snail2* (n=2/7) expression (data not shown). The Bmi-1 MO effect is most likely not secondary to changes in axial patterning because preliminary data suggest that expression of *HoxA2* may be unaltered (data not shown), which we found surprising in light of the role of Bmi-1 in homeotic repression in other organisms, although effects on other antero-posterior (AP) patterning genes were not examined (Lewis, 1978; van der Lugt et al., 1996; Cao et al., 2005). We hypothesize that these aberrant changes in gene expression may be secondary to the effect of Bmi-1 knock-down on the upstream specifier *Msx1* and possibly other unknown repressors or activators, as well as due to extensive cross-regulation between the neural crest specifiers (Gammill and Bronner-Fraser, 2002; Meulemans and Bronner-Fraser, 2004; Raible, 2006).

However, a large proportion of Bmi-1 MO-electroporated embryos assayed at late neurulation stages displayed no obvious phenotype (n=6/11 *FoxD3*, n=6/17 *Slug*, data not shown). In addition, condensation of ganglia and cranial and trunk neural crest migration patterns did not appear visibly altered in electroporated embryos assayed for *Sox10* and HNK-1 expression at later stages of development (data not shown). Because the neural crest is highly plastic and self-regulating as a cell population, examining effects of gene perturbations at later stages of development can be difficult due to extensive compensation (Le Douarin, 2004; Raible, 2006). Therefore, we can conclude from our analysis that the neural plate border specifier *Msx1* is negatively regulated by Bmi-1 during early neural crest development. However, we are unable to assess by *in situ* hybridization the later effects of Bmi-1 knock-down on downstream specifier genes and later events in neural crest migration and differentiation due to the extensive cross-regulatory relationships between such genes and the highly plastic and compensatory nature of this cell population.

Msx1, FoxD3, and Sox9 transcripts are quantifiably increased by Bmi-1 knock-down at HH6

To quantify changes in transcript levels as a result of Bmi-1 knock-down, we used real-time quantitative RT-PCR. HH4 embryos were electroporated with either Bmi-1 MO or control MO and cultured until HH6-10. Embryos collected at specific stages were then laterally bisected to separate the electroporated and control sides, followed by extraction of total RNA and cDNA synthesis from each embryo half. Real-time quantitative PCR was performed to compare changes in expression levels of several neural crest network genes between the control and

electroporated halves within the same embryo. In agreement with the *in situ* hybridization data, there is a twofold increase in *Msx1* expression in Bmi-1 MO-electroporated embryos assayed at HH6 (Fig. 3.6A,E, n=5, $p<0.01$). The fold change in transcript levels due to Bmi-1 knock-down is reduced or unchanged in embryos analyzed at later stages, likely due either to compensation by the neural crest population or dilution of MO as cells proliferate (Fig. 3.6A).

Similarly to *in situ* hybridization results, there is no significant change in *Pax7* (Fig. 3.6B) or *Sox10* (data not shown) expression with Bmi-1 MO. Changes in *Snail-2* expression are inconsistent, similar to *in situ* results, perhaps due to complex cross-regulatory interactions between the two genes and other neural crest specifiers (data not shown; Meulemans and Bronner-Fraser, 2004; Bermejo-Rodriguez et al., 2006; Sakai et al., 2006). In contrast, there is a greater than twofold increase in *FoxD3* (Fig. 3.6C,F, n=5, $p<0.05$) and *Sox9* (Fig. 3.6D, n=4, $p<0.01$) expression, respectively, in Bmi-1 MO-electroporated embryos collected at stage HH6, an effect that is difficult to discern by *in situ* hybridization due to low expression levels at this stage. As with *Msx1*, we do not see a significant effect on *FoxD3* and *Sox9* expression when we assay electroporated embryos at later developmental time points (Fig. 3.6C,D). This observation suggests that Bmi-1 also negatively regulates the neural crest specifiers *FoxD3* and *Sox9*, perhaps by preventing their early induction, upregulation or recruitment to the dorsal neural folds. Thus, quantification of transcript levels by real-time PCR is extremely sensitive and allows for detection of gene expression changes during early stages at which they are difficult to detect by *in situ* hybridization, and before phenotypic compensation occurs.

Upregulation of neural crest genes due to Bmi-1 MO occurs in the absence of changes in cell proliferation in the dorsal neural folds

Next, we investigated whether upregulation of neural crest network genes caused by Bmi-1 MO is the result of an increase in cell proliferation. We found a 19% increase in the mean number of phospho-histone H3 (PH3)-positive cells on the Bmi-1 MO-electroporated as compared to the control side in sections of six embryos which showed obvious upregulation of *Msx1* by *in situ* (Fig 3.5H, n=6, $p<0.05$). However, the effect was most often observed in adjacent non-neural ectoderm or within the lumen of the neuroepithelium, as opposed to the *Msx1*-positive dorsal aspect of the neural fold (Fig. 3.5A',B'). In contrast, we did not find a significant change in the number of PH3-positive cells in sections of four control MO embryos (Fig. 3.5E',F',H). In addition, we did not observe a decrease in cell proliferation or an abundance of pyknotic nuclei on the Bmi-1 MO-electroporated side in three embryos which showed a drastic decrease of *FoxD3* at HH8-9 (data not shown).

Therefore, although Bmi-1 transgenic mice exhibit strong defects in proliferation and cell survival, we did not observe a similar effect on progenitor cells within the dorsal neural fold and dorsal neural tube of HH6-9 chick embryos with *in vivo* Bmi-1 knock-down (Molofsky et al., 2003; Park et al., 2003). This is likely due to low penetrance of electroporated MO knock-down as compared with the mouse knockout system, as well as the fact that neural crest progenitors do not proliferate extensively until they begin migration, a time during which Bmi-1 may be acting more specifically on their cell cycle. Consequently, we conclude that Bmi-1 may act to regulate early transcription of neural crest network genes independently of changes in the cell cycle, possibly

by restricting the number of cells within the heterogeneous neural plate border population that express these genes and that are recruited as dorsal neural tube progenitors.

Co-over-expression of Bmi-1 and Ring1B causes a decrease in *Msx1* expression

We next performed the reciprocal experiment whereby Bmi-1 was overexpressed in the embryo under the control of the constitutively active chick beta-actin promoter (pCIG) to determine whether a large increase in Bmi-1 protein may enhance its repressive effect on neural crest genes. Although we did not examine large numbers of embryos, no significant or consistent change in expression of *Msx1* (n=6), *FoxD3* (n=4), or *HoxA2* (n=4) was observed when pCIG-Bmi-1-GFP was overexpressed at HH4 and embryos were subsequently assayed at stages ranging from HH6 to HH11. In addition, preliminary results suggest that there is no effect on *Snail2* and *Sox10* expression levels by *in situ* hybridization (data not shown). In order to determine whether over-expression of Bmi-1 may affect neural crest migration or contribution to sensory ganglia, we electroporated pCIG-Bmi-1-GFP into the neural fold on one side of the embryo at HH8 and cultured the embryos until HH13-17. We found that GFP-positive cells emigrated normally from the dorsal neural tube, migrated along unaltered pathways, expressed *Sox10* and HNK-1, contributed to cranial and dorsal root ganglia, and did not exhibit a change in cell proliferation (data not shown). However, we were unable to assess whether neural crest differentiation within the ganglia was affected by Bmi-1 over-expression due to the difficulty of culturing embryos to older stages, dilution of the electroporated construct with

cell division, and the highly self-regulating nature of the neural crest cell population.

In addition to the obstacles described above, it is also unlikely that over-expression of one member of a large protein complex would exhibit a significant increase in the functionality of the complex and a consequent effect on neural crest development. In accordance with this, over-expression of Ring1B alone had no effect on *Msx1* expression (data not shown). Therefore, we decided to co-electroporate pCIG-Bmi-1-GFP together with pCIG-Ring1B-memRFP (RFP with a membrane linker) at high concentrations into the prospective neural plate border at HH4, which resulted in an overabundance of translated Bmi-1 and Ring1B proteins by HH6 (Fig. 3.7A,B). Embryos co-electroporated with Bmi-1 and Ring1B exhibited a statistically significant decrease in *Msx1* staining intensity at HH6-8 (Fig. 3.7C,D,E, n=9/18, $p<0.05$) that was not observed in embryos electroporated with the empty control vector (Fig. 3.7F,G,E, n=2/17). However, expression of *FoxD3*, *Snail2*, or *Sox10* was unaffected when assayed at later stages (data not shown). This suggests that Bmi-1 cooperates with Ring1B to negatively regulate *Msx1* during early neural crest development. However, the effects on other, later-acting neural crest network genes were difficult to discern. Over-expression of at least three PcG genes may be required to elicit a strong effect on expression of neural crest genes. In particular, the specific expression pattern of *Phc1* during early neural crest development makes it a promising candidate for perturbation studies in combination with Bmi-1 and Ring1B. In summary, the preliminary co-over-expression results strongly suggest that Bmi-1, as part of PRC1, plays a role in repressing *Msx1*.

DISCUSSION

We have found that seven members the Polycomb group of epigenetic repressors are expressed in the chick embryo during early development in large and overlapping, but non-ubiquitous domains. During gastrulation, the PRC1 members *Bmi-1* and *Phc1* exhibit a strikingly specific expression pattern in the neural plate border, a region of the epiblast that has been shown to contain neural crest progenitors by fate-mapping analysis and explant experiments (Basch et al., 2006; Ezin et al., 2009). The expression domains of *Bmi-1* and *Phc1* are highly similar to that of *N-myc*, which is interesting in light of work that has demonstrated that myc genes collaborate with Bmi-1 in lymphomagenesis, a process that involves rapid proliferation of hematopoietic stem cells (Haupt et al., 1993; Jacobs et al., 1999b). We also found that *Ring1B*, *Cbx8*, *Suz12*, *Cbx2* and *Eed* transcripts are expressed in the epiblast during gastrulation, and although their domains are large, they include the presumptive neural plate border.

During neurulation, all PcG genes examined thus far are expressed in the neural folds, and some are additionally present in ectoderm. Intriguingly, we find that *Bmi-1* and other PcG genes are strongly expressed at HH8 in the anterior-most neural folds that contain forebrain and olfactory progenitors but do not generate neural crest. An intriguing possibility is that a Polycomb-mediated repressive mechanism restricts neural crest formation to the anterior boundary of the midbrain, consistent with the role of PcG genes in Hox boundary regulation and antero-posterior (AP) patterning (Alkema et al., 1995; van der Lugt et al., 1996; Le Douarin and Kalcheim, 1999; Cao et al., 2005). Accordingly, mouse knockouts of some PRC1 genes exhibit posterior

transformations and neural crest defects due to incorrect rhombomere and branchial arch patterning, although the phenotypes have not been examined at earlier stages of development (Takihara et al., 1997; Tomotsune et al., 2000).

We also find that all of the PcG genes that we examined thus far are expressed in migrating cranial neural crest at HH10, as well as in other tissues such as lateral non-placogenic ectoderm, lateral plate mesoderm, and blood. PRC expression in blood islands is not surprising since Polycomb genes are known regulators of hematopoietic stem cell development in other organisms (Lessard and Sauvageau, 2003; Park et al., 2003). Interestingly, the multipotent state of emigrating neural crest cells has been likened to that of hematopoietic stem cells, and these cell populations share some commonality of gene expression, suggesting some similarities in developmental mechanisms (Orkin and Zon, 1997; LaBonne and Bronner-Fraser, 1999).

We speculate that while the PcG genes likely play a role in development of a diverse set of cell types and tissues, the relatively specific expression domains of some complex members imply that they may be involved in development of specific cell types, or may function to recruit other, more ubiquitously present PcG proteins to specific cell populations. Indeed, it has been suggested that the composition of Polycomb complexes may differ depending on cell type or developmental process (Otte and Kwaks, 2003; Sparmann and van Lohuizen, 2006; Squazzo et al., 2006). Therefore, based on our expression analysis, we propose that Bmi-1 may participate specifically, but not uniquely, in the development of neural plate border cells which include neural, neural crest, and placode progenitors. Since Bmi-1 is continuously expressed by progenitors of this region until their terminal differentiation, this stem cell factor probably

functions in multiple stages and aspects of neural crest development that involve maintenance of multipotency.

In an attempt to gain insight into the functionality of Bmi-1 in neural crest development, we performed *in vivo* loss-of-function experiments by antisense morpholino (MO) electroporation. When Bmi-1 MO is electroporated at gastrula stage into the prospective neural plate, expression levels of *Msx1*, as assayed by QPCR and *in situ* hybridization, are increased by early neurula stages. By whole-mount *in situ* hybridization, we find that the severity of the phenotype varies, likely due to an inability to control precise localization and amount of injected material, as well as due to weak penetrance of morpholino in this type of experiment in general (Mende et al., 2008). In addition, it is unlikely that a strong phenotype would be elicited by reduction of a single PcG member, as evidenced by the fact that some transgenic mouse lines carrying null mutations in single PcG genes do not exhibit severe defects or embryonic lethality (Chamberlain et al., 2008; Pietersen and van Lohuizen, 2008). Accordingly, we do not see a phenotype as a result of Bmi-1 over-expression alone, and only a weak repression of *Msx1* when Ring1B is additionally co-electroporated. However, given the limitations of the system, we are encouraged by the fact that we are able to see reproducible and statistically significant phenotypes as a result of Bmi-1 knock-down and over-expression.

The Bmi-1 MO phenotype is mainly manifested within the normal expression domain of *Msx1*, which indicates that Bmi-1 regulates this factor specifically in the neural plate border cell population. No mediolateral shift in the position of the neural plate border was observed in our Bmi-1 MO or over-expression experiments, suggesting that cross-repressive interactions between

juxtaposed neural and non-neural tissues are not affected, despite widespread distribution of electroporated material (McLarren et al., 2003; Woda et al., 2003). Rather, there was an observable increase or decrease in staining intensity within the neural plate border, which contains a heterogeneous population of cells marked by "salt-and-pepper" expression of specifier genes, which we are not yet able to resolve on a single cell level. Therefore, it is possible that by knocking down Bmi-1 in this region, we are inducing *Msx1* in neural plate border cells that may not express it otherwise, and conversely, forced Bmi-1 over-expression may extinguish *Msx1* transcripts in some of these progenitors. Alternatively, Bmi-1 may function to maintain a threshold level of *Msx1* transcripts in neural plate border cells that is necessary for finely tuned control of downstream neural crest specifiers, but we are unable to distinguish between these possibilities at the present time.

It is likely that the phenotype elicited by Bmi-1 MO is due to a direct effect on transcription and is not secondary to changes in the cell proliferation. Although we detected a slight increase in cell proliferation in ectodermal and neural tissues that have been electroporated with Bmi-1 MO, dorsal neural fold progenitors were not affected. We found the proliferation increase surprising in light of mouse stem cell studies that have demonstrated a positive effect of Bmi-1 on the cell cycle (Molofsky et al., 2003; Park et al., 2003). It is possible that the phenotype we observe is a secondary consequence of an upstream effect of Bmi-1 MO on ectoderm- or neural-specific survival factors. In addition, the Ink4a/Arf locus through which Bmi-1 functions to regulate proliferation in the mouse embryo is not conserved in the chicken genome. Thus, the role of Bmi-1 in cell

cycle regulation may differ between the two species (Jacobs et al., 1999a; Kim et al., 2003).

We asked whether Bmi-1 regulates neural crest specifier genes in a similar manner to *Msx1* by assaying MO-electroporated embryos by *in situ* hybridization for expression of *FoxD3*, *Snail2*, and *Sox10* at HH8-10, stages during which these genes are highly expressed by pre-migratory and emigrating neural crest cells. Because the results were inconsistent, we suspect that these effects may occur as a secondary consequence of the Bmi-1 MO effect on upstream regulators and other neural crest specifier genes (Meulemans and Bronner-Fraser, 2004). Erratic changes in *Snail2* expression with Bmi-1 MO may also be due to perturbation of a feedback loop between the two factors, while *FoxD3* may be indirectly affected by an upregulation of an unknown repressor (Bermejo-Rodriguez et al., 2006). Therefore, by the time that we assay Bmi-1 MO embryos for changes in neural crest specifier expression by *in situ* hybridization, the results may already be confounded by perturbation of other, upstream regulatory interactions. In addition, the neural crest population is highly plastic and self-regulatory, which enables it to compensate for early effects of perturbations, especially if the phenotype is already weak. This has presented a challenge in our MO and over-expression experiments and we have been unable to determine whether neural crest migration or differentiation is altered by the electroporation because the phenotype appears normal when we culture embryos to the stages at which these processes may be examined.

In light of these limitations we decided to analyze Bmi-1 MO-electroporated embryos for changes in neural crest specifier expression by QPCR at HH6, when some of these factors first appear in the neural folds at low levels

(near or just below the threshold for detection by *in situ* hybridization), and when compensation for the MO effect may not yet have occurred. The results demonstrate a quantifiable increase of *FoxD3* and *Sox9* transcripts with Bmi-1 MO at HH6, suggesting that Bmi-1 is functioning to negatively regulate neural crest specifiers during early development. We hypothesize that this may serve to prevent their premature activation or upregulation in the neural folds, possibly in order to prevent premature commitment to the neural crest lineage. For example, although *FoxD3* is expressed in the neural plate border at HH4, it does not begin to accumulate in the dorsal neural folds until HH6-7 (Fig. 2.1, Chapter 2), and Bmi-1 may be preventing premature recruitment of *FoxD3* to dorsal neural tube progenitors. In turn, *Sox9* is not expressed in the chick embryo prior to HH6 (data not shown), and it is possible that PRC1-mediated repression is one of the mechanisms that prevent premature activation of late neural crest specifiers. Interestingly, some of the upstream factors that induce neural crest specifiers, such as *Msx1*, are present continuously during early development and may need to be modulated in some way that prevents continuous activation of target genes. This modulation may involve PcG repression at early stages in order to maintain *Msx1* levels below the threshold necessary for neural crest specifier induction or upregulation. In this case, the early increase in *FoxD3* and *Sox9* transcripts observed with MO may be a secondary consequence of an increase in *Msx1* levels due to Bmi-1 knock-down. Alternatively, these genes could be regulated independently. In conclusion, these data represent the first step in elucidating the role of Bmi-1 in neural crest development *in vivo*, which we demonstrate to involve early-acting negative regulation of neural plate border and neural crest specifier genes in the neural plate border region.

ACKNOWLEDGEMENTS

I am grateful to my co-advisor, Tatjana Sauka-Spengler, for providing sound collaboration, constructive discussion, and technical assistance and advice. I would also like to thank Matt Jones and Mary Flowers for their assistance. I am grateful to Kyoichi Isono for the generous gift of monoclonal Ring1B antibody. I would also like to thank Sujata Bhattacharyya, Meyer Barembaum, Jack Sechrist, and Sonja McKeown for helpful discussion and advice. This work was supported in part by the Ira Simon Fellowship.

Figure 3.1: *Bmi-1* is expressed during gastrulation in the chick embryo

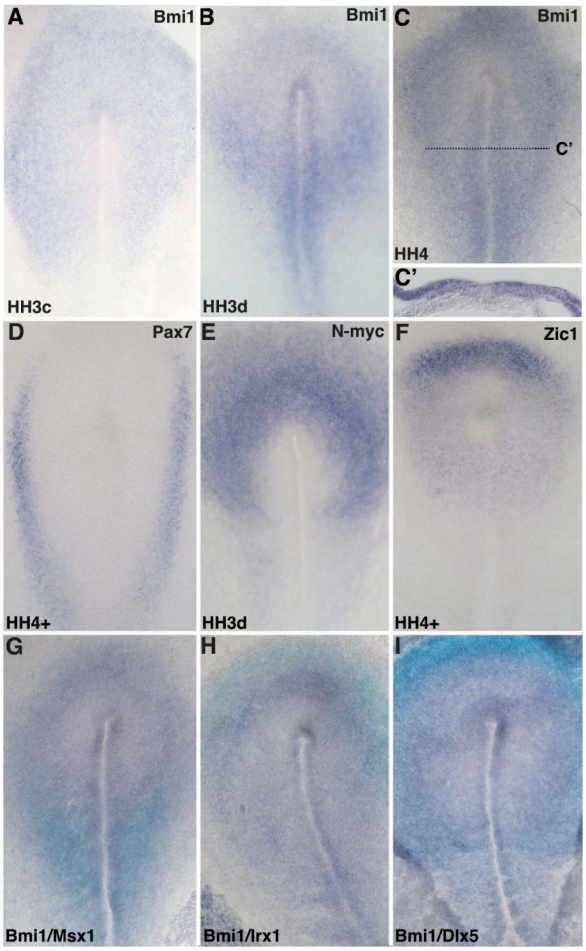

Figure 3.1. Chick *Bmi-1* is expressed in neural crest progenitors during gastrulation. **A.** At HH3c, *Bmi-1* is expressed at low levels throughout the epiblast. **B.** *Bmi-1* becomes restricted to the prospective posterior neural plate border at HH3d. **C** and **C′.** *Bmi-1* transcripts mark the prospective neural plate border both anteriorly and posteriorly at HH4. **D.** The expression pattern of *Bmi-1* resembles that of *Pax7* during HH4+. **E.** *N-myc* expression in the neural plate border is similar to *Bmi-1*. **F.** Anterior expression of *Bmi-1* is similar to *Zic1*. **G.** *Bmi-1* (purple) is co-expressed in the posterior border with *Msx1* (blue). **H.** *Bmi-1*

(purple) shares part of its anterior expression domain with placodal specifier *Irx1* (blue). **I.** *Bmi-1* (purple) expression is complementary to ectodermal specifier *Dlx5* (blue).

Figure 3.2: *Bmi-1* is expressed throughout development prior to differentiation

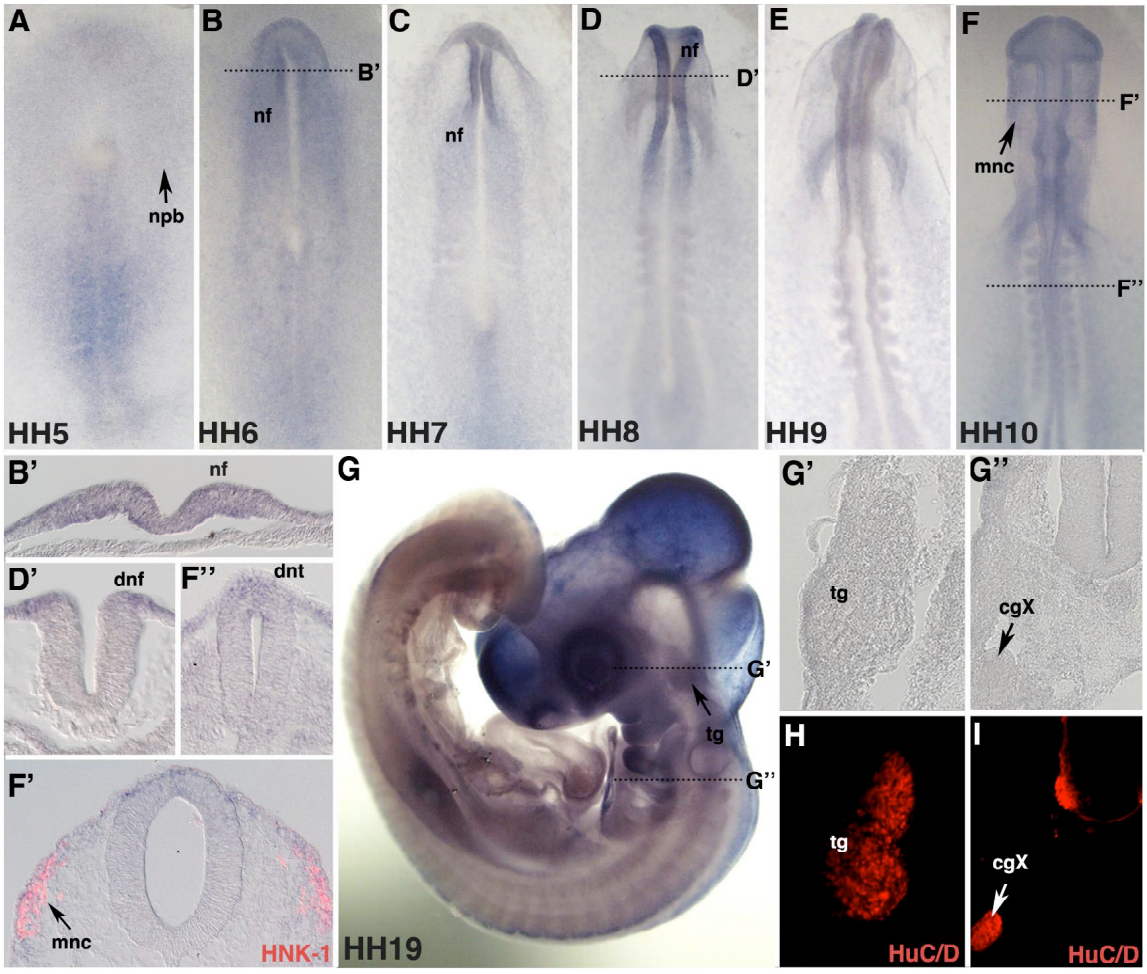

Figure 3.2. *Bmi-1* is expressed in neural crest progenitors during neurulation and early migration stages, but is downregulated in differentiated neural crest derivatives. **A.** At HH5, *Bmi-1* transcripts are localized in the neural plate border and primitive streak. **B** and **C.** At HH6 (**B**) and HH7 (**C**), *Bmi-1* is expressed in the neural folds and their border. **D.** At HH8, strong *Bmi-1* expression is observed in the dorsal aspect (**D'**) of the anterior neural folds. **E.** *Bmi-1* transcripts are maintained in neural tissue at HH9. **F.** At HH10, *Bmi-1* is expressed in migrating cranial neural crest cells that can be identified by HNK-1

immunostaining (**F′**), as well as in the dorsal neural tube at both cranial (**F′**) and trunk levels (**F′′**). **G.** By HH19, *Bmi-1* transcripts are absent from the trigeminal (**G′**) and tenth cranial (**G′′**) ganglia that express neuronal marker HuC/D (**H** and **I**, respectively). CgX, tenth cranial ganglion; dnf, dorsal neural fold; dnt, dorsal neural tube; mnc, migrating neural crest; nf, neural fold; npb, prospective neural plate border; tg, trigeminal ganglion.

Figure 3.3: Bmi-1 protein is actively translated during early development

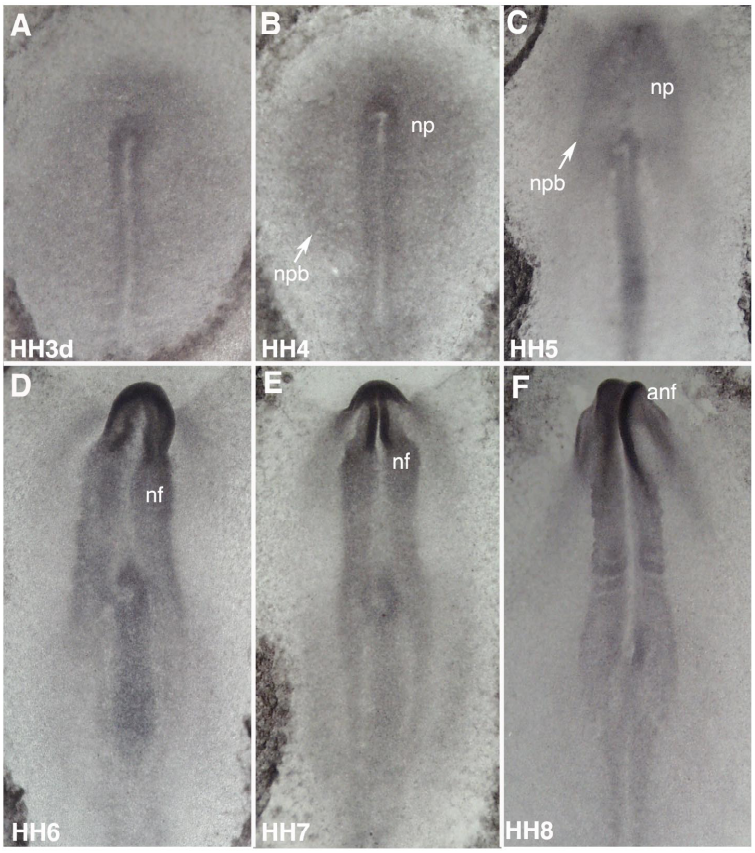

Figure 3.3. Bmi-1 protein expression recapitulates that of the mRNA during early developmental stages. Embryos were immunostained with a polyclonal Bmi-1 antibody and visualized with DAB enhanced with NiCo. **A.** Bmi-1 protein can be detected in the epiblast as early as HH3. **B.** Bmi-1 protein accumulates in the presumptive neural plate border (arrow) at HH4. It is also evident in the prospective neural plate. **C.** At HH5, Bmi-1 is expressed in forming neural tissue and neural plate border (arrow). **D** and **E.** Bmi-1 protein accumulates in the neural folds at high levels at HH6 and HH7. **F.** At HH8, Bmi-1 protein expression is highest in the anterior neural folds. Nf, anterior neural fold; nf, neural fold; np, neural plate; npb, prospective neural plate border.

Figure 3.4: PRC1 and PRC2 genes are expressed in the chick embryo

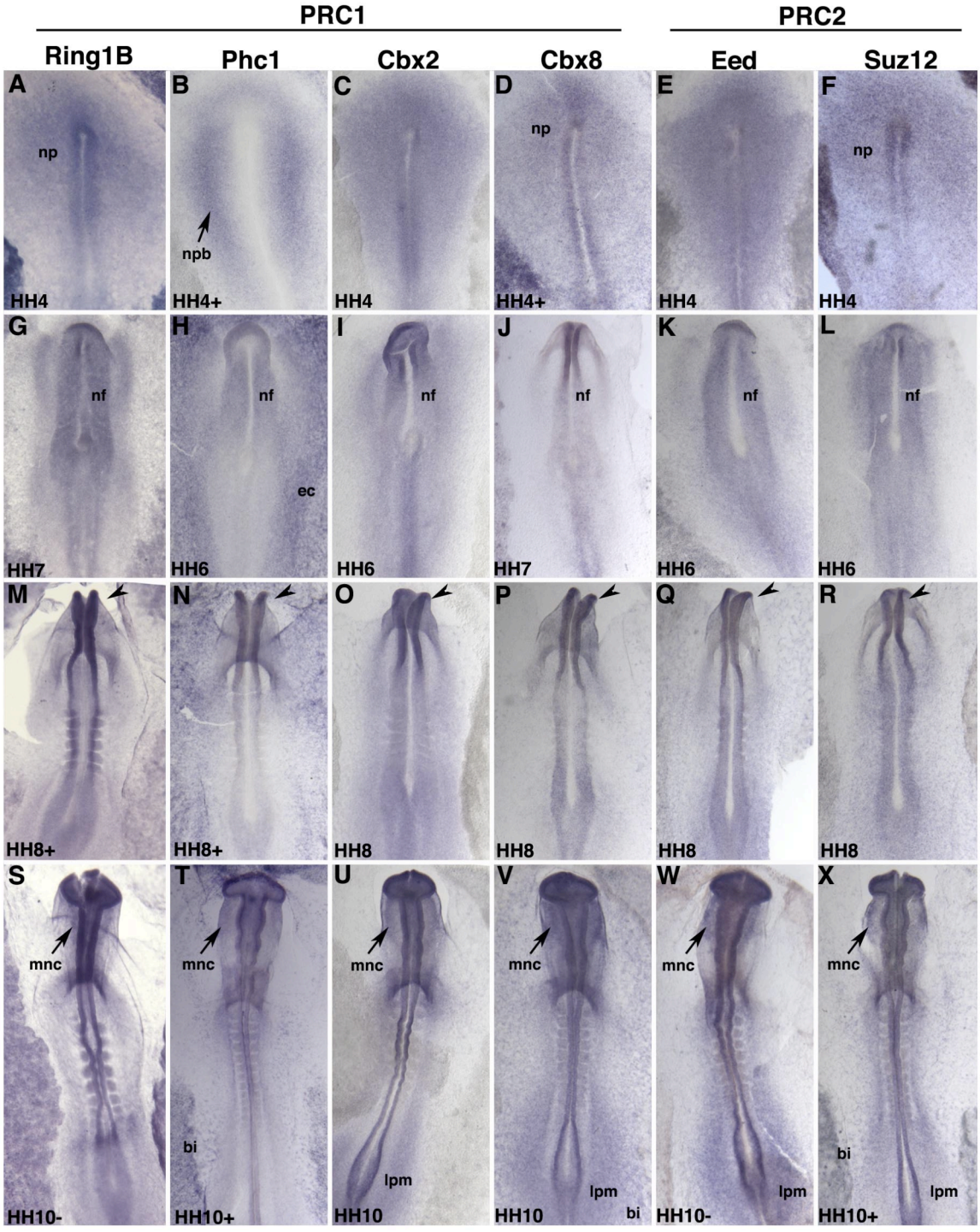

Figure 3.4. Four PRC1 genes and two PRC2 genes are expressed in overlapping but not identical domains during early stages of chick development. Embryos staged at approximately HH4 (**A-F**), HH6 (**G-L**), HH8 (**M-R**), and HH10 (**S-X**) were analyzed by whole-mount *in situ* hybridization using digoxigenin-labeled RNA probes for *Ring1B* (**A, G, M, S**), *Phc1* (**B, H, N, T**), *Cbx2* (**C, I, O, U**), *Cbx8* (**D, J, O, V**), *Eed* (**E, K, Q, W**), and *Suz12* (**F, L, R, X**). Expression in the anterior-most neural folds at HH8 and in migrating neural crest at HH10 is demarcated by arrowheads and arrows, respectively. Ao, area opaca; bi, blood islands; ec, ectoderm; lpm, lateral plate mesoderm; mnc, migrating neural crest; nf, neural fold; np, neural plate; npb, prospective neural plate border.

Figure 3.5: Effect of Bmi-1 knock-down on *Msx1* expression

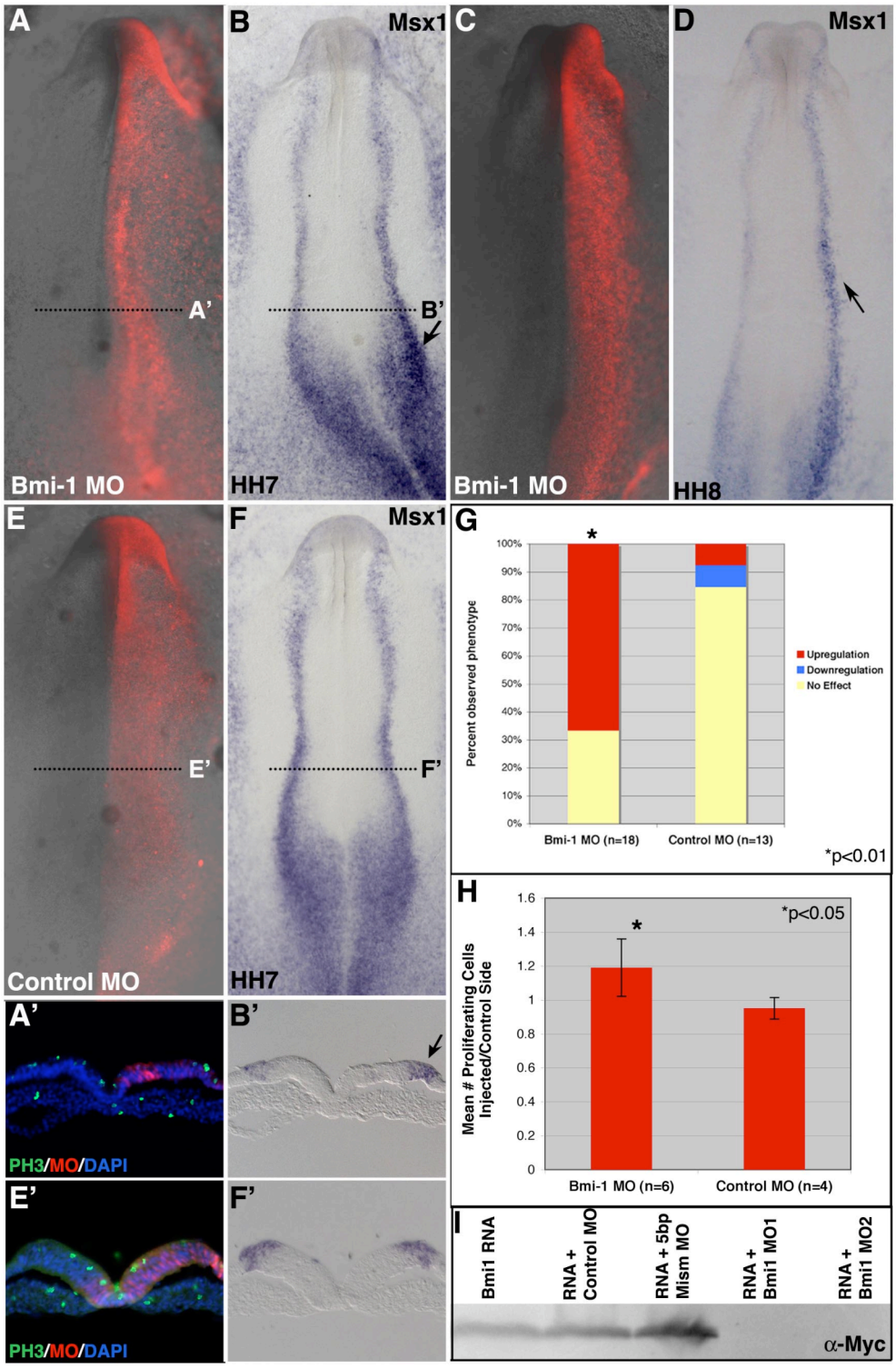

Figure 3.5. Bmi-1 MO knock-down causes upregulation of *Msx1* expression. **A** and **A′.** Embryo that was electroporated with Bmi-1 MO at HH4 showing distribution of the MO at HH7. **B** and **B′.** *Msx1* is upregulated (arrow) on the electroporated side of the embryo shown in A. **C** and **D.** Bmi-1 MO-electroporated embryo **(C)** collected at HH8 shows a weaker upregulation of *Msx1* **(D)**. **E, F, F′.** Control MO electroporation **(E)** does not affect *Msx1* expression **(F,F′)**. **G.** Quantification of embryos exhibiting specific phenotypes shows that the effect observed with Bmi-1 MO is statistically significant. **H.** Graph illustrating mean number of phospho-histone H3-positive cells on the electroporated versus control side in sections of embryos injected with Bmi-1 MO (**A′**) or control MO (**E′**). **I.** MO specificity test shows that two different Bmi-1 MOs inhibit translation of *Bmi-1* mRNA when co-injected into *Xenopus* embryos, while control MOs do not.

Figure 3.6: Quantification of changes in gene expression due to Bmi-1 MO

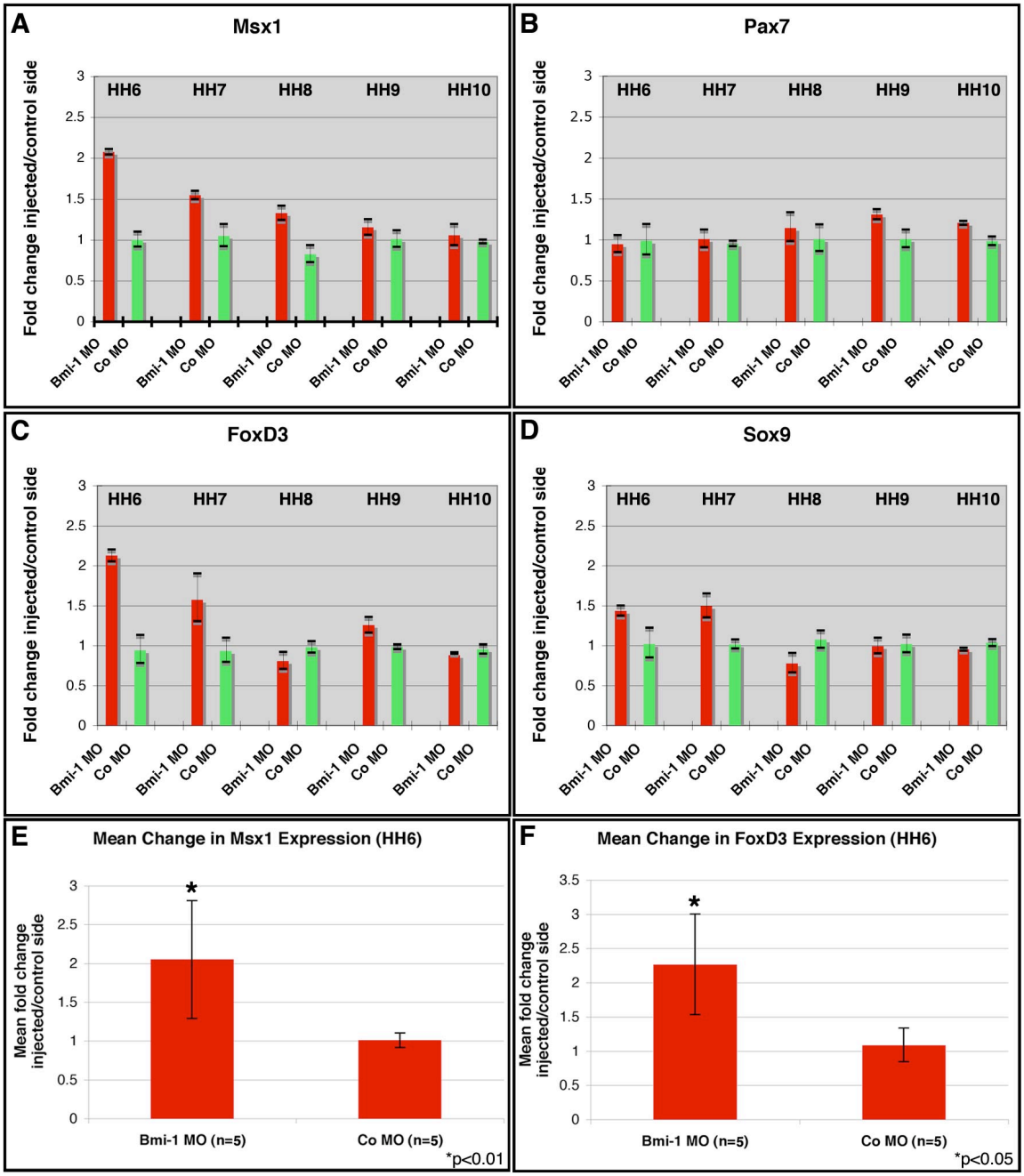

Figure 3.6. Fold change in transcript expression levels as a result of Bmi-1 MO knock-down was measured by QPCR. Embryos were electroporated at HH4 with either Bmi-1 MO or control MO and cultured until HH6-10. Electroporated

embryos collected at specific stages were laterally bisected to separate the electroporated and control sides and RT-QPCR was performed to compare changes in expression levels of target genes between the two halves within the same embryo. **A-D.** Fold change in expression levels of *Msx1* (**A**), *Pax7* (**B**), *FoxD3* (**C**), and *Sox9* (**D**) with Bmi-1 MO or control MO in single representative embryos collected at each stage indicated. **E** and **F.** Mean change in transcript levels of *Msx1* (**E**) and *FoxD3* (**F**) in 5 embryos that were electroporated with Bmi-1 or control MO and analyzed at HH6.

Figure 3.7: Bmi-1 and Ring1B co-over-expression causes *Msx1* downregulation

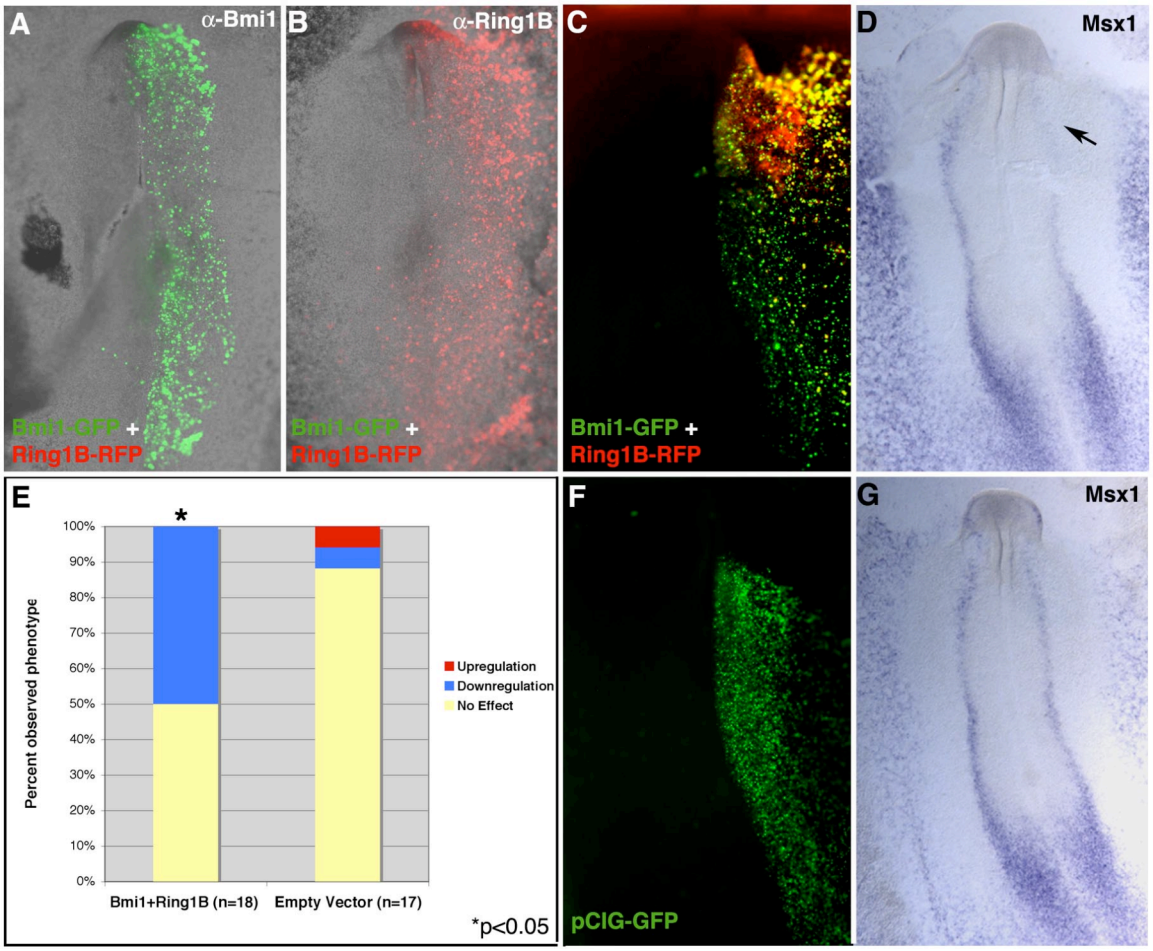

Figure 3.7. Co-over-expression of Bmi-1 and Ring1B in the chick gastrula results in a downregulation of *Msx1* transcripts at neurula stage. pCIG-Bmi-1-GFP and pCIG-Ring1B-memRFP constructs were co-electroporated at HH4 targeting the prospective neural plate border region. **A.** An electroporated embryo immunostained with anti-Bmi-1 antibody showing that large amounts of protein are translated on the injected side at HH6. **B.** Excess Ring1B protein can also be detected as early as HH6 in an embryo co-electroporated with Bmi-1 and Ring1B. **C** and **D.** An embryo that has been electroporated with pCIG-Bmi-1-GFP and

pCIG-Ring1B-memRFP shows distinct downregulation of *Msx1* transcripts on the electroporated side. **F** and **G.** Empty pCIG-GFP vector control electroporation (**F**) does not cause a significant change in *Msx1* expression (**G**). **E.** Downregulation of *Msx1* is observed in 50% of embryos co-electroporated with Bmi-1 and Ring1B (9/18, $p<0.05$). In contrast, 74% of embryos electroporated with pCIG-GFP empty vector do not exhibit a phenotype (14/19).

Chapter 4:

Characterization of alternatively spliced variants of Bmi-1 during early chick development

Jane Khudyakov, Tatjana Sauka-Spengler, and Marianne Bronner-Fraser

INTRODUCTION

The Polycomb group (PcG) of epigenetic repressors is a highly conserved bipartite protein complex that regulates gene expression in a vast number of organisms ranging from plants to mammals (Whitcomb et al., 2007; Kohler and Villar, 2008). Polycomb genes have been implicated in a number of key developmental processes such as maintenance of stem cell pluripotency, prevention of cell senescence, lineage restriction and differentiation, and axial patterning (Schuettengruber et al., 2007). The PcG was first identified in *Drosophila,* and orthologs of the fly Polycomb genes have since been identified in a number of organisms as core components of the repressive complexes. In recent years, a staggering number of other, non-core Polycomb Repressive Complex (PRC) partners have been characterized in vertebrates, many of which share great similarity in structure and function (Fig. 1.2B, Chapter 1, Whitcomb et al., 2007). Given that these genes regulate critical developmental processes and that mutations affecting PcG members often lead to embryonic lethality, carcinogenesis, deregulation of the stem cell state, and/or improper patterning of the body plan, careful regulation of the Polycomb complexes themselves is necessary for viable embryonic development (Pietersen and van Lohuizen, 2008). In addition to the antagonistically functioning Trithorax Group and upstream regulators such as the Asx family of Polycomb enhancers, an intriguing possibility is that alternative splice variants may modulate PcG protein function (Schwartz and Pirrotta, 2007; Baskind et al., 2009).

Alternative splicing has become widely recognized as one of the most prevalent means of generating proteomic diversity and phenotypic complexity in

higher-order eukaryotes, by modulating protein function. Pre-mRNA splicing events most commonly involve exon skipping or shuffling, usage of alternative 5′ and 3′ splice sites and retention of introns; and splicing factors that mediate these processes are expressed in a highly regulated, rapidly inducible, and tissue-specific manner (Maniatis and Tasic, 2002; Lareau et al., 2004; Stamm et al., 2005; Kim et al., 2008). Protein variants produced by alternative splicing commonly exhibit diverse changes in activity due to removal or alteration of functional domains or localization signals and often function as dominant-negatives. Functional modifications include changes in affinity for other proteins, ligands, or DNA, alteration in signaling or transactivation activity, and changes in intracellular localization, protein stability, and post-translational modifications. In addition, alternative splicing within 5′- and 3′-untranslated regions may control RNA expression levels or its localization, stability, and translation efficiency, respectively (Lareau et al., 2004; Stamm et al., 2005).

The prevalence of alternatively spliced isoforms in vertebrate proteomes and their high degree of evolutionary conservation suggest that splice variants may play important roles in vertebrate physiology. Indeed, alternatively spliced isoforms have been shown to regulate many important functions such as apoptosis, cell type specification, organ patterning, and neuronal activity. Accordingly, transgenic mice carrying variant-specific mutations often exhibit significant developmental and functional abnormalities (Venables, 2006; Moroy and Heyd, 2007; Holland and Short, 2008). Not surprisingly, differentially expressed splice isoforms are prevalent within large protein families of the signal transduction and transcription factor categories that regulate development and

differentiation, such as FGF and Pax, and are conserved across chordates (Holland and Short, 2008).

Perturbations of the delicate equilibrium between splice variants often lead to cancer, and many tumors are characterized by over-expression of alternatively spliced isoforms (Venables, 2006). A number of alternative splice variants have also been identified within chromatin-modifying protein families that are often perturbed in cancers; these include histone acetyltranferases, DNA methyltransferases, and Polycomb repressors. For example, a truncated variant of the DNA methyltransferase DNMT3 which lacks the conserved methytransferase motif has been shown to compete with the full-length protein for targeting to chromatin, leading to DNA hypomethylation, instability, and cancer (Saito et al., 2002). Likewise, many variants of PcG protein members such as Mph1, Mph2, Cbx6, Cbx7, and L3mbt1, have been identified and shown to lack key protein interaction and chromatin recognition motifs, although their physiological functions have not yet been analyzed (Alkema et al., 1997a; Yamaki et al., 2002; Tajul-Arifin et al., 2003; Li et al., 2005). Here, we show that that the PcG member Bmi-1 is characterized by five alternative splice variants, which we have examined within the *in vivo* context of the developing chicken embryo.

The Polycomb Repressive Complex 1 (PRC1) member Bmi-1 is the vertebrate homolog of *Drosophila posterior sex combs* (*psc*) which was one of the first PRC1 members to be identified in the mouse as a stem cell factor (Park et al., 2004). Mutant mice harboring null mutations or overexpressing Bmi-1 exhibit defects in proliferation of hematopoietic stem cells or develop lymphomas, respectively (Haupt et al., 1993; Park et al., 2003). Bmi-1 mutants also display defects in neural stem cell maintenance, as well as axial transformations due to

dysregulation of homeotic genes (van der Lugt et al., 1994; van der Lugt et al., 1996; Molofsky et al., 2003). In addition, Bmi-1 has been shown to function in mouse ESC development by directly associating with and repressing a large number of developmental regulator genes, thereby preventing premature differentiation (Bracken et al., 2006; Dietrich et al., 2007). In view of these findings, we hypothesized that Bmi-1 may play a similar role during development of multipotent neural crest progenitors. We have found that the chick Bmi-1 homolog is expressed by neural crest progenitors during early developmental stages and functions in cooperation with other PRC1 partners to negatively regulate members of the neural crest gene regulatory network (Chapter 3).

The biochemical activity and structure of the Bmi-1 protein have been thoroughly described. It is comprised of 326 amino acids and contains several highly conserved protein domains that are necessary its activity as well as interaction with other PRC1 members (Fig. 1.3A, Chapter 1). The N-terminal RING finger domain is characterized by a conserved cysteine-rich zinc finger binding motif and is necessary for interaction with the other RING finger-containing proteins, Ring1A and Ring1B. Two conserved cysteine residues within this domain and a stretch of several downstream amino acids have been shown to be critical for protein interaction (Hemenway et al., 1998). In addition, the RING finger domain and a downstream sequence containing a putative nuclear localization signal (NLS) are necessary for the oncogenic activity of Bmi-1 in transgenic mice and cell transformation in culture, as well as for prevention of replicative senescence in fibroblasts, suggesting that both the presence of the RING domain and subnuclear localization are critical for Bmi-1 function (Cohen

et al., 1996; Alkema et al., 1997b; Itahana et al., 2003). The full-length Bmi-1 protein also contains a centrally located helix-turn-helix-turn-helix-turn (HTHTHT) domain that is necessary for interaction with the mouse *polyhomeotic* homologs Mph1 and Mph2. In addition, presence of the HTHTHT domain is critical for transcriptional repression of Hox genes and skeletal transformation, and, to a lesser extent, for oncogenic potential (Cohen et al., 1996; Alkema et al., 1997a, 1997b). Finally, the C-terminal part of Bmi-1 contains a proline, glutamine, serine, and threonine-rich domain (PEST) that has no repressive or oncogenic function but may be involved in targeting the protein for degradation (Cohen et al., 1996; Alkema et al., 1997b). In addition, a putative MAPK pathway phosphorylation site is found within the PEST domain, which has been shown to regulate association of Bmi-1 with chromatin (Voncken et al., 1999; Voncken et al., 2005).

Bmi-1 deletion studies and *in vitro* interaction assays have demonstrated that truncated portions of the protein containing intact RING and HTHTHT domains can homodimerize with the full-length protein and bind to other PRC1 factors via homologous regions (Hemenway et al., 1998; Satijn and Otte, 1999). In addition, over-expression of mutant Bmi-1 constructs lacking any of the protein interaction domains in fibroblast cell culture causes a dominant-negative phenotype by inducing premature replicative senescence (Itahana et al., 2003). We hypothesized that naturally occurring truncated splice variants of Bmi-1 may function *in vivo* to modulate the activity of the full-length protein and affect interactions between partners of the PRC1, possibly in a dominant-negative manner. We have characterized three such splice variants that were identified in a chick cDNA library screen and found that two of them represent truncated N-

terminal isoforms containing the RING domain, while a third, C-terminal variant, contains the HTHTHT domain but lacks the RING finger. We have performed expression analysis by RT-PRC and QPCR using whole chick embryos and have found that the N-terminal variant V4 and the C-terminal variant V6 are expressed during early chick development from gastrulation to neural crest migration stages. We have also demonstrated by over-expression analysis that V4 likely functions in a dominant-negative manner to inhibit Bmi-1 activity, leading to upregulation of the *Msx1* target gene.

MATERIALS AND METHODS

Sequence analysis

A 600 bp fragment of the chick Bmi-1 homolog, amplified using degenerate PCR approach, was used to probe a 4-12 somite-stage macroarrayed cDNA library (Gammill and Bronner-Fraser, 2002; Fraser and Sauka-Spengler, 2004). Eight positive clones isolated in this screen were sequenced and the resulting sequences were analyzed and aligned using EditSeq and SeqMan applications (DNASTAR Lasergene 8, DNASTAR, Inc).

Genomic analysis and intron sequencing

The Bmi-1 genomic locus is very poorly characterized and, apart from a partial 3'-UTR sequence found within the unassembled random sequence collection, entirely absent from chick genome assembly. To gain further insight into genomic organization of Bmi-1, a macroarrayed chicken BAC library (Chori 261, purchased from BACPAC (http://bacpac.chori.org)) was screened using a chick Bmi-1 fragment and the resultant positive BAC clones were identified within the chicken genome assembly (http://genome.ucsc.edu). Analysis of BAC clones identified in our screen and positioning of BAC ends of clones absent in our screen have enabled us to narrow down the position of the Bmi-1 locus to ~20kb on chromosome 2 (chr2:17,642,600-17,662,000). The Bmi-1 gene is directly flanked by sperm associated antigen 6 and COMM domain-containing 3 genes and further analysis of synteny between chicken and mouse genomes confirms proper assignment of the Bmi-1 gene to this region. Mouse Bmi-1 protein sequence, which shares 93% identity with the chick, was used to predict the

location of intron-exon boundaries. We then designed several primer sets near the putative exon/intron boundaries in order to amplify the intronic regions by PCR using either ~1 μg of chick genomic DNA or 200 ng of BAC DNA template per reaction. The following primers were used: V123578F 5′-CGACCAGGATCAAAATCACC-3′, 2R 5′-GCAGTACTTGCTCGTCTC-3′, 2F 5′-GTCCAAGTGCACAAAACC-3′, 4R 5′-AGCAGCATAGAAATCCCT-3′, 4F 5′-TATGCTGCTCATCCGTCG-3′, 6R 5′- ATTTCCTTTTCGTTCCAGT-3′, 5F 5′-TCCATTGAGTTCTTTGAC-3′, 7R 5′-GCAGCGCAAATATCTTTT-3′, 7F 5′-AGTAAGATGGATATCCCC-3′, 9R 5′-GGGCCGCACGCGGTACTT-3′, RT1568 5′-TGTTTGCTTCCCGGTCCTTT-3′. Primers were designed using the EditSeq application (DNASTAR Lasergene 8, DNASTAR, Inc.). Reactions were carried out as follows: 94°C for 30 sec, 55°C for 30 sec, 72°C for 1 min, 30 cycles. PCR products were resolved on a 2% agarose gel and specific bands were isolated using the QIAquick Gel Extraction Kit (QIAGEN, Cat# 28706). The resulting products were cloned into pCR®2.1 TOPO vector using the TOPO® TA Cloning® Kit (Invitrogen, Cat# K4500-01) and transformed into One® Shot Top10 Chemically Competent Cells (Invitrogen, Cat# C4040-03). Positive colonies were picked and grown in a 96-well mini culture plate. QIAprep 96 Turbo Miniprep Kit (QIAGEN, Cat# 27191) was used to purify DNA from bacterial cultures. DNA sequencing reactions were set up using the BigDye® Terminator v3.1 Cycle Sequencing Kit (Applied Biosystems, Cat# 4337455) with 1 pmol/μL of each SP6 and T7 primers and 1 μL miniprep DNA in each reaction. Sequencing was performed by Miki Yun (Davidson lab, Caltech). Sequences were aligned using the SeqMan application (DNASTAR Lasergene 8, DNASTAR,

Inc). The following BAC clones, used in PCR reactions, were obtained from BACPAC (http://bacpac.chori.org): CH261-130E19, CH261-107L20, CH261-180F13.

V6 protein translation assay

Sequence analysis of the V6 clone identified two possible open reading frames (ORF), both containing a different C-terminal portion of the Bmi-1 protein. The first putative truncated protein, if produced, would contain the NLS but none of the characterized protein domains. Alternatively, a longer putative protein would include the majority of the HTHTHT protein interaction domain, in addition to the NLS. To determine which of the reading frames is used to produce the V6 protein, *Xenopus* oocytes were injected with V6 mRNA in which either the short or long putative protein was myc-tagged. Western blot analysis of protein extracts from injected embryos using anti-myc and anti-Bmi-1 antibodies demonstrates that the protein translated from V6 mRNA corresponds to the second ORF and contains the HTHTHT domain and a NLS (data not shown).

Chick embryo incubation

Fertilized chicken eggs were obtained from AA Enterprises (Ramona, CA) and incubated at 38°C in a humidified incubator (Lyon Electric, Chula Vista, CA). Embryos were staged according to the Hamburger and Hamilton chick staging system (Hamburger and Hamilton, 1992).

RT-PCR

Whole embryos for RT-PCR were collected and trimmed to remove extra-embryonic membranes in Ringer's solution on ice. Several embryos of each approximate stage were pooled together and lysed in RNAqueous® Lysis Buffer (Ambion, Cat# AM1912). Total RNA was isolated using the RNAqueous® Kit according to manufacturer's protocol (Ambion, Cat# AM1912). Reverse transcription was carried out using First Strand cDNA Synthesis Kit for RT-PCR (AMV) (Roche Applied Science, Cat# 11483188001). Specific RT primers were designed within the unique 3'-UTR of V4 (corresponding to intron 4, RT4 5'-AACCGCCAAAGCTGCAAACT-3'), the distal 3'-UTR exon shared by V2 and V3/7 (RT237 5'-TCGACCAAAGCAAAGCACGA-3'), and within the proximal 3'-UTR portion shared by full-length variants and V6 (RT1568 5'-TGTTTGCTTCCCGGTCCTTT-3'). PCR reactions were carried out using 500 ng of cDNA template and Taq DNA polymerase (Invitrogen, Cat# 10342-020). PCR primers for amplifying specific variant sequences from cDNA were designed as follows: full-length variants were amplified using the primer set designed within the coding region of Bmi-1, with a forward primer in exon 1 (V123578F 5'-CGACCAGGATCAAAATCACC-3') and a reverse primer in exon 9 (V135678R 5'-TATGGAGGATTTCCGTGCTC-3'). The following PCR settings were used: 94°C for 30 sec, 65°C for 30 sec, 72°C for 1 min, 30 cycles. V2 was detected using the same forward primer (V123578F) and a reverse primer in the distal 3'-UTR exon (V237R 5'-TCCATCTCATCTCCCTCGAC-3'). Amplification conditions were the same as above, with the exception of 30 sec elongation at 72°C. This primer set also amplified the V3/7 full-length variant, yielding a larger size

fragment, albeit with lower efficiency. V4 was amplified using the primer set designed within its 3'-UTR region, with a forward primer in intron 2 (V46F 5'-AACCTCAGCCCCCGAACTC-3') and a reverse primer in intron 4 (V4R 5'-AAAAGGAAAGAGCGGAGCA-3'). The PCR reaction was carried out for 35 cycles, with a 45 sec elongation step. V6 was amplified using the same V46F forward primer, situated in its 5'-UTR, and the V135678R reverse primer in exon 9, described above. The V6 PCR reaction was performed for 35 cycles with a 1 min 20 sec elongation step. All primers were designed using Primer3 software (http://frodo.wi.mit.edu) and synthesized by IDT. PCR products were resolved on a 1% or 2% agarose gel.

QPCR

cDNA for use in QPCR was synthesized using RNA extracted from single whole chick embryos prepared by Pablo Strobl and Tatjana Sauka-Spengler. The reverse transcription (RT) reaction was probed using random hexamers and each sample was accompanied by a minus RT control. QPCR was performed using the 96-well plate ABI 7000 QPCR machine (Applied Biosciences) with SYBRGreen iTaq Supermix with ROX (Bio-Rad, Cat# 172-5101). Primers were used at a concentration of 450 nM with the exception of *Gapdh*, which was used at 150 nM, in a 20 μL reaction. Variant-specific sets of primers were designed using the Primer3 software (http://frodo.wi.mit.edu) and synthesized by IDT. The sequences of primers used are as follows: V13578spec1F 5'-AGAGAAAGAAAAGTCGAAGGAGG-3', V13578spec2F 5'-TCACGTCGATCTGGAAAGTG-3', V6spec4F 5-GATGCTCCTTTCCAGGTCAG-

3′, V6spec4R 5′-ATTAGAGCCATTGGCAGCAT-3′, V2spec2F 5′-CTCGTACCGGGCCTTTTC-3′, V2spec2R 5′-CACGTCAATGACTTCCATCTC-3′, V4spec6F 5′-GAGTGCCTGCACTCCTTCTG-3′, V4spec6R 5′-TTCACGGCTCCTTTCAGATT-3′. Each sample was run in three replicates to reduce errors created by pipetting. The baseline and threshold levels were set according to the Applied Biosystem software, and gene expression was calculated by the standard curve assay method as described in Applied Biosystems protocols. In detail, the results for different samples were interpolated from a line created by running four point standard curves for each primer set and then normalized against results for the *Gapdh* housekeeping gene. The standard cDNA was prepared from chick embryos collected between stages HH4 and HH10, at which we have shown expression of Bmi-1 variants by RT-PCR. Minus RT controls were tested for each set of primers, and showed no amplification. cDNA from three separate single embryos collected at HH4, HH6, HH8, and HH10 was individually tested in this assay.

Over-expression constructs

Using a high fidelity enzyme (Expand High FidelityPLUS PCR System, Roche, Cat# 03300242001), the open reading frame of the V4 variant, including the endogenous Kozak sequence, was amplified using full-length V4 cDNA obtained from a chick cDNA library screen (see above). The obtained fragment was ligated into several expression vectors: pCIG-IRES-GRP (pCIG-V4-GFP), pCIG-H2B-RFP (pCIG-V4-H2B-RFP), and pCIG-mem-RFP (pCIG-V4-memRFP (RFP with a membrane linker)). The V2 fragment was prepared in a similar manner and cloned into pCIG-H2B-RFP vector. Maxi preps were prepared using the QIAGEN

EndoFree Plasmid Maxi Kit (QIAGEN, Cat# 12362) and DNA was resuspended in Buffer EB (QIAGEN, Cat# 19086). Plasmids were diluted to 2-5 μg/μL concentration with Buffer EB (10 mM Tris pH 8) and 0.01% Blue Vegetable Dye (FD&C Blue 1, Spectra Colors Corp, Cat# 3844-45-9) for injection into chick embryos. Empty vectors were used as electroporation controls.

Electroporation

HH stage 3-5 chick embryos were explanted on Whatman filter paper rings and placed ventral-side up in Ringer's solution in an electroporation dish containing a platinum plate electrode in a shallow well. pCIG-V4-H2B-RFP or pCIG-V4-memRFP (or a combination of the two constructs), pCIG-V2-H2B-RFP, or the control pCIG-GFP empty vector was unilaterally injected into the lumen between the epiblast and vitelline membrane targeting the prospective neural plate border. The embryo was covered with a flattened-tip platinum electrode and five 7-volt, 50-millisecond pulses with 100-millisecond pauses in between were applied using a square-pulse electroporator. Embryos were cultured in thin albumin in a humidified 37°C incubator. After 6-8 hours, embryos were fixed in 4% paraformaldehyde at 4°C overnight and dehydrated to 100% methanol for analysis by *in situ* hybridization.

***In situ* hybridization**

Chick embryos were dissected in Ringer's solution and fixed in 4% paraformaldehyde at 4°C overnight. Whole-mount *in situ* hybridization was performed as described previously (Nieto et al., 1996; Xu and Wilkinson, 1998),

with some modifications involving more extensive washing adapted from a lamprey *in situ* protocol (Sauka-Spengler et al., 2007). The digoxigenin-labeled antisense *Msx1* probe was reverse transcribed from the chick EST template ChEST900p21 (BBSRC ChickEST Database (http://www.chick.umist.ac.uk)) using Promega buffers and RNA polymerases (Promega Corp), and purified with illustra ProbeQuant™ G-50 Micro Columns (GE Healthcare, product code 28-9034-08). Stained embryos were photographed in 50% glycerol on a Zeiss Stemi SV11 microscope using AxioVision software (Release 4.6) and processed using Photoshop 7.0 (Adobe Systems).

RESULTS

Bmi-1 is characterized by five alternatively spliced isoforms

Using the full-length Bmi-1 gene as a probe in a high stringency chick cDNA library screen, we have identified eight positive clones corresponding to Bmi-1 variants. Five clones contain an open reading frame (ORF) of 981 base pairs (bp), encoding the full-length 326-amino acid (aa) Bmi-1 protein. These clones are identical in coding sequence but vary within untranslated regions. In addition, we identified three clones that encode truncated Bmi-1 isoforms with ORFs ranging from approximately 200 to 450 bp. We found that the putative proteins encoded by these transcripts lack some of the functional domains present in the full-length Bmi-1 protein, which is illustrated in Figure 4.1. In order to determine whether Bmi-1 clones represent naturally occurring splicing isoforms of the Bmi-1 gene, we performed thorough characterization of Bmi-1 genomic locus and structural analysis of Bmi-1 variants.

In order to identify splicing events that generated Bmi-1 variants, we mapped and characterized the genomic locus of Bmi-1 and obtained intronic sequences by PCR using chick genomic DNA and BAC templates (see Materials and Methods for details). The full-length Bmi-1 gene contains nine coding exons, intercepted by eight introns and at least two non-coding exons contributing to 5'- and 3'-untranslated regions (UTR). The RING finger protein interaction motif is generated by the first two exons. One of two putative nuclear localization signals (NLS) lies within the fourth exon similarly to the mouse Bmi-1 protein, while the other one is found in the ninth exon. The helix-turn-helix-turn-helix (HTHTHT) domain is generated by the last three exons (Fig. 4.1).

The five full-length Bmi-1 clones (V1, V5, V8, V3, V7) have identical open reading frames; however, they differ in the 3'-UTR as two of the variants (V3, V7) contain a supplementary non-coding exon (Fig. 4.1A). Two distinct N-terminal variants, termed V2 and V4, are truncated in the C-terminal portion and thus lack the HTHTHT protein interaction domain. Variant V2, generated by the first three coding exons and the second 3'-UTR exon, contains the RING domain and a NLS, whereas the short V4 variant contains the first two exons and includes the RING domain only (Fig. 4.1B,C). The putative NLS found in the C-terminal region of V2 is generated when the last exon, which contributes to the 3'-UTR in the full-length V3/V7 clones, is spliced in frame with the third coding exon and is translated as part of the V2 protein. This rearrangement extends the N-terminal portion of V2, encoded by the first three exons, by approximately 60 amino acids and contributes a 21 amino acid-region that encodes an experimentally confirmed NLS motif (http://www.rostlab.org/cgi/var/nair/resonline.pl). A C-terminal variant, V6, is generated by the last three exons, encoding a protein that lacks the RING domain and the first five amino acids of the HTHTHT domain (Fig. 4.1D). Therefore, we have characterized several splice isoforms of Bmi-1, which include two unique full-length variants that are alternatively spliced in untranslated regions and N-terminal and C-terminal truncated variants lacking protein interaction and nuclear localization motifs.

Bmi-1 variants are expressed in the chicken embryo during early development in a stage-specific manner

We used RT-PCR to examine whether Bmi-1 variants are expressed in the chicken embryo during early stages of neural crest development. Total RNA was extracted from a pooled sample of several whole embryos collected at each stage of development from HH4 to HH10. Reverse transcription (RT) was performed using specific variant RT primers to ensure detection of low expression levels of variant mRNA and to exclude the possibility of genomic contamination in the cDNA library. Specific PCR primers for amplification of variant sequences from cDNA were designed as described in Materials and Methods. Each set of primer pairs was first tested for specificity in a PCR reaction using variant clones isolated from the chick library as templates. Stage-specific RT-PCR results demonstrate that full-length *Bmi-1*, which we refer to as *V8* for simplicity, and N-terminal variant *V4* are expressed during each stage of development from HH4 to HH10 (Fig. 4.2A,C). In contrast, a very weak *V2*-specific band is only detectable at HH9 (Fig. 4.2B). Intriguingly, *V6* is present at HH4 and is progressively downregulated at later stages (Fig. 4.2D).

Next, we used quantitative RT-PCR (QPCR) to accurately measure levels of truncated variant transcripts at several developmental stages and to examine how they differ between these time points. In addition, since we hypothesized that the short variants may be acting to modify full-length Bmi-1 function during development, we also wanted to quantitatively compare their expression levels. We analyzed expression at four specific stages – HH4, HH6, HH8, and HH10 – representative of events occurring during chick neural crest development. cDNA used in variant QPCR was synthesized from total RNA extracted from single embryos (Pablo Strobl and Tatjana Sauka-Spengler), and three embryos of each stage were individually tested in our assay. Variant-specific primer sets for

QPCR analysis were designed similarly to those used in RT-PCR reactions and tested for specificity using specific variant DNA templates as well as genomic DNA. Variant expression results were normalized to expression of the housekeeping gene *Gapdh*, allowing for control of the amount of input material.

We found that although expression levels varied slightly between single embryos due to stochastic variation of endogenous transcriptional levels and slight variations in the age of the embryos, trends in expression levels from stage to stage were conserved. Therefore, we present data using one representative embryo of each stage in Figure 4.3. We were unable to amplify *V2* at any stage including HH9, at which we found low expression by RT-PCR from pooled sample cDNA primed with V2-specific primers, suggesting that *V2* may not be transcribed at levels that are detectable in a single embryo. *V4* was expressed unvaryingly at low levels at every stage tested (Fig. 4.3A). In contrast, *V6* was expressed at high levels at HH4 and HH8 and at low levels that were similar to *V4* at HH6 and HH10. Its expression was highest at HH8 (Fig. 4.3A). *V8* transcripts were present in at higher levels than either of the truncated variants. However, similar to *V6*, its expression was highest at HH8, and slightly lower at HH4, HH6 and HH10. Expression levels of *V6* and *V8* were similar at HH8 (Fig. 4.3A).

We next calculated *V4* and *V6* transcript levels as a function of *V8* expression (*V4*/*V8* and *V6*/*V8*). We find that *V4* is expressed at low levels relative to *V8* at each stage, similar to the results described above, suggesting that V4 may function in a dominant-negative manner to moderate *V8* expression during development (Fig. 4.3B). In contrast, *V6* expression relative to *V8* is much higher at stages HH4, HH6, and HH8. There is a fourfold, twofold, and eightfold

difference between *V6*/*V8* and *V4*/*V8* at HH4, HH6, and HH8, respectively. However, the two measurements are similar at HH10 (Fig. 4.3B). Based on these expression data, we hypothesize that while V4 may be acting as a negative regulator, V6 may function in a dominant-active manner to enhance full-length Bmi-1 activity, especially during gastrulation (HH4) and late neurulation (HH8) stages.

V4 over-expression causes upregulation of *Msx1*, mimicking a loss-of-function phenotype

To examine whether the N-terminal truncated variant V4 may function as a dominant-negative regulator of Bmi-1, we performed *in vivo* over-expression experiments in the chick embryo. The V4 fragment was cloned into an expression vector and injected unilaterally into the prospective neural plate border of the chick gastrula in an electroporation procedure that was described for MO experiments. Electroporated embryos were cultured until HH6-8 and analyzed by *in situ* hybridization for *Msx1* expression. We find that *Msx1* is upregulated weakly in a statistically significant proportion of embryos expressing pCIG-V4-memRFP (Fig. 4.4A-D,G, 8/22, $p<0.05$), but not in control embryos injected with empty pCIG vector (Fig. 4.4E,F). The phenotype is similar to that seen with Bmi-1 MO knock-down. The increase in staining intensity is always observed within the normal expression domain of *Msx1* and is usually most obvious in the open neural plate, which suggests that the phenotype preferentially affects neural plate border progenitors at earlier stages of development (Fig. 4.4B-D). This may be due to the ability of neural crest cells to compensate for the weak phenotype elicited by V4 as electroporated embryos develop.

In summary, our experiments demonstrate that V4 over-expression mimics the Bmi-1 MO effect on *Msx1*, suggesting that it may function to negatively regulate Bmi-1 during neural crest development. The effect is weak despite injection of high concentrations of the over-expression construct, suggesting that either V4 is not translated efficiently under these conditions or, more likely, that it does not alter full-length Bmi-1 protein activity to the same extent as the MO. Given that V4 contains the RING domain but lacks a NLS, it may act as dominant-negative regulator by binding to the full-length protein and preventing it from entering the nucleus. Additionally, V4 may bind to the Ring proteins via the RING domain and prevent them from interacting with other members of PRC1. Based on these preliminary studies, we propose that V4 is expressed during embryonic development at low concentrations, which may serve to regulate or tone down Bmi-1 activity to necessary critical levels. Thus controlled, Bmi-1 may restrict expression of neural crest network genes to levels that may be below the threshold for differentiation or lineage restriction.

DISCUSSION

We have characterized five distinct Bmi-1 variants that were identified in a chick macroarrayed cDNA library (Gammill and Bronner-Fraser, 2002). Identification of intron/exon sequences by PCR from chick BAC templates and alignment of variant sequences has enabled us to make some predictions about splicing events that may have generated these alternative isoforms. We have found that the N-terminal truncated variant V4 contains the RING protein interaction domain generated by the first two exons, but no functional NLS, suggesting a possible role as a dominant-negative regulator of the full-length protein. Another N-terminal variant, V2, contains the RING domain and a potential NLS formed by splicing in and translation of a 3'-UTR exon containing a stretch of amino acids contributing to this domain. Although we saw very weak expression of this variant in stage HH9 embryos by RT-PCR, we were unable to amplify it by QPCR from single embryo cDNA. In addition, in preliminary over-expression experiments with a pCIG-V2-memRFP construct, expression of *Msx1* was not affected (n=4, data not shown). Therefore, although this variant was isolated from a chick neural crest cDNA library and appears to be a true splice isoform based on its sequence, it may not be expressed during the stages that we examined at detectable levels, or may be the result of a very rare splicing event or splicing error amplified in the library. Therefore, we did not pursue this variant further. Finally, we have also characterized a C-terminal truncated variant, V6, and identified the functional translation site, which is found within the HTHTHT domain in the seventh exon. This variant lacks the

RING domain and the first five amino acids of the HTHTHT domain, but contains an alternate putative NLS near the C-terminus.

Variant expression analysis was performed by RT-PCR and QPCR using whole chick embryos collected at several distinct stages of development. We found that *V4* was continuously expressed throughout early chick development from HH4 until HH10 at low levels compared with full-length *Bmi-1*. *V6* expression was quantitatively higher and was characterized by peaks at HH4 and HH8. Full-length *Bmi-1* was expressed at higher levels than the truncated variants with a peak at HH8, similarly to *V6*. The fact that *V4* is expressed at low levels throughout development, while *V6* was detected at similar levels and temporal pattern as the full-length protein, suggests that these variants may be functioning to modify Bmi-1 activity in a dominant-negative and dominant-active manner, respectively. In addition, the peaks of *V6* and full-length variant expression at HH4 and HH8 suggest that Bmi-1 function may be more critical at gastrulation and late neurulation, as opposed to other stages. It is possible that higher Bmi-1 activity in the neural plate border at gastrulation functions to maintain neural crest genes at levels that are sufficient for commitment, but too low for specification and differentiation. At HH8, Bmi-1 activity may be high in the anterior neural folds in order to repress neural crest genes in this region.

In order to obtain some insight into Bmi-1 variant function in the context of the developing neural crest, we electroporated an overexpression construct containing V4 into the prospective neural plate of the chick gastrula. We find that V4 over-expression recapitulates the effect of Bmi-1 MO knock-down on *Msx1*, although the effect is much weaker and primarily observed at younger stages. This suggests that V4 may function to partially inhibit the repressive activity of

Bmi-1 during development, possibly by dimerizing with the full-length protein and preventing it from binding to other PRC1 members and/or from entering the nucleus, and we intend to pursue biochemical studies to elucidate this mechanism. We also plan to examine the function of V6 during neural crest progenitor development using similar *in vivo* over-expression technique. Based on the similarity in expression levels of V6 and full-length Bmi-1, as well as the presence of a putative NLS and the HTHTHT repressive domain in this variant, we predict that over-expression would result in a gain-of-function phenotype similar to that observed with Bmi-1 and Ring1B co-electroporation.

In conclusion, we have isolated and characterized several truncated splice isoforms of Bmi-1, which are expressed in the chick embryo, and have demonstrated that the N-terminal variant V4 negatively regulates Bmi-1 during early neural crest development. However, a large amount of work remains in order to characterize the spatiotemporal expression pattern of Bmi-1 variants during chick neural crest development and to elucidate the functional mechanism by which they modulate Bmi-1 function.

ACKNOWLEDGEMENTS

I am grateful to my co-advisor, Tatjana Sauka-Spengler, for helpful discussion and technical assistance and advice. I would also like to thank Matt Jones and Mary Flowers for their assistance. I am grateful to Miki Yun for help with intron sequencing.

Figure 4.1: Bmi-1 genomic locus and splicing of variants

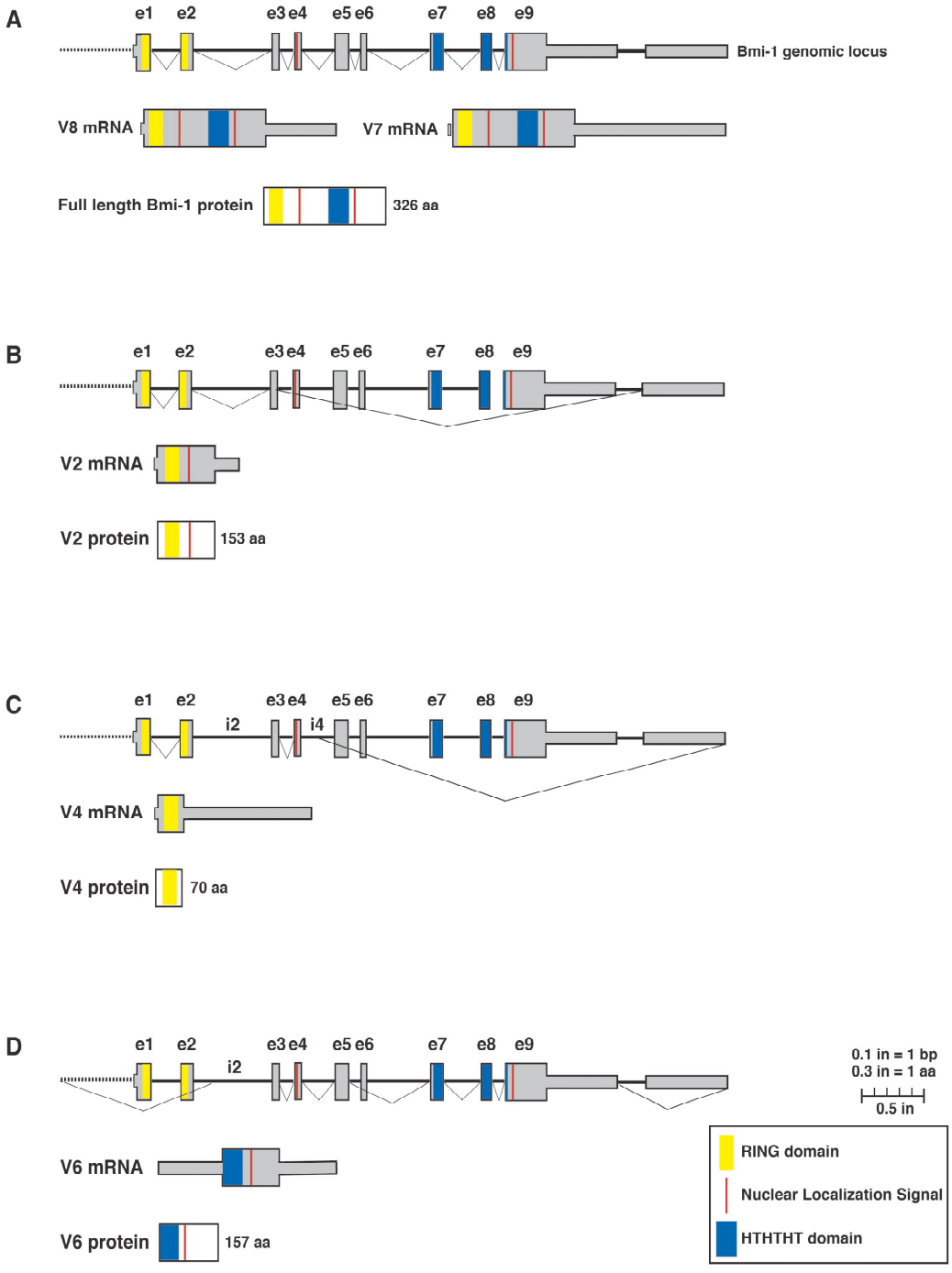

Figure 4.1. Genomic structure of the Bmi-1 locus and predictions of splicing events that yield Bmi-1 isoforms. The chick Bmi-1 gene is characterized by nine coding and at least two non-coding exons. **A.** Full-length Bmi-1 variants V8 and V7 have identical coding sequences and vary only in the 3'-untranslated region (UTR) of the mRNA. V7 contains a supplementary 3'-UTR exon. V7 and V8 encode the full-length 326-amino acid (aa) long Bmi-1 protein containing the RING (yellow box) and HTHTHT (blue box) protein interaction domains and two nuclear localization signals (NLS, red stripe). **B.** A 153-aa long protein encoded by V2 is a result of splicing events assembling the first three exons that contribute the RING domain and the distal 3'-UTR exon, which, when spliced in frame, contributes a putative NLS with an amino acid composition that has been previously experimentally confirmed as functional in other nuclear proteins. **C.** V4 mRNA includes the first four exons as well as the second and fourth introns, which have been retained. Only the first two exons are translated, giving rise to a 70-aa long protein that only contains the RING domain. **D.** V6 is comprised of the second intron and the third, fourth, fifth, seventh, and ninth exons. The functional translation initiation site of V6 lies within the HTHTHT domain in the seventh exon, giving rise to a 175-aa long protein that lacks the RING domain and first five amino acids of the HTHTHT domain. Schematic is drawn to scale.

Figure 4.2: Variant expression during chick development

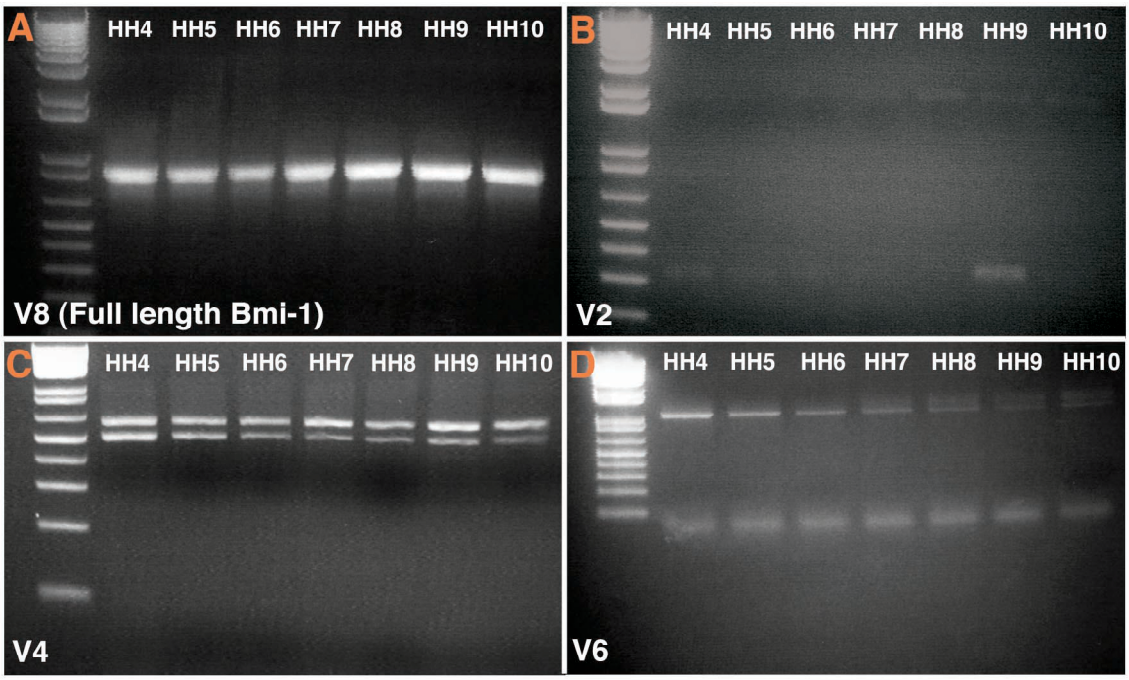

Figure 4.2. Bmi-1 variants are differentially expressed in the chick embryo during early neural crest development. RT-PCR reactions were carried out using material from whole chick embryos collected at HH4-10 and specific variant primer sets described in Materials and Methods. **A.** Full-length Bmi-1 variant *V8* is expressed at all developmental stages tested. **B.** *V2* is amplified at very low levels at HH9 only. **C.** *V4* is expressed throughout HH4-10. **D.** *V6* is expressed at early developmental stages and is progressively downregulated at later stages.

Figure 4.3: Quantification of Bmi-1 variant expression

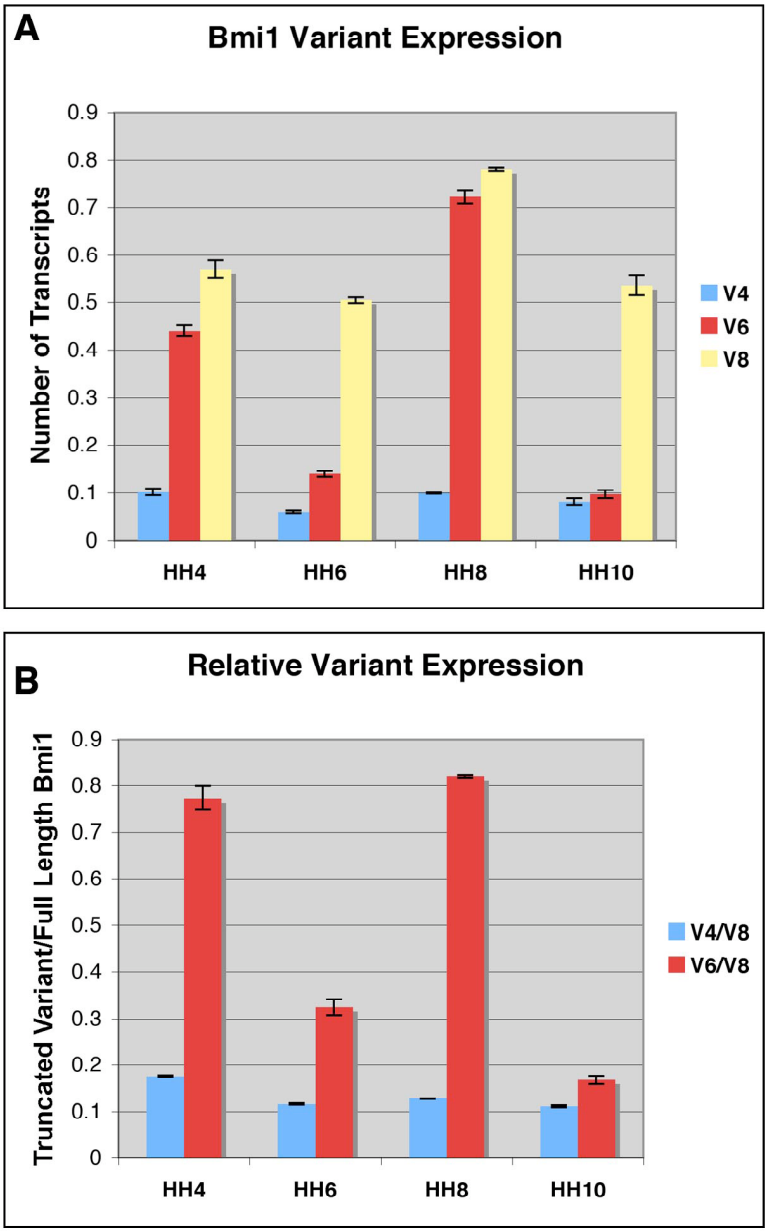

Figure 4.3. Quantitative analysis of Bmi-1 variant expression during early chick development. RT-QPCR was carried out using material from single whole chick embryos staged HH4, HH6, HH8, and HH10 using specific Bmi-1 variant primer pairs. Data shown is from one representative embryo out of three analyzed at

each stage. QPCR reactions were performed in triplicate and relative abundance of transcript was calculated by standard curve method and normalized to *Gapdh*. **A.** The full-length variant *V8* is expressed at high levels at all stages examined with a peak at HH8. In contrast, *V4* levels remain relatively low throughout development. *V6* expression is biphasic: it is expressed at levels comparable to *V8* at HH4 and HH8 but at low levels similarly to *V4* at HH6 and HH10. **B.** Expression levels of truncated variants were compared to that of full-length Bmi-1 variant *V8*. *V4* transcripts are present at low levels compared to *V8* at all stages tested. In contrast, *V6* expression is high compared to *V8* with large peaks at HH4 and HH10.

Figure 4.4: V4 over-expression elicits a dominant-negative phenotype

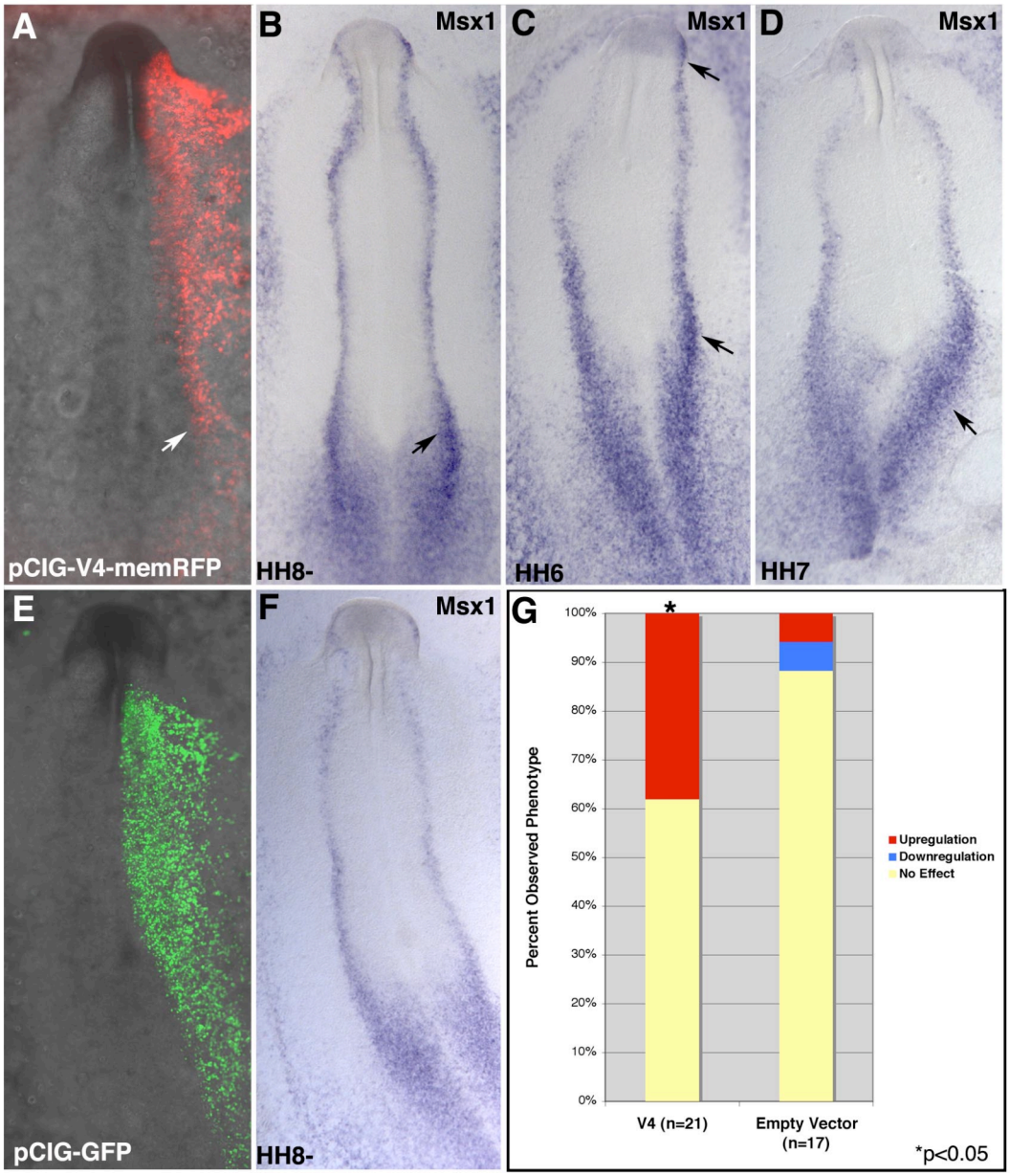

Figure 4.4. Over-expression of pCIG-V4-memRFP results in weak upregulation of *Msx1* during neurulation. **A** and **B.** An embryo that was electroporated with pCIG-V4-memRFP overexpression construct (**A**) exhibits weak upregulation of *Msx1* in the open neural plate at HH8- (**B**, arrow). **C** and **D.** pCIG-V4-memRFP-

electroporated embryos demonstrate more obvious phenotypes when analyzed at HH6 (**C**) or HH7 (**D**). **E** and **F**. In a control embryo electroporated with empty pCIG-GFP vector (**E**), *Msx1* expression is not affected (**F**). **G.** Quantification of phenotypes demonstrates that the effect observed in V4-electroporated embryos is statistically significant and not due to chance (8/21, $p<0.05$).

Chapter 5:

Summary and Perspectives

Current molecular definition of the neural plate border progenitor population

The neural crest has fascinated developmental biologists ever since it was first described by His in 1868 as *zwischenstrang*, or a strip of tissue between the neural tube and epidermis (Le Douarin and Kalcheim, 1999). Although inductive signals that contribute to the emergence of this cell population have been studied for some time, neural crest research in recent years has been aimed toward understanding the regulatory interactions between molecules that guide neural crest development, especially during its earliest stages. Despite a dearth of knowledge about direct regulatory relationships, many epistatic interactions between neural crest genes have been studied and information gathered from functional experiments has been compiled into a putative neural crest gene regulatory network (NC-GRN), which proposes that progressive acquisition of neural crest cell fate is driven by discrete groups of developmental regulators.

As such, the neural crest is induced at the border of the presumptive neural plate by a combination of diffusible growth factor signals that segregate neural plate from adjacent non-neural ectoderm. As a result, a group of transcription factors are activated at the junction between the two tissues that specify this region as the neural plate border, a relatively wide domain containing a heterogeneous population of progenitors with overlapping neural, neural crest, placode, and ectodermal fates. Specification of these cell fates occurs extremely early in development, even before gastrulation or bona fide neural induction. It is therefore likely that the neural plate border contains an intermixed population of multipotent stem-like cells as well as progenitors with restricted potential for the formation of specific lineages. However, it is unknown how they segregate. It is difficult to visually identify neural crest precursors

within this region because there are no known neural crest specific genes, and even canonical neural crest specifiers such as *Snail2* are expressed at pre-migratory neural crest stages by both neural crest and dorsal neural tube progenitors. In addition, expression domains of neural plate border, neural plate, ectoderm, and placodal specifiers are large and are characterized by a "salt-and-pepper" distribution. Therefore, I sought to thoroughly characterize early expression patterns of neural crest network genes in the hopes of finding an overlap between them, which may illuminate the locations of specific cell populations within this region.

I examined expression of ten members of the NC-GRN in the chick embryo during early development and found that neural crest specifiers *c-myc*, *N-myc*, *FoxD3*, and *AP-2* are expressed in the gastrula at the neural plate border. Early expression of most neural crest specifiers has not been examined previously in the chick in the context of neural crest development, and these data confirm the early specification status of this cell population. In addition, this work demonstrates conservation in timing of neural crest developmental events because studies in *Xenopus* and lamprey have also demonstrated concomitant expression of neural plate border and neural crest specifiers during gastrulation. Based on side-by-side comparison of individual gene expression domains and double *in situ* hybridization data, I propose that the chick neural plate border can be divided into posterior and anterior domains characterized by the combinatorial expression of a number of neural plate border and neural crest specifiers, which is summarized in Fig. 5.1. The anterior border of the neural plate which contains forebrain and placodal progenitors is defined by co-expression of *Zic1*, *N-myc*, *FoxD3*, *Dlx5*, *Dlx3*, and *AP-2*, which overlap with

placodal specifiers such as *Irx1*. The posterior portion of the neural plate border containing dorsal neural tube progenitors is characterized by co-expression of *Msx1*, *Pax7*, *c-myc, N-myc*, *Zic1*, *Dlx3*, and *AP-2*. As mentioned previously, the expression domains of these transcription factors are relatively large, and many of them overlap in other regions of the embryo such as the neural plate (*Zic1*, *N-myc*, *FoxD3*, *Dlx3*) and non-neural ectoderm (*Msx1*, *N-myc*, *Dlx3*, *Dlx5*, *AP-2*), suggesting potential roles in specification of several distinct cell types.

Interestingly, I noted that as development proceeds, several specifiers (*FoxD3*, *c-myc*, *AP-2*) are extinguished in neural plate border progenitors and are instead recruited to other embryonic structures, subsequently re-appearing in dorsal neural folds during late neurulation. Conversely, other genes were expressed continuously in progenitors of the dorsal neural tube but turned off in migrating neural crest cells (*Zic1*, *N-myc*). I propose that many members of the NC-GRN play separable roles in early specification and later maintenance of neural crest fate, and that activation of neural crest specifiers occurs extremely early in chick development, either concomitant with neural plate border specifiers or shortly thereafter during gastrulation. This is supported by striking similarities in expression patterns of some neural plate border and neural crest specifiers at this stage (*Msx1* and *c-myc*; *Zic1* and *FoxD3*). However, the precise timing of neural plate border and neural crest specifier induction is still unknown, and resolving this question necessitates further *in situ* hybridization and QPCR analysis of gene expression at developmental stages preceding HH4.

Prospects for cellular resolution at the neural plate border

While these studies bring us closer to defining the neural plate border region, we are still unable to resolve gene expression on a single-cell basis. Therefore, we are currently optimizing fluorescent *in situ* hybridization techniques that will enable us to obtain cellular resolution of combinatorial expression of up to three specifier genes at once (Denkers et al., 2004). In such an experiment, it will be important to define the overlap between markers of neural plate, non-neural ectoderm, neural plate border, and placodes with high resolution which is not possible by chromogenic means. Ultimately, the best approach to this question would involve live imaging of chick embryos expressing fluorescent reporter constructs driven by specific neural crest gene enhancers, enabling precise cellular resolution of spatiotemporal changes in gene expression as they occur during development. Such neural crest gene specific enhancer elements are currently being investigated in our laboratory, and the comprehensive characterization of spatiotemporal expression patterns of chick neural crest genes conducted here will serve as valuable background for further identification of potential regulatory elements.

Discovery of epigenetic regulators in the developing chick embryo

In light of these findings, it is intriguing that despite exposure to a plethora of regulatory signals from the time of specification to terminal differentiation several days later, neural crest cells maintain some degree of multipotency, even upon reaching their targets. The multipotent progenitor state of the neural crest has been demonstrated by a number of lineage tracing, back-transplantation, and clonogenic studies; however, potential mechanisms

responsible for maintenance of this plastic state have been elusive (Crane and Trainor, 2006). Therefore, we hypothesized that members of the NC-GRN may be regulated by a yet-unknown mechanism that serves to prevent premature lineage decisions and differentiation. The Polycomb group (PcG) of epigenetic repressors emerged as promising candidates because these proteins have been demonstrated to mediate global repression of developmental regulator genes in a variety of stem cells and stem-like progenitors, including mouse and human embryonic stem cells, fibroblasts, hematopoietic stem cells, and cancers (Sparmann and van Lohuizen, 2006). In addition, the PcG has been shown to be necessary during lineage restriction and differentiation by repressing pluripotency factors and regulators of alternative cell fates. Although epigenetic repression mechanisms have not been investigated during *in vivo* neural crest development, neural crest derived neuroblastomas often exhibit dysregulation of chromatin-modifying genes, including Polycomb, consistent with possible involvement in normal development (Cui et al., 2006).

Therefore, I first set out to examine whether PcG genes are expressed at the right time and place for participation in neural crest development. I found that Polycomb Repressive Complex 2 (PRC2) members *Suz12* and *Eed* and Polycomb Repressive Complex 1 (PRC1) proteins *Bmi-1*, *Ring1B*, *Cbx2*, *Cbx8*, and *Phc1* are expressed throughout early chick development in large domains that include the neural plate border, neural folds, and migrating neural crest, which is summarized in Fig. 5.1. While some of the PRC gene expression patterns were more specific than others, none were ubiquitously expressed at all stages. Widespread PcG expression in the gastrula is strongly suggestive of a role in maintenance of multipotency and regulation of tissue specification signals.

Interestingly, I found that all seven Polycomb genes examined are localized at high levels in the anterior neural folds, which do not express neural crest specifiers and do not generate neural crest. We hypothesize that the PcG, in combination with anteriorizing neural signals such as Wnt inhibitors, may act to repress neural crest cell fate in anterior neural folds, possibly by selectively inhibiting neural crest regulator genes while leaving forebrain and placode specifiers unaffected. Furthermore, specific PcG expression in migratory neural crest cells, which are characterized by rapid proliferation and a high degree of cell fate plasticity, suggests that Polycomb-mediated epigenetic repression may be involved in regulating these processes as well. Therefore, the PcG might function to modulate a number of processes during neural crest development, likely by negatively regulating NC-GRN genes.

In vivo functional analysis of Polycomb Group factor Bmi-1

To investigate the *in vivo* function of Polycomb proteins in the chick neural crest, we undertook a morpholino (MO) knock-down approach focusing on the PRC1 member Bmi-1, which has been shown to regulate self-renewal of neural, hematopoietic, and enteric neural crest cells in culture (Molofsky et al., 2003). We found that Bmi-1 MO electroporation into the prospective neural plate border during gastrulation results in consistent upregulation of *Msx1*, *FoxD3*, and *Sox9* transcripts by early neurulation stage HH6. In the case of *Msx1*, which showed an obvious phenotype by *in situ* hybridization, the Bmi-1 MO-induced increase in expression is not due to ectopic expansion of the *Msx1* domain or an increase in cell proliferation, but is a direct result of an increase in expression within the endogenous neural fold territory. The visible enhancement of *Msx1*

expression is likely a consequence of either an increase in intracellular transcript concentrations or an increase in the number of neural plate border and neural fold cells that are recruited to express it. Due to the lack of cellular resolution of gene expression and the heterogeneity of the target cell population, we cannot yet distinguish between these alternate possibilities, which are not mutually exclusive. However, we can definitively conclude that Bmi-1 represses *Msx1* because its expression is conversely decreased in embryos overexpressing high levels of Bmi-1 protein and its partner Ring1B.

Likewise, Bmi-1 MO knock-down results in an increase in *FoxD3* and *Sox9* transcript quantities at early neurulation stage HH6 as measured by QPCR. This derepression leads to *FoxD3* and *Sox9* being expressed during HH6 at levels which are not usually seen until much later in development, and may cause premature commitment or segregation to the dorsal neural tube/neural crest lineage. However, we have been unable to examine how these transcriptional changes functionally affect neural crest development because early transcriptional derepression leads to misregulation of neural crest specifiers at later stages. This secondary effect probably results from a perturbation of the delicate balance between these factors, which is controlled by highly complex cross- and auto-regulatory interactions. In addition, by the time that neural crest cells begin migrating in electroporated embryos, this highly plastic cell population has compensated for the early phenotype, such that no effect on migration or differentiation is observable.

Therefore, we plan to continue to examine the role of Bmi-1 in neural crest differentiation and proliferation in an *in vitro* explant culture system, which will allow us to minimize the number of variables confounding this question. A

homogeneous population of isolated neural crest stem-like cells, such as EPI-NCSC, would present an ideal system (Sieber-Blum and Hu, 2008). However, it may be also possible to use a culture system such as demonstrated by Basch et al., in which explants of tissue containing neural crest progenitors are cultured for a week in the absence of exogenous factors until differentiation occurs autonomously. We have attempted to replicate this system and have found that explants of gastrula-stage medial epiblast and neurula-stage midbrain dorsal neural folds generate migratory neural crest cells that express the HNK-1 antigen within 36 hours in growth factor restricted culture medium. Although we were unable to observe a difference in neural crest cell emigration from explants that have been electroporated with Bmi-1 MO as compared to control MO (data not shown), we also have not examined these cultures for changes in expression of differentiation markers, and plan to repeat these experiments using a more stringent knock-down approach. For example, we will attempt to inactivate the upstream PRC2 complex in neural crest cell cultures with the chemical inhibitor DZNep, which has been shown to effectively and specifically disrupt PRC2 function in cancer cells, and examine the effect on cell survival, proliferation, and differentiation (Tan et al., 2007).

Optimizing Polycomb loss-of-function approaches

We are significantly limited by the fact that our perturbations are specific to one member of the downstream complex of a large bipartite protein group, and although some biochemical studies have shown that knock-down of single PRC members can disrupt activity of the entire complex, PRC1 proteins may function somewhat redundantly during development (Lee et al., 2006).

Therefore, in future knock-down experiments we will apply several PRC1 morpholinos together, targeting Bmi-1 along with the catalytically active partner Ring1B and the specifically expressed PRC1 member Phc1. Co-electroporation of three morpholinos at high concentrations in the gastrula has been shown to result in viable chick embryos with a drastic and specific neural crest phenotype at later stages (Betancur and Sauka-Spengler, personal communication). Experiments with three PRC1 morpholinos will undoubtedly result in a stronger phenotype and may lead to more obvious effects on later developmental events.

In addition, recent development of shRNA cassettes driven by discrete neural crest-specific enhancers in our laboratory shows great promise for studies in which target genes necessitate inactivation in a cell-specific, temporally controlled manner. These neural crest-specific enhancer elements drive mir-shRNA constructs at levels comparable to endogenous expression of the targeted gene, which overcomes the problem of non-specific effects that have been reported with ubiquitously driven shRNA by us and others (data not shown, Mende et al., 2008). This approach may allow us to examine late effects of Bmi-1 knock-down and to overcome early specificity and compensation issues.

Strategies for large-scale analysis of Polycomb function

In the meantime, it will be interesting to examine whether PRC1 knock-down also affects expression of other specifier genes in the chick embryo in a similar manner to *Msx1*, *FoxD3*, and *Sox9*. For instance, are other neural plate border specifiers affected? We did not observe a significant effect of Bmi-1 MO on expression of *Pax7*, which may suggest that either *Msx1* is repressed specifically, or that *Pax7* is less sensitive to the effects of Bmi-1, which we may be

able to resolve in a double or triple PRC1 knock-down experiment. Does the Polycomb complex repress neural crest network genes that have been shown to stimulate proliferation and inhibit differentiation, such as *Zic1*, *c-myc*, *AP-2*, and *Id2*? It is possible that these genes cooperate with PRC1 during stages of neural crest development that necessitate extensive proliferation and multipotency (i.e., migration), and are therefore not repressed at that time. Are specifiers of other neural plate border fates, such as placodes, also regulated? We presume that placodal specifiers such as *Irx1* would be repressed by PRC1, given that Bmi-1 and its partners are co-expressed with these genes in the pre-placodal region. Does Polycomb knock-down affect the cell cycle of neural crest progenitors in a way that cannot be detected by phospho-histone H3 immunostaining? Are factors that regulate AP patterning in the chick embryo, such as Hox genes, Krox20, and Wnt, dysregulated in these experiments?

In order to examine whether PRC1 knock-down affects NC-GRN genes specifically or globally, we plan to assay electroporated embryos at HH6 for changes in expression of a number of other neural plate border and neural crest specifiers, induction factors, ectoderm, placode, neural plate, and axial patterning specifiers, and mitotic and apoptotic markers. To this end, we will use the NanoString nCounter Gene Expression Assay system, which allows for large-scale multiplex quantitative analysis of mRNA expression directly without the necessity for RNA extraction, reverse transcription or amplification procedures (Geiss et al., 2008; Su et al., 2009). This incredibly sensitive assay can also be used to quantify changes in gene expression as a result of PRC1 over-expression, either alone or in combination with Bmi-1 MO in a rescue experiment. We imagine that Bmi-1 and other PRC1 partners repress developmental regulator

genes in the chick embryo selectively, due to the presence of other complex regulatory interactions, unlike the global repression which has been observed in homogeneous ESC populations.

However, definitive conclusions about direct regulation of NC-GRN genes by PRC1 will require experimental evidence of association of Polycomb proteins with the chromatin context of target genes and simultaneous presence of repressive histone methylation marks. Therefore, we plan to first investigate whether PRC1 members such as Bmi-1, Ring1B, Cbx8, and the PRC2 member Suz12 are associated with upstream regulatory regions of Msx1, FoxD3, and Sox9 during early chick development by chromatin immunoprecipitation (ChIP). This experiment will allow us to determine whether the neural crest specifiers are repressed by Bmi-1 directly or secondarily through Msx1 regulation. We have identified antibodies that immunoprecipitate PRC1 complex partners from protein extracts of chick embryos, and are currently optimizing chromatin sonication conditions and cross-linking procedures in order to minimize background and increase specific signal. We are also testing specific primer sets that we have designed within highly conserved upstream regulatory sequences of Msx1 and FoxD3 that have shown PcG occupancy in human and mouse ESC ChIP assays (Stock et al., 2007). Additionally, we would like to address whether de-repression of neural crest genes observed in Bmi-1 knock-down experiments occurs as a consequence of the removal of Polycomb complexes and H3K27me^3 marks from chromatin. Finally, an ideal experiment would involve large-scale investigation of PcG chromatin association during several distinct stages of chick development using the ChIP-on-Chip method, allowing us to determine how epigenetic regulation of lineage specifier genes changes in the embryo with time.

Alternative splicing as an additional regulatory mechanism

In addition to the challenges of studying a large, multifunctional complex of epigenetic regulator proteins *in vivo*, we discovered another level of complexity when we isolated several truncated splice isoforms of Bmi-1 from a chick cDNA library. Understanding the splicing events responsible for generating these variants necessitated thorough characterization of the chick Bmi-1 genomic region, which lies on an unassigned chromosome and is not annotated in the chick genome. We have found that truncated variant V4 contains the conserved RING finger domain which is necessary for interaction between Bmi-1 and Ring1B proteins, but lacks a nuclear localization signal (NLS) and other C-terminal functional domains. In contrast, variant V6 lacks the N-terminal RING finger but contains a NLS and the helix-turn-helix-turn-helix-turn (HTHTHT) motif which mediates interaction with the Ph proteins and is responsible for repressive activity; however, a small portions of the HTHTHT motif is missing in V6, suggesting possible reduced functionality.

Preliminary expression studies using QPCR have demonstrated that *V6* is expressed at similar levels as full-length *Bmi-1* during early development, suggesting that it may be a positive regulator of its expression. In addition, we have found that *V4* transcripts are present throughout early chick development at levels significantly below those of full-length Bmi-1, and that over-expression of this variant at the gastrula stage recapitulates the effect of Bmi-1 MO on *Msx1* expression. We predict that it functions in this manner by binding to full-length Bmi-1 and the Ring proteins and preventing them from engaging in the PRC1 complex and translocating to the nucleus. It would be interesting to investigate whether V4 inhibits Bmi-1 activity in a cell type-specific manner, or whether it

acts more generally within the neural fold to restrict Bmi-1 activity to a critical level.

Unfortunately, the RT-PCR techniques used in our experiments do not provide spatial information about variant expression, and we are unable at present to distinguish whether the Bmi-1 isoforms function specifically within the neural crest progenitor population or are differentially expressed in other tissues. Specific variant probe synthesis for *in situ* hybridization proves problematic due to the small size of truncated isoforms and large regions of homology shared between them, especially within 3'-UTR. In addition, variant transcripts may be present at levels below detection by standard whole-mount *in situ* hybridization technique. Therefore, we have designed fluorescently labeled locked nucleic acid (LNA) probes, which are highly stable RNA analogs with high affinities toward even very short complementary sequences, and which have been used successfully to analyze microRNA expression in vertebrate embryos by whole-mount *in situ* hybridization (Kloosterman et al., 2006; Kubota et al., 2006). We are currently testing these LNA probes in the chick embryo using an *in situ* hybridization technique that includes additional signal amplification steps.

Although we have not yet obtained spatiotemporal resolution of V4 expression or tested its ability to interact with other PRC1 proteins, the data generated so far strongly suggest that V4 may be a naturally occurring dominant-negative modulator of Bmi-1 activity. We next plan to examine the biochemical mechanism by which V4 functions in a cell culture system using bimolecular fluorescence complementation analysis (BiFC), which has been successful in visualizing protein interactions in live cells (Hu and Kerppola, 2003;

Grinberg et al., 2004; Shyu et al., 2006). We are currently making fluorescent fusion constructs containing full-length Bmi-1, truncated variants, and other PRC1 members such as Ring1B and Phc1 together with truncated fluorophores, which will be transfected into live cells for imaging studies. We expect that V4 associates with full-length Bmi-1 and Ring1B via the RING finger domain, but is not able to interact with Phc1 or to translocate to the nucleus. In contrast, V6 should not be able to interact with Ring1B, but may bind Phc1. However, since the V6 translation initiation site is located within the HTHTHT domain, the translated V6 protein lacks five amino acids of this protein interaction motif, and it will be interesting to examine whether its affinity for interaction with Phc1 is reduced. If the truncated HTHTHT domain of V6 retains protein-binding and repressive activity, it is possible that V6 may act as a substitute for Bmi-1 in PRC1 complexes. Alternatively, V6 may be able to bind to Bmi-1 and stimulate its activity within the complex. In addition, the culture experiments should be able to demonstrate whether the alternative putative NLS located near the C-terminus of V6 is functional, giving this variant the ability to translocate to the nucleus. Luciferase assays may be useful for determining whether the HTHTHT domain truncation reduces the repressive activity of V6.

Finally, we also plan to investigate the function of V6 *in vivo* by over-expression. We have prepared a pCIG-V6-GFP construct, which we plan to inject into HH4 embryos for analysis at HH6 and HH10, stages when endogenous levels of V6 are relatively low, as demonstrated by QPCR. Alternatively, we may overexpress V6 at HH6 and assay electroporated embryos for changes in neural crest gene expression at later stages. Based on the similarity in expression levels of V6 and full-length Bmi-1, as well as the presence of a putative NLS and the

HTHTHT repressive domain in this variant, we predict that over-expression would result in a gain-of-function phenotype similar to that observed with Bmi-1 and Ring1B co-electroporation. If this variant indeed functions in a dominant-active manner, it is possible that it may be compensating for full-length Bmi-1 in our MO knock-down experiments, explaining the weak phenotype that we observe. In addition, the high expression peak of V6 at HH8 may explain why we do not see a consistent effect on neural crest network genes when we analyze Bmi-1 MO-electroporated embryos at later stages. Therefore, we also plan to design a morpholino targeting the unique V6 start site for use in co-electroporation experiments with the 5' Bmi-1 MO (as well as with MOs against other PRC1 members).

Although these studies are far from complete, they present novel evidence for regulation of Bmi-1 by alternative splicing. Given the high incidence of strongly conserved splice variants within large protein families involved in key aspects of development, such as FGF, Dlx, and Pax, it is likely that modulation of protein function by alternative splicing is a common regulatory mechanism in vertebrate development. Accordingly, inappropriate expression of splice isoforms of PcG members has been demonstrated in cancers, highlighting the importance of precise control of Polycomb activity and critical involvement of alternatively spliced variants in developmental processes.

Conclusions

In summary, in my thesis project I have demonstrated that a number of neural crest specifiers are co-expressed in the neural plate border of the chick gastrula with early neural plate border specifier genes, which has contributed to

the identification of this region by combinatorial gene expression. I have also investigated how neural crest network gene expression domains resolve over time and found that most specification signals are continuously present throughout neural crest development, suggesting a need for upstream regulation. I have demonstrated that members of the Polycomb Group of epigenetic regulators are co-expressed with neural crest network genes throughout early chick development, and that the Polycomb Repressive Complex 1 member Bmi-1 functions to negatively regulate *Msx1*, *FoxD3*, and *Sox9* in the neural plate border of the chick neurula. Finally, I have characterized the Bmi-1 genomic locus and identified several truncated splice variants which are expressed during early development, and have demonstrated that one of the variants possesses dominant-negative activity *in vivo*. Therefore, I have characterized some of the molecular and epigenetic events that participate in neural crest formation and have found that multiple levels of regulation, including genetic, epigenetic, and biochemical inputs, are involved in development of this cell population.

Figure 5.1: NC-GRN and PcG expression during early development

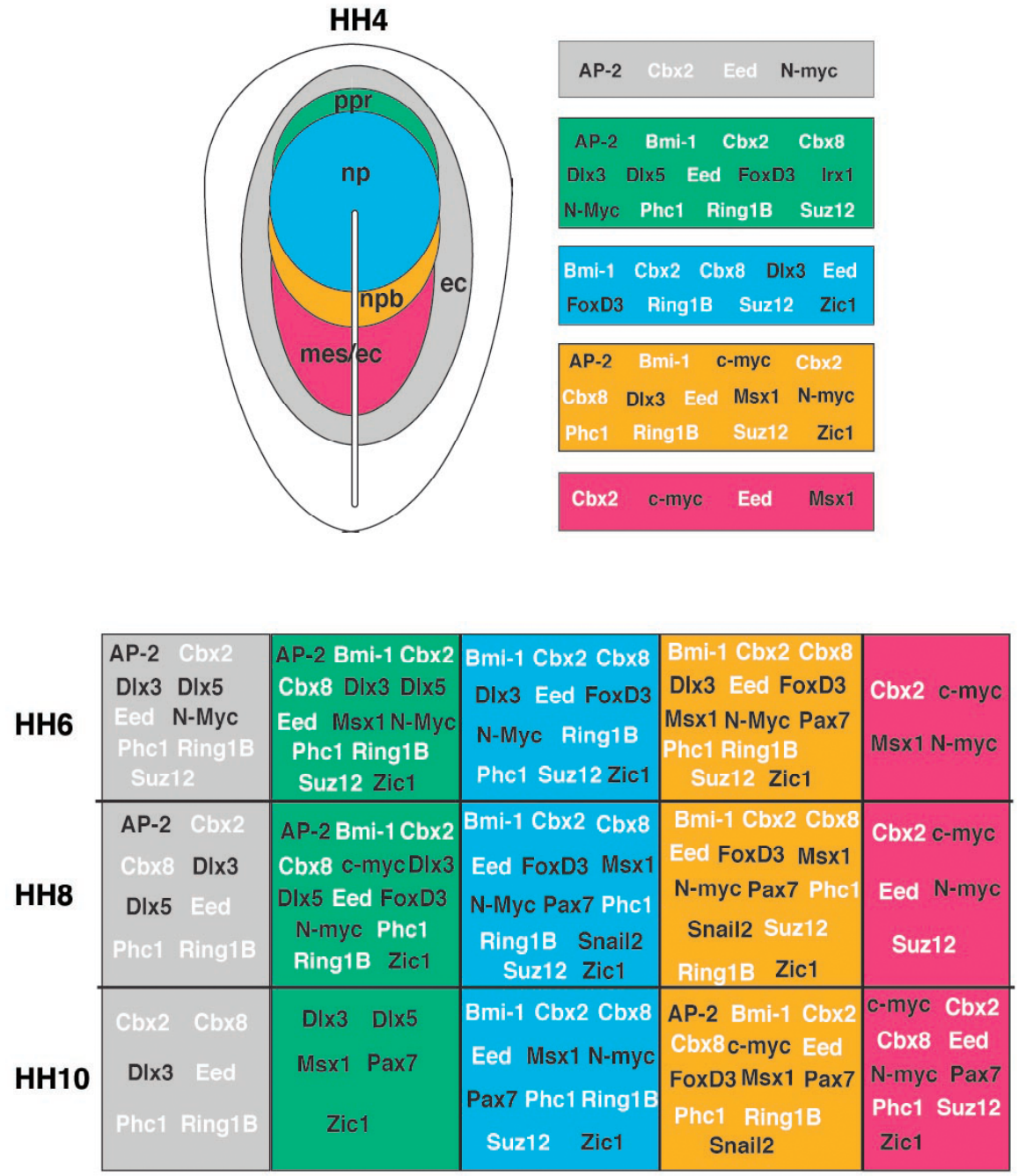

Fig. 5.1. Schematic diagram illustrating respective locations of the following presumptive tissues in the chick gastrula: non-neural ectoderm (gray), pre-placodal and anterior neural region (green), neural plate (blue), neural plate

border (orange), and posterior mesectoderm (pink). Neural crest network genes (black type) and Polycomb Group genes (white type), which were found to be expressed in each of these subregions, are listed in color-coded blocks. A summary color-coded chart lists the neural crest and Polycomb genes which were found to be expressed in progenitors of the aforementioned lineages at HH6, HH8, and HH10. Note that many genes share expression in closely apposed tissues, such as neural (dorsal neural tube) and neural plate border (neural crest).

Cited Literature

Alkema MJ, Bronk M, Verhoeven E, Otte A, van 't Veer LJ, Berns A, and van Lohuizen M. (1997a) Identification of Bmi-1-interacting proteins as constituents of a multimeric mammalian Polycomb complex. *Genes Dev* 11:226-240.

Alkema MJ, Jacobs H, van Lohuizen M, and Berns A. (1997b) Pertubation of B and T cell development and predisposition to lymphomagenesis in Emu Bmi-1 transgenic mice require the Bmi-1 RING finger. *Oncogene* 15:899-910.

Alkema MJ, van der Lugt NM, Bobeldijk RC, Berns A, and van Lohuizen M. (1995) Transformation of axial skeleton due to over-expression of bmi-1 in transgenic mice. *Nature* 374:724-727.

Atsuta T, Fujimura S, Moriya H, Vidal M, Akasaka T, and Koseki H. (2001) Production of monoclonal antibodies against mammalian Ring1B proteins. *Hybridoma* 20:43-46.

Aybar MJ and Mayor R. (2002) Early induction of neural crest cells: lessons learned from frog, fish and chick. *Curr Opin Genet Dev* 12:452-458.

Baker JC, Beddington RS, and Harland RM. (1999) Wnt signaling in Xenopus embryos inhibits bmp4 expression and activates neural development. *Genes Dev* 13:3149-3159.

Bang AG, Papalopulu N, Kintner C, and Goulding MD. (1997) Expression of Pax-3 is initiated in the early neural plate by posteriorizing signals produced by the organizer and by posterior non-axial mesoderm. *Development* 124:2075-2085.

Basch ML, Bronner-Fraser M, and Garcia-Castro MI. (2006) Specification of the neural crest occurs during gastrulation and requires Pax7. *Nature* 441:218-222.

Baskind HA, Na L, Ma Q, Patel MP, Geenen DL, and Wang QT. (2009) Functional conservation of asxl2, a murine homolog for the Drosophila enhancer of trithorax and Polycomb group gene asx. *PLoS ONE* 4:e4750.

Baylin SB and Ohm JE. (2006) Epigenetic gene silencing in cancer - a mechanism for early oncogenic pathway addiction? *Nat Rev Cancer* 6:107-116.

Bellmeyer A, Krase J, Lindgren J, and LaBonne C. (2003) The protooncogene c-myc is an essential regulator of neural crest formation in xenopus. *Dev Cell* 4:827-839.

Bermejo-Rodriguez C, Perez-Caro M, Perez-Mancera PA, Sanchez-Beato M, Piris MA, and Sanchez-Garcia I. (2006) Mouse cDNA microarray analysis uncovers Slug targets in mouse embryonic fibroblasts. *Genomics* 87:113-118.

Bernstein BE, Mikkelsen TS, Xie X, Kamal M, Huebert DJ, Cuff J, Fry B, Meissner A, Wernig M, Plath K, Jaenisch R, Wagschal A, Feil R, Schreiber SL, and Lander ES. (2006) A bivalent chromatin structure marks key developmental genes in embryonic stem cells. *Cell* 125:315-326.

Bhattacharyya S, Bailey AP, Bronner-Fraser M, and Streit A. (2004) Segregation of lens and olfactory precursors from a common territory: cell sorting and reciprocity of Dlx5 and Pax6 expression. *Dev Biol* 271:403-414.

Boyer LA, Plath K, Zeitlinger J, Brambrink T, Medeiros LA, Lee TI, Levine SS, Wernig M, Tajonar A, Ray MK, Bell GW, Otte AP, Vidal M, Gifford DK, Young RA, and Jaenisch R. (2006) Polycomb complexes repress developmental regulators in murine embryonic stem cells. *Nature* 441:349-353.

Bracken AP, Kleine-Kohlbrecher D, Dietrich N, Pasini D, Gargiulo G, Beekman C, Theilgaard-Monch K, Minucci S, Porse BT, Marine JC, Hansen KH, and Helin K. (2007) The Polycomb group proteins bind throughout the INK4A-ARF locus and are disassociated in senescent cells. *Genes Dev* 21:525-530.

Bracken AP, Dietrich N, Pasini D, Hansen KH, and Helin K. (2006) Genome-wide mapping of Polycomb target genes unravels their roles in cell fate transitions. *Genes Dev* 20:1123-1136.

Bronner-Fraser M. (2002) Molecular analysis of neural crest formation. *J Physiol Paris* 96:3-8.

Bronner-Fraser M. (1998) Inductive interactions underlie neural crest formation. *Adv Pharmacol* 42:883-887.

Bronner-Fraser M and Fraser SE. (1989) Developmental potential of avian trunk neural crest cells in situ. *Neuron* 3:755-766.

Bronner-Fraser M and Fraser SE. (1988) Cell lineage analysis reveals multipotency of some avian neural crest cells. *Nature* 335:161-164.

Brown ST, Wang J, and Groves AK. (2005) Dlx gene expression during chick inner ear development. *J Comp Neurol* 483:48-65.

Cao R, Tsukada Y, and Zhang Y. (2005) Role of Bmi-1 and Ring1A in H2A ubiquitylation and Hox gene silencing. *Mol Cell* 20:845-854.

Chamberlain SJ, Yee D, and Magnuson T. (2008) Polycomb repressive complex 2 is dispensable for maintenance of embryonic stem cell pluripotency. *Stem Cells* 26:1496-1505.

Cheung M and Briscoe J. (2003) Neural crest development is regulated by the transcription factor Sox9. *Development* 130:5681-5693.

Cohen KJ, Hanna JS, Prescott JE, and Dang CV. (1996) Transformation by the Bmi-1 oncoprotein correlates with its subnuclear localization but not its transcriptional suppression activity. *Mol Cell Biol* 16:5527-5535.

Crane JF and Trainor PA. (2006) Neural crest stem and progenitor cells. *Annu Rev Cell Dev Biol* 22:267-286.

Cui H, Ma J, Ding J, Li T, Alam G, and Ding HF. (2006) Bmi-1 regulates the differentiation and clonogenic self-renewal of I-type neuroblastoma cells in a concentration-dependent manner. *J Biol Chem* 281:34696-34704.

Davidson EH, Rast JP, Oliveri P, Ransick A, Calestani C, Yuh CH, Minokawa T, Amore G, Hinman V, Arenas-Mena C, Otim O, Brown CT, Livi CB, Lee PY, Revilla R, Rust AG, Pan Z, Schilstra MJ, Clarke PJ, Arnone MI, Rowen L, Cameron RA, McClay DR, Hood L, and Bolouri H. (2002) A genomic regulatory network for development. *Science* 295:1669-1678.

del Barrio MG and Nieto NM. (2002) Over-expression of Snail family members highlights their ability to promote chick neural crest formation. *Development* 129:1583-1593.

Delcuve GP, Rastegar M, and Davie JR. (2009) Epigenetic control. *J Cell Physiol* 219:243-250.

Denkers N, Garcia-Villalba P, Rodesch CK, Nielson KR, and Mauch TJ. (2004) FISHing for chick genes: Triple-label whole-mount fluorescence in situ hybridization detects simultaneous and overlapping gene expression in avian embryos. *Dev Dyn* 229:651-657.

Dietrich N, Bracken AP, Trinh E, Schjerling CK, Koseki H, Rappsilber J, Helin K, and Hansen KH. (2007) Bypass of senescence by the Polycomb group protein CBX8 through direct binding to the INK4A-ARF locus. *Embo J* 26:1637-1648.

Dottori M, Gross MK, Labosky P, and Goulding M. (2001) The winged-helix transcription factor Foxd3 suppresses interneuron differentiation and promotes neural crest cell fate. *Development* 128:4127-4138.

Ezin AM, Fraser SE, and Bronner-Fraser M. (2009) Fate map and morphogenesis of presumptive neural crest and dorsal neural tube. *Dev Biol* Epub ahead of print.

Fernandez-Garre P, Rodriguez-Gallardo L, Gallego-Diaz V, Alvarez IS, and Puelles L. (2002) Fate map of the chicken neural plate at stage 4. *Development* 129:2807-2822.

Fraser PE and Sauka-Spengler T. (2004) Expression of the Polycomb group gene bmi-1 in the early chick embryo. *Gene Expr Patterns* 5:23-27.

Gammill LS and Bronner-Fraser M. (2003) Neural crest specification: migrating into genomics. *Nat Rev Neurosci* 4:795-805.

Gammill LS and Bronner-Fraser M. (2002) Genomic analysis of neural crest induction. *Development* 129:5731-5741.

Gans C and Northcutt RG. (1983) Neural crest and the origin of vertebrates: a new head. *Science* 220:268-273.

Garcia-Castro MI, Marcelle C, and Bronner-Fraser M. (2002) Ectodermal Wnt function as a neural crest inducer. *Science* 297:848-851.

Garcia-Martinez V, Alvarez IS, and Schoenwolf GC. (1993) Locations of the ectodermal and nonectodermal subdivisions of the epiblast at stages 3 and 4 of avian gastrulation and neurulation. *J Exp Zool* 267:431-446.

Geiss GK, Bumgarner RE, Birditt B, Dahl T, Dowidar N, Dunaway DL, Fell HP, Ferree S, George RD, Grogan T, James JJ, Maysuria M, Mitton JD, Oliveri P, Osborn JL, Peng T, Ratcliffe AL, Webster PJ, Davidson EH, Hood L, and Dimitrov K. (2008) Direct multiplexed measurement of gene expression with color-coded probe pairs. *Nat Biotechnol* 26:317-325.

Grinberg AV, Hu CD, and Kerppola TK. (2004) Visualization of Myc/Max/Mad family dimers and the competition for dimerization in living cells. *Mol Cell Biol* 24:4294-4308.

Hall BK. (2000) The neural crest as a fourth germ layer and vertebrates as quadroblastic not triploblastic. *Evol Dev* 2:3-5.

Hamburger V and Hamilton HL. (1992) A series of normal stages in the development of the chick embryo. 1951. *Dev Dyn* 195:231-272.

Haupt Y, Bath ML, Harris AW, and Adams JM. (1993) bmi-1 transgene induces lymphomas and collaborates with myc in tumorigenesis. *Oncogene* 8:3161-3164.

Haupt Y, Alexander WS, Barri G, Klinken SP, and Adams JM. (1991) Novel zinc finger gene implicated as myc collaborator by retrovirally accelerated lymphomagenesis in E mu-myc transgenic mice. *Cell* 65:753-763.

Hemenway CS, Halligan BW, and Levy LS. (1998) The Bmi-1 oncoprotein interacts with dinG and MPh2: the role of RING finger domains. *Oncogene* 16:2541-2547.

Hemmati HD, Nakano I, Lazareff JA, Masterman-Smith M, Geschwind DH, Bronner-Fraser M, and Kornblum HI. (2003) Cancerous stem cells can arise from pediatric brain tumors. *Proc Natl Acad Sci U S A* 100:15178-15183.

Hemmati-Brivanlou A and Melton D. (1997) Vertebrate neural induction. *Annu Rev Neurosci* 20:43-60.

Holland LZ and Short S. (2008) Gene duplication, co-option and recruitment during the origin of the vertebrate brain from the invertebrate chordate brain. *Brain Behav Evol* 72:91-105.

Hong CS and Saint-Jeannet JP. (2007) The activity of Pax3 and Zic1 regulates three distinct cell fates at the neural plate border. *Mol Biol Cell* 18:2192-2202.

Hu CD and Kerppola TK. (2003) Simultaneous visualization of multiple protein interactions in living cells using multicolor fluorescence complementation analysis. *Nat Biotechnol* 21:539-545.

Huang X and Saint-Jeannet JP. (2004) Induction of the neural crest and the opportunities of life on the edge. *Dev Biol* 275:1-11.

Itahana K, Zou Y, Itahana Y, Martinez JL, Beausejour C, Jacobs JJ, Van Lohuizen M, Band V, Campisi J, and Dimri GP. (2003) Control of the replicative life span of human fibroblasts by p16 and the Polycomb protein Bmi-1. *Mol Cell Biol* 23:389-401.

Jacobs JJ, Kieboom K, Marino S, DePinho RA, and van Lohuizen M. (1999a) The oncogene and Polycomb-group gene bmi-1 regulates cell proliferation and senescence through the ink4a locus. *Nature* 397:164-168.

Jacobs JJ, Scheijen B, Voncken JW, Kieboom K, Berns A, and van Lohuizen M. (1999b) Bmi-1 collaborates with c-myc in tumorigenesis by inhibiting c-myc-induced apoptosis via INK4a/ARF. *Genes Dev* 13:2678-2690.

Khudyakov J and Bronner-Fraser M. (2009) Comprehensive spatiotemporal analysis of early chick neural crest network genes. *Dev Dyn* 238:716-723.

Kim E, Goren A, and Ast G. (2008) Alternative splicing: current perspectives. *Bioessays* 30:38-47.

Kim SH, Mitchell M, Fujii H, Llanos S, and Peters G. (2003) Absence of p16INK4a and truncation of ARF tumor suppressors in chickens. *Proc Natl Acad Sci U S A* 100:211-216.

Kloosterman WP, Wienholds E, de Bruijn E, Kauppinen S, and Plasterk RH. (2006) In situ detection of miRNAs in animal embryos using LNA-modified oligonucleotide probes. *Nat Methods* 3:27-29.

Knecht AK and Bronner-Fraser M. (2002) Induction of the neural crest: a multigene process. *Nat Rev Genet* 3:453-461.

Kohler C and Villar CB. (2008) Programming of gene expression by Polycomb group proteins. *Trends Cell Biol* 18:236-243.

Kos R, Reedy MV, Johnson RL, and Erickson CA. (2001) The winged-helix transcription factor FoxD3 is important for establishing the neural crest lineage and repressing melanogenesis in avian embryos. *Development* 128:1467-1479.

Ku M, Koche RP, Rheinbay E, Mendenhall EM, Endoh M, Mikkelsen TS, Presser A, Nusbaum C, Xie X, Chi AS, Adli M, Kasif S, Ptaszek LM, Cowan CA, Lander ES, Koseki H, and Bernstein BE. (2008) Genomewide analysis of PRC1 and PRC2 occupancy identifies two classes of bivalent domains. *PLoS Genet* 4:e1000242.

Kubota K, Ohashi A, Imachi H, and Harada H. (2006) Improved in situ hybridization efficiency with locked-nucleic-acid-incorporated DNA probes. *Appl Environ Microbiol* 72:5311-5317.

Kuroda H, Wessely O, and De Robertis EM. (2004) Neural induction in Xenopus: requirement for ectodermal and endomesodermal signals via Chordin, Noggin, beta-Catenin, and Cerberus. *PLoS Biol* 2:E92.

LaBonne C and Bronner-Fraser M. (2000) Snail-related transcriptional repressors are required in Xenopus for both the induction of the neural crest and its subsequent migration. *Dev Biol* 221:195-205.

LaBonne C and Bronner-Fraser M. (1999) Molecular mechanisms of neural crest formation. *Annu Rev Cell Dev Biol* 15:81-112.

LaBonne C and Bronner-Fraser M. (1998) Neural crest induction in Xenopus: evidence for a two-signal model. *Development* 125:2403-2414.

Lareau LF, Green RE, Bhatnagar RS, and Brenner SE. (2004) The evolving roles of alternative splicing. *Curr Opin Struct Biol* 14:273-282.

Launay C, Fromentoux V, Shi DL, and Boucaut JC. (1996) A truncated FGF receptor blocks neural induction by endogenous Xenopus inducers. *Development* 122:869-880.

Le Douarin N, Creuzet S, Couly G, and Dupin E. (2004) Neural crest cell plasticity and its limits. *Development* 131:4637-4650.

Le Douarin N. (2004) The avian embryo as a model to study the development of the neural crest: a long and still ongoing story. *Mech Dev* 121:1089-1102.

Le Douarin N and Kalcheim C. (1999) The Neural Crest. New York: Cambridge University Press, 2nd edn.

Lee TI, Jenner RG, Boyer LA, Guenther MG, Levine SS, Kumar RM, Chevalier B, Johnstone SE, Cole MF, Isono K, Koseki H, Fuchikami T, Abe K, Murray HL, Zucker JP, Yuan B, Bell GW, Herbolsheimer E, Hannett NM, Sun K, Odom DT, Otte AP, Volkert TL, Bartel DP, Melton DA, Gifford DK, Jaenisch R, and Young RA. (2006) Control of developmental regulators by Polycomb in human embryonic stem cells. *Cell* 125:301-313.

Lessard J and Sauvageau G. (2003) Bmi-1 determines the proliferative capacity of normal and leukaemic stem cells. *Nature* 423:255-260.

Lewis EB. (1978) A gene complex controlling segmentation in Drosophila. *Nature* 276:565-570.

Li J, Bench AJ, Piltz S, Vassiliou G, Baxter EJ, Ferguson-Smith AC, and Green AR. (2005) L3mbtl, the mouse orthologue of the imprinted L3MBTL, displays a complex pattern of alternative splicing and escapes genomic imprinting. *Genomics* 86:489-494.

Light W, Vernon AE, Lasorella A, Iavarone A, and LaBonne C. (2005) Xenopus Id3 is required downstream of Myc for the formation of multipotent neural crest progenitor cells. *Development* 132:1831-1841.

Luo T, Lee YH, Saint-Jeannet JP, and Sargent TD. (2003) Induction of neural crest in Xenopus by transcription factor AP2alpha. *Proc Natl Acad Sci U S A* 100:532-537.

Luo T, Matsuo-Takasaki M, Thomas ML, Weeks DL, and Sargent TD. (2002) Transcription factor AP-2 is an essential and direct regulator of epidermal development in Xenopus. *Dev Biol* 245:136-144.

Luo T, Matsuo-Takasaki M, Lim JH, and Sargent TD. (2001a) Differential regulation of Dlx gene expression by a BMP morphogenetic gradient. *Int J Dev Biol* 45:681-684.

Luo T, Matsuo-Takasaki M, and Sargent TD. (2001b) Distinct roles for Distal-less genes Dlx3 and Dlx5 in regulating ectodermal development in Xenopus. *Mol Reprod Dev* 60:331-337.

Maniatis T and Tasic B. (2002) Alternative pre-mRNA splicing and proteome expansion in metazoans. *Nature* 418:236-243.

Mayor R, Morgan R, and Sargent MG. (1995) Induction of the prospective neural crest of Xenopus. *Development* 121:767-777.

McKeown SJ, Lee VM, Bronner-Fraser M, Newgreen DF, and Farlie PG. (2005) Sox10 over-expression induces neural crest-like cells from all dorsoventral levels of the neural tube but inhibits differentiation. *Dev Dyn* 233:430-444.

McLarren KW, Litsiou A, and Streit A. (2003) DLX5 positions the neural crest and preplacode region at the border of the neural plate. *Dev Biol* 259:34-47.

Mende M, Christophorou NA, and Streit A. (2008) Specific and effective gene knock-down in early chick embryos using morpholinos but not pRFPRNAi vectors. *Mech Dev* 125:947-962.

Mendenhall EM and Bernstein BE. (2008) Chromatin state maps: new technologies, new insights. *Curr Opin Genet Dev* 18:109-115.

Merzdorf CS. (2007) Emerging roles for zic genes in early development. *Dev Dyn* 236:922-940.

Meulemans D and Bronner-Fraser M. (2004) Gene-regulatory interactions in neural crest evolution and development. *Dev Cell* 7:291-299.

Mikkelsen TS, Ku M, Jaffe DB, Issac B, Lieberman E, Giannoukos G, Alvarez P, Brockman W, Kim TK, Koche RP, Lee W, Mendenhall E, O'Donovan A, Presser A, Russ C, Xie X, Meissner A, Wernig M, Jaenisch R, Nusbaum C, Lander ES, and Bernstein BE. (2007) Genome-wide maps of chromatin state in pluripotent and lineage-committed cells. *Nature* 448:553-560.

Mohn F, Weber M, Rebhan M, Roloff TC, Richter J, Stadler MB, Bibel M, and Schubeler D. (2008) Lineage-specific Polycomb targets and de novo DNA methylation define restriction and potential of neuronal progenitors. *Mol Cell* 30:755-766.

Molofsky AV, He S, Bydon M, Morrison SJ, and Pardal R. (2005) Bmi-1 promotes neural stem cell self-renewal and neural development but not mouse growth and survival by repressing the p16Ink4a and p19Arf senescence pathways. *Genes Dev* 19:1432-1437.

Molofsky AV, Pardal R, Iwashita T, Park IK, Clarke MF, and Morrison SJ. (2003) Bmi-1 dependence distinguishes neural stem cell self-renewal from progenitor proliferation. *Nature* 425:962-967.

Monsoro-Burq AH, Wang E, and Harland R. (2005) Msx1 and Pax3 cooperate to mediate FGF8 and WNT signals during Xenopus neural crest induction. *Dev Cell* 8:167-178.

Montero-Balaguer M Lang MR, Sachdev SW, Knappmeyer C, Stewart RA, De La Guardia A, Hatzopoulos AK, and Knapik EW. (2006) The mother superior mutation ablates foxd3 activity in neural crest progenitor cells and depletes neural crest derivatives in zebrafish. *Dev Dyn* 235:3199-3212.

Moroy T and Heyd F. (2007) The impact of alternative splicing in vivo: mouse models show the way. *RNA* 13:1155-1171.

Morrison SJ, White PM, Zock C, and Anderson DJ. (1999) Prospective identification, isolation by flow cytometry, and in vivo self-renewal of multipotent mammalian neural crest stem cells. *Cell* 96:737-749.

Nieto MA, Patel K, and Wilkinson DG. (1996) In situ hybridization analysis of chick embryos in whole mount and tissue sections. *Methods Cell Biol* 51:219-235.

Nieto MA, Sargent MG, Wilkinson DG, and Cooke J. (1994) Control of cell behavior during vertebrate development by Slug, a zinc finger gene. *Science* 264:835-839.

Odenthal J and Nusslein-Volhard C. (1998) fork head domain genes in zebrafish. *Dev Genes Evol* 208:245-258.

Orkin SH and Zon LI. (1997) Genetics of erythropoiesis: induced mutations in mice and zebrafish. *Annu Rev Genet* 31:33-60.

Otte AP and Kwaks TH. (2003) Gene repression by Polycomb group protein complexes: a distinct complex for every occasion? *Curr Opin Genet Dev* 13:448-454.

Park IK, Morrison SJ, and Clarke MF. (2004) Bmi-1, stem cells, and senescence regulation. *J Clin Invest* 113:175-179.

Park IK, Qian D, Kiel M, Becker MW, Pihalja M, Weissman IL, Morrison SJ, and Clarke MF. (2003) Bmi-1 is required for maintenance of adult self-renewing haematopoietic stem cells. *Nature* 423:302-305.

Pasini D, Bracken AP, Hansen JB, Capillo M, and Helin K. (2007) The Polycomb group protein Suz12 is required for embryonic stem cell differentiation. *Mol Cell Biol* 27:3769-3779.

Pasini D, Bracken AP, Jensen MR, Lazzerini Denchi E, and Helin K. (2004) Suz12 is essential for mouse development and for EZH2 histone methyltransferase activity. *Embo J* 23:4061-4071.

Pera E, Stein S, and Kessel M. (1999) Ectodermal patterning in the avian embryo: epidermis versus neural plate. *Development* 126:63-73.

Phillips BT, Kwon HJ, Melton C, Houghtaling P, Fritz A, and Riley BB. (2006) Zebrafish msxB, msxC and msxE function together to refine the neural-nonneural border and regulate cranial placodes and neural crest development. *Dev Biol* 294:376-390.

Pietersen AM, van Lohuizen M. 2008. Stem cell regulation by Polycomb repressors: postponing commitment. Curr Opin Cell Biol 20:201-207.

Raible DW. (2006) Development of the neural crest: achieving specificity in regulatory pathways. *Curr Opin Cell Biol* 18:698-703.

Ross RA and Spengler BA. (2007) Human neuroblastoma stem cells. Semin *Cancer Biol* 17:241-247.

Saito Y, Kanai Y, Sakamoto M, Saito H, Ishii H, and Hirohashi S. (2002) Over-expression of a splice variant of DNA methyltransferase 3b, DNMT3b4, associated with DNA hypomethylation on pericentromeric satellite

regions during human hepatocarcinogenesis. *Proc Natl Acad Sci U S A* 99:10060-10065.

Sakai D, Suzuki T, Osumi N, and Wakamatsu Y. (2006) Cooperative action of Sox9, Snail2 and PKA signaling in early neural crest development. *Development* 133:1323-1333.

Sasai N, Mizuseki K, and Sasai Y. (2001) Requirement of FoxD3-class signaling for neural crest determination in Xenopus. *Development* 128:2525-2536.

Satijn DP and Otte AP. (1999) RING1 interacts with multiple Polycomb-group proteins and displays tumorigenic activity. *Mol Cell Biol* 19:57-68.

Sato T, Sasai N, and Sasai Y. (2005) Neural crest determination by co-activation of Pax3 and Zic1 genes in Xenopus ectoderm. *Development* 132:2355-2363.

Sauka-Spengler T and Bronner-Fraser M. (2008) A gene regulatory network orchestrates neural crest formation. *Nat Rev Mol Cell Biol* 9:557-568.

Sauka-Spengler T, Meulemans D, Jones M, and Bronner-Fraser M. (2007) Ancient evolutionary origin of the neural crest gene regulatory network. *Dev Cell* 13:405-420.

Schuettengruber B, Chourrout D, Vervoort M, Leblanc B, and Cavalli G. (2007) Genome regulation by Polycomb and trithorax proteins. *Cell* 128:735-745.

Schwartz YB and Pirrotta V. (2008) Polycomb complexes and epigenetic states. *Curr Opin Cell Biol* 20:266-273.

Schwartz YB and Pirrotta V. (2007) Polycomb silencing mechanisms and the management of genomic programmes. *Nat Rev Genet* 8:9-22.

Selleck MA and Bronner-Fraser M. (1996) The genesis of avian neural crest cells: a classic embryonic induction. *Proc Natl Acad Sci U S A* 93:9352-9357.

Shyu YJ, Liu H, Deng X, and Hu CD. (2006) Identification of new fluorescent protein fragments for bimolecular fluorescence complementation analysis under physiological conditions. *Biotechniques* 40:61-66.

Sieber-Blum M and Hu Y. 2008. Epidermal Neural Crest Stem Cells (EPI-NCSC) and Pluripotency. *Stem Cell Rev* 4:256-60.

Sparmann A and van Lohuizen M. (2006) Polycomb silencers control cell fate, development and cancer. *Nat Rev Cancer* 6:846-856.

Squazzo SL, O'Geen H, Komashko VM, Krig SR, Jin VX, Jang SW, Margueron R, Reinberg D, Green R, and Farnham PJ. (2006) Suz12 binds to silenced regions of the genome in a cell-type-specific manner. *Genome Res* 16:890-900.

Stamm S, Ben-Ari S, Rafalska I, Tang Y, Zhang Z, Toiber D, Thanaraj TA, and Soreq H. 2005. Function of alternative splicing. *Gene* 344:1-20.

Stewart RA, Arduini BL, Berghmans S, George RE, Kanki JP, Henion PD, and Look AT. (2006) Zebrafish foxd3 is selectively required for neural crest specification, migration and survival. *Dev Biol* 292:174-188.

Stock JK, Giadrossi S, Casanova M, Brookes E, Vidal M, Koseki H, Brockdorff N, Fisher AG, and Pombo A. (2007) Ring1-mediated ubiquitination of H2A restrains poised RNA polymerase II at bivalent genes in mouse ES cells. *Nat Cell Biol* 9:1428-1435.

Streit A and Stern CD. (1999) Establishment and maintenance of the border of the neural plate in the chick: involvement of FGF and BMP activity. *Mech Dev* 82:51-66.

Su YH, Li E, Geiss GK, Longabaugh WJ, Kramer A, and Davidson EH. (2009) A perturbation model of the gene regulatory network for oral and aboral ectoderm specification in the sea urchin embryo. *Dev Biol* 329:410-21.

Suzuki A, Ueno N, and Hemmati-Brivanlou A. (1997) Xenopus msx1 mediates epidermal induction and neural inhibition by BMP4. *Development* 124:3037-3044.

Tajul-Arifin K, Teasdale R, Ravasi T, Hume DA, and Mattick JS. (2003) Identification and analysis of chromodomain-containing proteins encoded in the mouse transcriptome. *Genome Res* 13:1416-1429.

Takihara Y, Tomotsune D, Shirai M, Katoh-Fukui Y, Nishii K, Motaleb MA, Nomura M, Tsuchiya R, Fujita Y, Shibata Y, Higashinakagawa T, and Shimada K. (1997) Targeted disruption of the mouse homologue of the Drosophila polyhomeotic gene leads to altered anteroposterior patterning and neural crest defects. *Development* 124:3673-3682.

Tan J, Yang X, Zhuang L, Jiang X, Chen W, Lee PL, Karuturi RK, Tan PB, Liu ET, and Yu Q. (2007) Pharmacologic disruption of Polycomb-repressive complex 2-mediated gene repression selectively induces apoptosis in cancer cells. *Genes Dev* 21:1050-1063.

Taneyhill LA, Coles EG, and Bronner-Fraser M. (2007) Snail2 directly represses cadherin6B during epithelial-to-mesenchymal transitions of the neural crest. *Development* 134:1481-1490.

Teng L, Mundell NA, Frist AY, Wang Q, and Labosky PA. (2008) Requirement for Foxd3 in the maintenance of neural crest progenitors. *Development* 135:1615-1624.

Tomotsune D, Shirai M, Takihara Y, and Shimada K. (2000) Regulation of Hoxb3 expression in the hindbrain and pharyngeal arches by rae28, a member of the mammalian Polycomb group of genes. *Mech Dev* 98:165-169.

Tribulo C, Aybar MJ, Nguyen VH, Mullins MC, and Mayor R. (2003) Regulation of Msx genes by a Bmp gradient is essential for neural crest specification. *Development* 130:6441-6452.

van der Lugt NM, Alkema M, Berns A, and Deschamps J. (1996) The Polycomb-group homolog Bmi-1 is a regulator of murine Hox gene expression. *Mech Dev* 58:153-164.

van der Lugt NM, Domen J, Linders K, van Roon M, Robanus-Maandag E, te Riele H, van der Valk M, Deschamps J, Sofroniew M, van Lohuizen M, et al. (1994) Posterior transformation, neurological abnormalities, and severe hematopoietic defects in mice with a targeted deletion of the bmi-1 proto-oncogene. *Genes Dev* 8:757-769.

van der Stoop P, Boutsma EA, Hulsman D, Noback S, Heimerikx M, Kerkhoven RM, Voncken JW, Wessels LF, and van Lohuizen M. (2008) Ubiquitin E3 ligase Ring1b/Rnf2 of Polycomb repressive complex 1 contributes to stable maintenance of mouse embryonic stem cells. *PLoS ONE* 3:e2235.

Venables JP. (2006) Unbalanced alternative splicing and its significance in cancer. *Bioessays* 28:378-386.

Voncken JW, Niessen H, Neufeld B, Rennefahrt U, Dahlmans V, Kubben N, Holzer B, Ludwig S, and Rapp UR. (2005) MAPKAP kinase 3pK phosphorylates and regulates chromatin association of the Polycomb group protein Bmi-1. *J Biol Chem* 280:5178-5187.

Voncken JW, Roelen BA, Roefs M, de Vries S, Verhoeven E, Marino S, Deschamps J, and van Lohuizen M. (2003) Rnf2 (Ring1b) deficiency causes gastrulation arrest and cell cycle inhibition. *Proc Natl Acad Sci U S A* 100:2468-2473.

Voncken JW, Schweizer D, Aagaard L, Sattler L, Jantsch MF, and van Lohuizen M. (1999) Chromatin-association of the Polycomb group protein BMI-1 is cell cycle-regulated and correlates with its phosphorylation status. *J Cell Sci* 112:4627-4639.

Wakamatsu Y, Watanabe Y, Nakamura H, and Kondoh H. (1997) Regulation of the neural crest cell fate by N-myc: promotion of ventral migration and neuronal differentiation. *Development* 124:1953-1962.

Wang H, Wang L, Erdjument-Bromage H, Vidal M, Tempst P, Jones RS, and Zhang Y. (2004) Role of histone H2A ubiquitination in Polycomb silencing. *Nature* 431:873-878.

Whitcomb SJ, Basu A, Allis CD, and Bernstein E. (2007) Polycomb Group proteins: an evolutionary perspective. *Trends Genet* 23:494-502.

Wilson SI and Edlund T. (2001) Neural induction: toward a unifying mechanism. *Nat Neurosci* 4 Suppl:1161-1168.

Wilson SI, Rydstrom A, Trimborn T, Willert K, Nusse R, Jessell TM, and Edlund T. (2001) The status of Wnt signalling regulates neural and epidermal fates in the chick embryo. *Nature* 411:325-330.

Wilson SI, Graziano E, Harland R, Jessell TM, and Edlund T. (2000) An early requirement for FGF signalling in the acquisition of neural cell fate in the chick embryo. *Curr Biol* 10:421-429.

Woda JM, Pastagia J, Mercola M, and Artinger KB. (2003) Dlx proteins position the neural plate border and determine adjacent cell fates. *Development* 130:331-342.

Xu Q and Wilkinson D. (1998) In situ hybridisation of mRNA with hapten labeled probes. In Situ Hybridisation: A Practical Approach. Oxford: Oxford University Press, 87-106.

Yamaki M, Isono K, Takada Y, Abe K, Akasaka T, Tanzawa H, and Koseki H. (2002) The mouse Edr2 (Mph2) gene has two forms of mRNA encoding 90- and 36-kDa polypeptides. *Gene* 288:103-110.

Yang L, Zhang H, Hu G, Wang H, Abate-Shen C, and Shen MM. (1998) An early phase of embryonic Dlx5 expression defines the rostral boundary of the neural plate. *J Neurosci* 18:8322-8330.

Yu JK, Meulemans D, McKeown SJ, and Bronner-Fraser M. (2008) Insights from the amphioxus genome on the origin of vertebrate neural crest. *Genome Res* 18:1127-1132.